SOLUTE TRANSPORT THROUGH CEMENT-BENTONITE BARRIERS

September 2004

Punlop Visudmedanukul

SOLUTE TRANSPORT THROUGH CEMENT-BENTONITE BARRIERS

by

Punlop Visudmedanukul

A dissertation submitted in partial fulfillment
of the requirements for the degree of
Doctor of Engineering

Graduate School of Civil Engineering
September 2004

To my family and ancestors

ABSTRACT

Cement-bentonite (CB) slurry walls have been substantially used as a barrier to contaminant migration in groundwater for the last two decades. Despite their significance, researches concerning the behaviors of these self-hardening materials under the attack of contaminant are not so comprehensive as those on landfill liners. Thus, this research deals with the solute transport through CB mixtures by taking a number of factors into account.

The study begins with the combination of black-box model and conventional column testing to relate retardation factor R_d and hydrodynamic dispersion coefficient D to a timely-averaged concentration, called reference concentration C_R. The reference concentration calculated by numerical technique is transformed into empirical equations for practical use. The reference concentration is a function of column Peclet number P_e, and the number can be obtained using two theoretical charts proposed herein.

Five kinds of experiments i.e., column testing, batch testing, diffusion testing, scanning electron microscopy (SEM), and laser diffraction (LD) technique are presented in this thesis. Column testing is the most important experiment by which the behaviors of CB mixtures under the transport of chloride ions have been investigated. The selected factors which are believed to affect the chloride migration are curing period, seepage velocity v, concentration, particle size d_{avg}, porosity n, and mix design. The effect of concentration is studied using the concept of reference concentration mentioned above. Transport mechanisms considered are advection, diffusion, dispersion, and adsorption.

Main conclusions from the experiments are as follows. Adsorption, hydrodynamic dispersion, and tortuosity decrease when concentration goes up. Increased seepage diminishes adsorption, but augments hydrodynamic dispersion after a yielding seepage velocity. Longer curing periods lower all hydraulic conductivity, adsorption and hydrodynamic dispersion. The hydrodynamic curves of CB mixtures, Barricalla clay and sand data do not match one another, and also their normalized versions are not coincident. Chloride ions are bound by the formation of Friedel's salt and perhaps some other chloro-complexes. The SEM images of CB columns suggest that the shape of the salt is hexagonal.

Then, concentration-dependent parameters from a series of column tests are used to predict the results of two diffusion tests by semi-analytical method (POLLUTE). Good agreement between predicted results and diffusion data could be explained in terms of concentration level. Finally, several design methods are suggested for contaminant barriers.

ACKNOWLEDGMENTS

First of all, I would like to express my deep appreciation to my research supervisor, Professor Masashi Kamon, Graduate School of Global Environmental Studies, for his valuable academic guidance, warm stimulation, and constant nonacademic support during three years of my life in Japan. Professor Kamon not only provided me the best opportunity to challenge for D.Eng. at Kyoto University, but he also introduced me to the world of environmental geotechnics about which my knowledge was little before coming to Japan. He is one of the most respectable people I have known so far.

Sincere thanks are given to Professor Yuzo Ohnishi and Professor Shinsuke Morisawa, from Department of Urban and Environment Engineering, for their review of the manuscript and constructive comments as committee members of my doctoral degree.

I thankfully acknowledge Professor Dennes T. Bergado, my former supervisor at AIT, for his introduction of myself to Professor Kamon during his visit to Kochi, Japan in the year 2000. The current head of geotechnical division at AIT also expressed his kind concern about my study in Japan. Simultaneously, special thanks go towards Professor Hiroyasu Ohtsu, Department of Urban Management, who introduced me to the International Doctoral Course in Kyoto University during his visit to AIT.

I would like to thank Dr. Takeshi Katsumi, Associate Professor at Graduate School of Global Environmental Studies, for his suggestion on my experimental work. Grateful am I to Dr. Toru Inui, Research Associate, who has given me continual supports throughout the doctoral program.

My appreciation to Professor Susumu Iai, from Disaster Prevention Research Institute (DPRI), Kyoto University, must be expressed due to his permission to utilize facilities in his laboratory. Dr. Mamoru Mimura, Associate Professor at DPRI, provided me kind hospitality and concern during my laboratory works in DPRI.

Mr. Hiroki Shimizu, a technician at DPRI, did give me a great deal of assistance in my laboratory, and I cannot but appreciate. I also thank Dr. Jae-Hyeung Jeoung, formerly a doctoral student, for his several suggestions when I began my experiments. Many thanks are due to Miss Youko Morimoto, Professor Kamon's Secretary, for her continuous help, especially in documentary work.

During my laboratory life in DPRI, I enjoyed good communication with Mr. Daisuke Miyagi, Mr. Satoru Hamada, and Mr. Yan Li. Mr. Li was my first companion when I came

to Japan, and he has been my best friend for the last three years. I appreciate his trustworthy character and believe that he will be a good professor in the near future. In addition, I also wish to thank the former and present members of Professor's Kamon research group for their friendship and support, such as Mr. Hae-Hoon Lee, Mr. Saravanan Mariappan, Mr. Tae-Hoon Lee, Mr. Giancarlo A. Flores, Mr. Yutaka Shouji, Mr. Yasuhiro Ogawa, Mr. Kenichiro Yajima, and Mr. Shotaro Sanada.

I am indebted to my Japanese language teacher, Kazuko Kudo. Not only Teacher Kudo voluntarily taught Japanese to me, but also she introduced me to many aspects of Japan and Japanese. Her sincere hospitality and support made my life in Japan easier. She deserves my respect with no doubt.

Acknowledgement is without fail directed to the Japanese Ministry of Education, Culture, Sports, Science and Technology for allocating a scholarship for my life and study in Japan. I have put much effort into my research based on the fact that the scholarship came from Japanese tax.

Last but not least, words are not enough to convey my gratitude to my beloved parents and wife for their patience, understanding, encouragement, and invaluable support to my life and study in Japan. Many thanks for their believing in me.

TABLE OF CONTENTS

LIST OF TABLES

LIST OF FIGURES

NOTATION

A_{eff} = effective area of column ($A_{eff} = V_v/L$) [L^2]

B = sodium bentonite

BS = blastfurnace slag

BSC = blastfurnace slag cement

C_e = effluent or exit concentration [M/L^3]

C_i = background concentration [M/L^3]

C_o = source concentration [M/L^3]

C_r = resident concentration [M/L^3]

C_R = reference concentration [M/L^3]

C_T = concentration in source solution [M/L^3]

Cl = chloride

CB = cement-bentonite

CMR = cumulative mass ratio (CMR = cumulative mass/V_vC_o) [-]

d_{avg} = average grain size [L]

d_{50} = grain size at 50% finer [L]

D = hydrodynamic dispersion coefficient ($D = D^* + D_{md}$) [L^2/T]

D_{md} = mechanical dispersion ($D_{md} = \alpha v$) [L^2/T]

D_o = free-solution diffusion coefficient [L^2/T]

D^* = effective diffusion coefficient [L^2/T]

e = void ratio [-]

erfc(z) = complementary error function = $1-\frac{2}{\sqrt{\pi}}\sum_{m=0}^{\infty}\frac{(-1)^m z^{2m+1}}{m!(2m+1)}$

f_T = mass flux of contaminant into soil [M/L^2T]

GM = geomembrane

G_s = specific gravity [-]

h_{loss} = head loss [L]

H_f = height of leachate [L]

i = hydraulic gradient [-]

IMR = incremental mass ratio in cumulative mass approach [-]

ISE = ion selective electrode

k = hydraulic conductivity [L/T]

K	=	partitioning or distribution coefficient [L^3/M]
L	=	column length [L]
LD	=	laser diffraction
$M_{adsorbed}$	=	adsorbed mass [M]
M_{pore}	=	resident or pore mass [M]
M_{total}	=	total mass [M]
n	=	total porosity [-]
n_e	=	effective porosity [-]
OPC	=	ordinary Portland cement
P	=	Peclet number ($P = vd_{avg}/D_o$) [-]
P_e	=	column Peclet number ($P_e = vL/D$) [-]
PSD	=	particle size distribution
q	=	adsorbed concentration [-]
Q	=	discharge [L^3/T]
R_d	=	retardation factor [-]
SB	=	soil-bentonite
SEM	=	scanning electron microscopy
t	=	time [T]
t_{limit}	=	time to obtain M_{pore} equal to ?% of total pore capacity V_vC_o [T]
T	=	pore volumes of flow ($T = vt/L$) [-]
TRD	=	trench cutting and re-mixing deep wall
v	=	seepage velocity [L/T]
V_v	=	void volume [L^3]
w_c	=	water content [-]
x	=	distance [L]
α	=	dispersivity [L]
ε	=	empirical exponent in Freundlich adsorption model [-]
ρ_d	=	dry bulk density [M/L^3]
ρ_t	=	total density [M/L^3]
τ_a	=	apparent tortuosity factor [-]

CHAPTER 1
INTRODUCTION

1.1 BACKGROUND

In recent decades, slurry walls have been used as contaminant barriers in addition to their use as barriers to water flow in more traditional construction (Sharma and Lewis 1994). Most of the remediation works are conducted after isolating contaminated areas with slurry walls. The advantages of this technique are that: (1) wall construction is simple and cost-effective, and (2) an inward flow can be supplied by lowering groundwater level inside the barrier system, thus controlling contaminant transport.

The design of a slurry wall depends on its application. Aspects like stress-strain behavior, strength, and consolidation shall be considered when the wall works as a structural element. However, when the wall is used for pollution prevention, more attentions are paid to hydraulic conductivity and contaminant-wall interaction (Jefferis 1996). Knowledge of hydraulic conductivity leads to the determination of leakage rate (seepage) through the wall, and the discharge of contaminant mass by seepage is known as advection. In fact, the total mass discharged not only depends on advection, but also depends on hydrodynamic dispersion and adsorption inside the wall. Hydrodynamic dispersion is called diffusion at low seepage velocities, and merely called dispersion at high seepage. This phenomenon makes contaminant mass reach the end of the barrier sooner than pure advection alone. Adsorption is normally considered negligible in conservative design. Yet, if the contaminant of interest is very reactive to the barrier, this negligence will make the design too conservative and not economical. Despite the importance of hydrodynamic dispersion and adsorption phenomena, most of the current designs of slurry walls are mainly based on only hydraulic conductivity.

Cement-bentonite (CB) slurry wall is one of the slurry wall types used in present construction. This type of wall has self-hardening behavior, and the wall physical and chemical properties change with curing time. The hydration of cement with pore fluid changes the hydraulic conductivity of this self-hardening material. Hydraulic conductivity at 28-day curing is normally used for design; however, a number of researches show that decreases in hydraulic conductivity values of CB mixtures rarely stop at 28 days, but rather go on for months or years (Fratalocchi and Pasqualini 1998). The decreases in hydraulic

conductivity imply that both hydrodynamic dispersion and adsorption should not remain constant with time as well. Nevertheless, comprehensive studies regarding the two phenomena have not been provided.

Apart from curing time, such factors as seepage, porosity, and concentration could influence the dispersion and adsorption inside CB materials. Even though conventional batch testing (Roy et al. 1991) can be used to study the concentration-dependent adsorption behavior of ordinary soils, the test has many limitations in terms of interpretation, and it is not applicable to self-hardening materials like CB. Furthermore, hydrodynamic dispersion phenomenon cannot be studied by batch testing.

Column testing (see Shackelford 1994) overcomes the difficulties in batch testing. Not only it is possible to simulate such field conditions as water content, effective stress, and seepage velocity, but also the test can be used to evaluate adsorption and hydrodynamic dispersion parameters simultaneously. Such parameters generally are obtained by fitting a selected analytical solution to concentration data, usually a series of effluent concentrations. As implied from batch testing, adsorption in column testing would also depend on the level of concentration in pore volume, and likewise hydrodynamic dispersion phenomenon, to a certain extent, could be related to this resident concentration. The analytical solution is generally based on the assumption of constant transport parameters; therefore, the results of column testing may just provide average transport parameters of a solute of interest along a flow path under an induced seepage velocity. In addition, the determination of hydrodynamic dispersion parameter from column testing needs nonlinear regression involving complementary error function (see Kreyszig 1993) which is not available in most curve-fitting softwares. This difficulty may prevent people from choosing column testing as their tool to evaluate the transport parameters of porous media.

This research deals with the comprehensive studies of solute transport mechanisms inside CB materials under diverse influencing factors. Attentions are especially paid to adsorption and hydrodynamic dispersion phenomena which have always been neglected in other previous researches. Column testing is selected as the main tool to evaluate transport parameters. The test has two drawbacks which need to be resolved. Firstly, transport parameters deduced from column testing shall be related to resident concentration. Second, simpler parameter interpretation may attract more attention to the test.

It is motivated that if the behaviors of CB walls are fully understood, the design and analysis of these reactive and time-dependent barriers can be carried out with more

confidence and accuracy. This research is the first volume that provides a great deal of information regarding solute transport through CB barriers.

1.2 OBJECTIVES OF THE STUDY

The main objectives of this research are as follows:

1. To develop an approach to understand solute transport in view of concentration levels.
2. To simplify the interpretation of column testing.
3. To study solute transport through CB mixtures, taking a number of factors into account.
4. To propose practical applications of CB walls: design and analysis.

1.3 SCOPE OF THE STUDY

This research work begins with the origination of an approach to cope with the concentration-dependent behaviors of adsorption and hydrodynamic dispersion parameters. The formulation of the approach comes from the combination of a well-known method for column testing and numerical techniques. Then, a simple algorithm to find the transport parameters without nonlinear regression is proposed in this study. Most mathematical calculations are carried out with the aid of MATHEMATICA software.

Experimental works mainly consisting of column, batch, and pure diffusion tests have been performed to provide evidence towards the approach. There are 42 column tests, 2 series of batch tests, and 2 pure diffusion tests. Cement-bentonite (CB) mixtures are investigated, and the chemical solutions used throughout the study are sodium chloride (NaCl), with various concentrations. Chloride ions are the only ions to be focused. The significant factors, which are likely to affect the transport of chloride ions through CB mixtures, are curing period, seepage velocity, concentration, particle size, porosity, and mix design.

In addition, two special tests namely laser diffraction (LD) technique and scanning electron microscopy (SEM) are also conducted to provide more supporting information to the experimental results. Theoretical predictions appeared in a part of the dissertation are carried out using POLLUTE software (Rowe et al. 1998). Predicted results are compared with the experimental results of the diffusion tests.

1.4 DISSERTATION OUTLINE

This research volume is divided into 6 chapters. Chapter 1 here sets the introductory stage of informing the readers of the importance of this research. Four objectives and scope of the work are clarified. The second chapter deals with present basic knowledge essential for the understanding of the novel contents in following chapters.

Chapter 3 explains the tools and ideas which are used by the author in order to give an insight into the solute transport mechanisms inside CB mixtures. Chapter 4 shows the experimental results of column and batch testing, together with their discussions. Other results such as properties of materials used, LD and SEM analyses are also provided.

Chapter 5 deals with the possible applications of this research. The results from diffusion tests and their theoretical predictions using POLLUTE are included in this chapter. The last chapter then gives conclusions from Chapters 3, 4 and 5, and recommendations for future research. Figure 1.1 shows the structure of this dissertation.

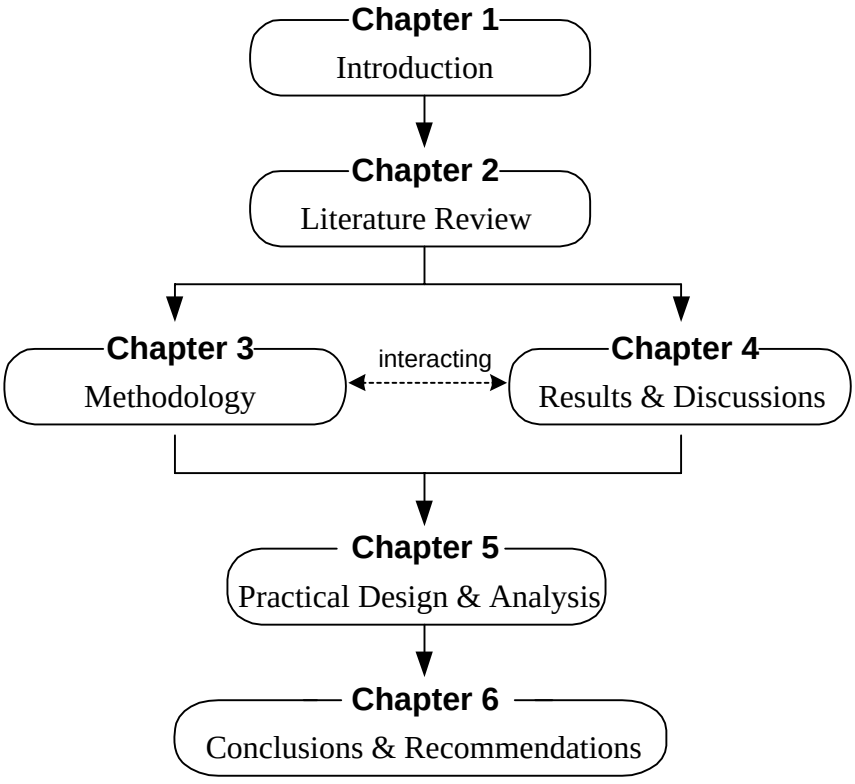

Figure 1.1 Structure of the dissertation.

The dotted line in Figure 1.1 means that the tools and ideas appeared in Chapter 3 are implemented in Chapter 4. Then, Chapter 5 is developed based on both Chapters 3 and 4 before Chapter 6 marks the end of the dissertation.

1.5 RESEARCH MAIN IDEAS

Described in Chapter 1, the author chooses CB barrier as the target of the study because the behaviors of CB materials are time-dependent, reactive, and still mysterious in many aspects. In order to study these self-curing barriers, the author believes that conventional batch testing for soils is not an appropriate tool because construction process (material mixing) and field conditions cannot be simulated. It is believed that column testing conducted on a massive porous specimen should provide more reliable parameters for the design. Thus, column testing has been chosen as the main tool of the research.

Explained in Chapter 3, the selected factors, which are believed to affect solute transport through CB barriers, are: (1) curing period, (2) seepage velocity, (3) concentration level, (4) particle size, (5) porosity, and (6) mix design. To deal with the third factor, the concept of "reference concentration" for column testing is newly introduced herein to reveal that varied transport parameters are obtained from column tests performed at different concentration levels. Next, because the parameter interpretation of column testing is not attractive, the author has simplified the interpretation of the test, and this method is called "instant column Peclet number". At this point, it is suggested that column testing be used to evaluate the transport parameters of CB barriers.

In order to design and/or analyze CB barriers with high confidence, shown in this research in Chapter 4 are a number of column experiments on CB mixtures permeated with chloride ions. Many trends of transport parameters under the six factors mentioned above are clarified. Thus, barrier designers and/or analyzers can realize what they ought to consider in the design of CB walls and how the behaviors of CB barriers under chemical attack look like. Main findings from the experiments are as follows. Adsorption, hydrodynamic dispersion, and tortuosity decrease when concentration goes up. Increased seepage diminishes adsorption, but augments hydrodynamic dispersion after a yielding seepage velocity. Longer curing periods lower all hydraulic conductivity, adsorption and hydrodynamic dispersion. The hydrodynamic curves of different porous media do not match one another, and also their normalized versions are not coincident. Chloride ions are bound by the formation of chloro-complexes including Friedel's salt.

The behaviors of CB barriers under the attack of other solute ions apart from the chloride ions might be similar to or different from this research; nevertheless, this dissertation aims to give a framework of solute transport through CB barriers as comprehensively as possible by considering many influencing factors.

After revealing the behaviors of CB barriers, Chapter 5 of the dissertation subsequently gives some practical design methods for a single-layer vertical barrier, based on conservative and economical cases. Design parameters should be obtained corresponding with field conditions (the six factors). Furthermore, examples of analyses using concentration-dependent parameters are also given, and the way to obtain such parameters is clearly explained.

CHAPTER 2
LITERATURE REVIEW

2.1 HISTORY OF SLURRY WALLS

Ressi di Cervia (1992) reported that the construction of slurry walls started in Italy in the 1940's and spread throughout the world in three decades. There is also evidence that some shallow slurry walls were built in California in the mid forties. In Italy, ICOS corporation of America first acquired patents on slurry wall construction in the late forties. The discovery of the technique stems from the use of bentonite mud during the drilling of piles. The observation that bentonite mud can stabilize the excavation led to extensive experiments on this underground structure. After the expiration of the original patents, a number of foundation companies began to develop equipments and techniques for the construction of slurry walls.

2.2 TYPES AND CURRENT USES OF SLURRY WALLS

According to Millet et al. (1992), two basic underground walls are constructed by slurry wall technique: (1) structural diaphragm walls, and (2) cutoff barrier walls. The structural diaphragm walls are the first applications of slurry wall construction. They work as retaining walls and/or foundation-bearing walls. On the other hand, the cutoff barrier walls are constructed to provide:

1. A barrier to seepage beneath dams and canals, seepage through dams and dikes, seepage from ponds and lakes, etc.
2. A barrier to water inflow into excavation areas.
3. A barrier to contaminant migration in groundwater.

The third use of the cutoff walls has been substantially increased in the last 20 years. The cutoff walls are often used to isolate polluted areas before remediation works are carried out. They are constructed by simultaneously excavating a trench and filling the trench with a supporting fluid (normally bentonite slurry), and thereafter backfilling the trench with a specified material. There are four basic types of slurry cutoff walls: (1) soil-bentonite or SB, (2) cement-bentonite or CB, (3) plastic concrete, and (4) concrete. Sometimes, special

additives such as fly ash, slag or silica gel are introduced in the backfill material to attain some desired properties [e.g., Jefferis (1997); Czurda and Haus (2002)]. A geomembrane can also be inserted into the trench to make a nearly impermeable slurry wall. SB and CB walls are the most typical types of slurry walls used to contain contaminated groundwater. Figure 2.1 gives an example of a cutoff wall placed into the ground to prevent contaminant transport in groundwater.

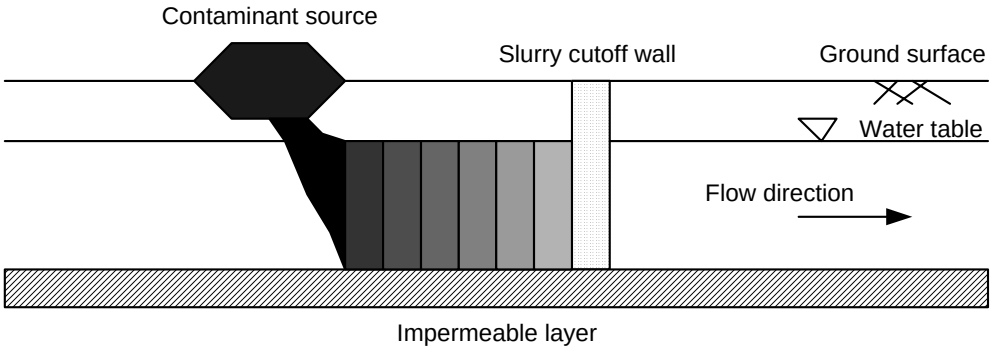

Figure 2.1 Application of a slurry cutoff wall to prevent contaminant transport.

2.3 CEMENT-BENTONITE (CB) WALLS

2.3.1 Construction

Cement-bentonite (CB) walls are mainly used in Europe. These self-hardening walls are constructed by excavating a trench and filling the trench with a supporting liquid prepared from water, bentonite and cement (Figure 2.2). The trench stabilizing slurry finally hardens in the trench and becomes the backfill material. The typical wall width is from 0.4 to 1.6 m, and the maximum wall depth could be down to 170 m (Brandl 1994). Slag is commonly incorporated in the backfill material to lower hydraulic conductivity of the hardened wall. Because the slurry and the backfill material are the same, the construction of CB walls appears simpler and faster. CB walls may be the cutoff wall of choice when the need for a material stronger than soil-bentonite (SB) is required.

The construction process of CB walls starts by pumping water from dewatering wells into a colloidal mixer. A desired amount of bentonite is then added to the mixer, and mixing continues to disperse the bentonite and produce a homogeneous suspension of bentonite slurry. The slurry is then allowed to hydrate for hours (normally 1 night). It is important to assure that the bentonite be fully hydrated with water prior to the addition of cement. With this procedure done, the final properties of CB walls will be mainly controlled by the hydration of cement with time.

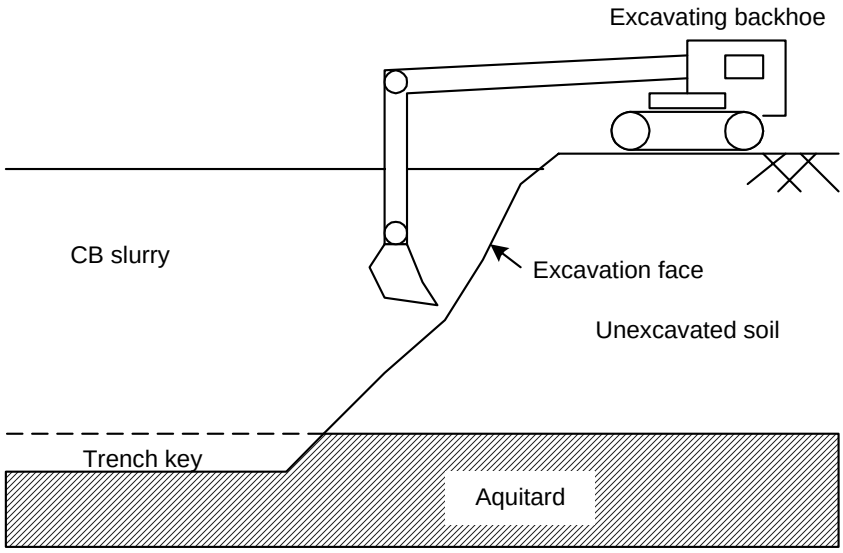

Figure 2.2 Construction of a CB wall using a backhoe.

Thereafter, the mixing is continued by adding cement to the prepared bentonite slurry. The resultant CB slurry is further mixed to obtain a homogeneous product with cement particles completely dispersed (but not fully hydrated). Lastly, the final CB slurry is then pumped to the trench where continuous excavation is being performed.

Mentioned above is the method which excavation is carried out following by backfilling. Furthermore, there is a recently-developed method called the trench cutting and re-mixing deep wall (TRD) which is considered highly cost-effective for constructing a vertical barrier. In this method, a trench is made while a solidifying agent (cement slurry) is injected into the trench; therefore, mixing of the solidifying liquid with in-situ loosened soil occurs in place. According to Kamon (1997), the TRD method has the following advantages:

1. The continuity of the wall is very high, and the permeability is very low.
2. The wall is homogeneous over the whole depth.
3. The digging capability of the TRD machine is high enough to be applied to gravel and cobble grounds.
4. The height of the machine is low, so the machine stability is high.

Figure 2.3 shows the schematic of the TRD method. More information on the TRD method can be referred to Kamon et al. (1998). Nevertheless, it should be noted that the order of material mixing in the TRD method is different from that of the conventional excavate-and-backfill method. In this research, laboratory material mixing is done in the same way as the conventional construction.

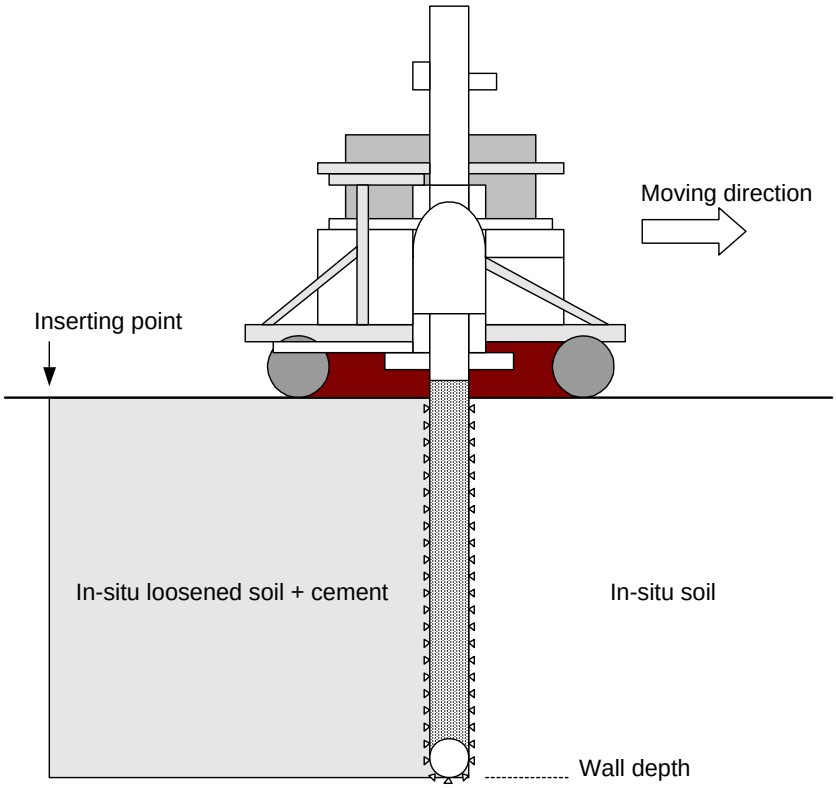

Figure 2.3 Schematic of TRD method.

2.3.2 Design Criteria

When slurry walls are used as structural elements, design criteria could be hydraulic conductivity (k), strength, modulus of elasticity, erosion resistance, and so forth. However, if they are utilized to retard contaminant transport in groundwater, the mentioned criteria are not enough. As in case of compacted clayey liners constructed in landfills, the design of slurry walls should deal with: (1) hydraulic conductivity, and (2) adsorption and hydrodynamic dispersion (or diffusion at low velocities).

For CB walls, hydraulic conductivity decreases with curing time due to cement hydration process. This reduction may continue for months or years, depending on the type of cement and pore fluid. The typical range of k values of CB mixtures varies between 10^{-5} to 10^{-7} cm/s. Lower k values can be occasionally obtained when the mixtures contain special additives. The hydraulic conductivity value at 28 days of curing is normally used as a design parameter. Fratalocchi and Pasqualini (1998) suggested that this design approach can be too conservative because the cement hydration rarely ceases at 28 days.

Hydraulic conductivity testing (ASTM D 5084) is always carried out to determine the reduction in k values as a function of curing time. There are a large number of literatures that provide information about CB hydraulic conductivity [e.g., Khera and Tirumala (1992);

Fratalocchi et al. (1996); Jefferis (1997); Fratalocchi and Pasqualini (1998); Bouazza et al. (1999)]. The conductivity test can also be used to study compatibility problems between contaminants and CB mixtures. Main concern is the possible increase in hydraulic conductivity under chemical leaching. Manassero et al. (2000) claimed that both low-k mixtures and high confining stress tend to reduce the sensitivity of the mixtures to chemical attack, at least in the short term. Jefferis (1992) and Tedd et al. (1993) showed that only strong acids and/or sulphates can cause problems for the CB mixtures in the long term. More information on compatibility problems is provided in Manassero et al. (1995), Jefferis (1996), and Garvin and Hayles (1999).

2.3.3 Limited Knowledge

Many of the researches concerning CB walls appear in the proceedings of international and local conferences. They mainly concentrate on the hydraulic conductivity of these self-hardening materials. Besides tap, distilled, and site water, chemical solutions or leachate have been used as permeants in hydraulic conductivity testing. Thus, the design aspect hydraulic conductivity has been considerably studied so far.

In contrast, comprehensive studies regarding adsorption and hydrodynamic dispersion have not been provided. Omission of adsorption can make the design too conservative, and diffusion or dispersion allows contaminants to breakthrough the walls faster than advection does alone. In fact, pure advection never occurs in field condition, especially at low seepage velocities where diffusion would rather dominate. Manassero et al. (2000) claimed that diffusion parameters are fully comparable with the same parameters from compacted clayey liners even though the total porosity of typical CB mixtures can be even 2 to 10 times greater. This quote needs further warranty.

Moreover, significant factors influencing the adsorption and hydrodynamic dispersion phenomena inside CB mixtures have not been discussed. For instance, the effects of curing period, concentration level, and porosity on adsorption and hydrodynamic dispersion are still mysterious. Other factors such as seepage velocity, particle size, and mix design are also likely to affect the two phenomena.

At this point, it can be realized that only the use of hydraulic conductivity in the design of CB walls is inadequate. As long as the understanding of CB behaviors is not clear, the design and analysis of CB walls cannot be done with full confidence. As a result, this research focuses on many aspects of solute transport through these time-dependent underground structures.

2.4 PRINCIPLES OF SOLUTE TRANSPORT IN POROUS MEDIA

2.4.1 Definition

Solution means a mixture of two or more substances in which the molecules or atoms of the substances are completely dispersed, solvent means a substance capable of dissolving or dispersing one or more other substances, and solute means a substance in a solution that is dissolved. In this context, solute transport means the migration of dissolved contaminants in saturated porous media. Since the dissolved contaminants are the most mobile and can affect a tremendous amount of groundwater, this research deals with the transport mechanisms of this class of contaminants. The transport mechanisms considered are advection, diffusion, dispersion and adsorption.

2.4.2 Macroscopic Equation

Considering the one-dimensional transient solute transport through a saturated homogeneous medium under steady-state flow, the most common partial differential equation accounting advection, hydrodynamic dispersion and adsorption can be written as [e.g., van Genuchten and Alves (1982)]:

$$R_d \frac{\partial C_r}{\partial t} = D \frac{\partial^2 C_r}{\partial x^2} - v \frac{\partial C_r}{\partial x} \tag{2.1}$$

where C_r = resident (volume-averaged) solute concentration; R_d = retardation factor; D = diffusion-dispersion (or hydrodynamic dispersion) coefficient; v = seepage velocity; x = distance; and t = time. The retardation factor R_d accounts for linear and reversible equilibrium adsorption.

2.4.3 Advection

Advective transport or advection involves the movement of solutes with flowing pore water. Advection is driven by hydraulic gradient (i). The average rate of transport is equal to the seepage velocity v which can be calculated by dividing Darcy velocity (ki) by porosity. The actual transport velocity within pore space remains subtle. Pore water in fact moves at velocities both greater and less than the average velocity. Normally the movement along the center of the pores is faster than at the boundary.

In highly permeable media such as sand and gravel, advection is the most significant transport process. Hydraulic conductivity is the most important factor controlling advection.

2.4.4 Hydrodynamic Dispersion

Hydrodynamic dispersion coefficient D is a combination of effective molecular diffusion D^* and mechanical dispersion D_{md} coefficients. It is simply formulated as follows (Freeze and Cherry 1979):

$$D = D^* + D_{md} \tag{2.2}$$

For the movement of contaminants through porous media at relatively low velocities, the hydrodynamic dispersion coefficient D is reduced to the effective molecular diffusion coefficient (i.e. $D \approx D^*$). When seepage velocity exceeds the yielding velocity of material, D coefficient will increase as a function of velocity. The effect of velocity on mixing is quantified by mechanical dispersion coefficient D_{md}.

2.4.5 Diffusion

Diffusion in this context is the migration of solutes in water from a region of higher to a region of lower concentration. Diffusion can occur in the absence of any bulk water movement. The driving force is the random movement of molecules and ions under the influence of their kinetic activity called Brownian motion.

Maximum rates of migration by diffusion occur in free water at infinite dilution. Diffusion in free solution depends on free solution diffusion coefficient D_o and concentration gradient. Typical values for D_o [Li and Gregory (1974); Lerman (1979); Shackelford and Daniel (1991)] are listed in Table 2.1 for several species of cations and anions that are normally encountered. These values would represent the maximum values measurable in any laboratory or field condition. It can be noticed that most D_o values vary from 0.6×10^{-5} to 2×10^{-5} cm^2/s at 25°C. Shackelford (1989) showed that concentration level has slight effect on the D_o coefficient. Free solution coefficients are also found to increase linearly with temperature (Rowe et al. 1995b). For example, the D_o of chloride ions is reduced from 20.3×10^{-6} cm^2/s at 25°C to about 10×10^{-6} cm^2/s at 0°C.

Diffusion in soil is more complicated than in free solution. This involves the diffusive movement of the species of interest in the pore water between soil particles. According to Mitchell (1993), several reasons for this complication are listed as follows:

1. The pathways for migration are more tortuous in soil.
2. The cross-sectional area of flow is reduced because of solid particles in soil.

Table 2.1 Free solution diffusion coefficients for representative ions at infinite dilution in water at 25°C [Li and Gregory (1974); Lerman (1979); Shackelford and Daniel (1991)]

Anion	D_o x 10^{-6} cm^2/s	Cation	D_o x 10^{-6} cm^2/s
OH^-	52.7 (high)	H^+	93.1 (high)
F^-	14.6	Li^+	10.3
Cl^-	20.3	Na^+	13.3
Br^-	20.8	K^+	19.6
I^-	20.4	Rb^+	20.6
HS^-	17.3	Cs^+	20.7
HCO_3^-	11.8	NH_4^+	19.8
NO_2^-	19.1	Be^{2+}	5.98
NO_3^-	19.0	Mg^{2+}	7.05
SO_4^{2-}	10.7	Ca^{2+}	7.93
CO_3^{2-}	9.55	Sr^{2+}	7.94
CrO_4^{2-}	11.2	Ba^{2+}	8.48
--	--	Pb^{2+}	9.45
--	--	Ra^{2+}	8.89
--	--	Mn^{2+}	6.88
--	--	Cu^{2+}	7.33
--	--	Fe^{2+}	7.19
--	--	Cd^{2+}	7.17
--	--	Zn^{2+}	7.15
--	--	Ni^{2+}	6.79
--	--	Fe^{3+}	6.07
--	--	Cr^{3+}	5.94
--	--	Al^{3+}	5.95

3. The electrical fields of the solid particles may affect the pathways of a diffusing chemical species.
4. Retardation of some chemical species may occur as a result of ion exchange and adsorption with host material.

To consider the effect of soil on the diffusion of chemical species, the effective molecular diffusion coefficient D^* is often used. There is a wide variation in the definition of D^* coefficient, yet Shackelford and Daniel (1991) proposed a practical definition as follows:

$$D^* = \tau_a D_o \tag{2.3}$$

where τ_a = apparent tortuosity factor. This parameter not only includes the actual geometric tortuosity but also all other inherent factors such as solute-solute and solute-solvent interactions. At present, tortuosity factors cannot be measured independently. They are calculated after knowing the D^* coefficient. Mitchell (1991) suggested that the values of D^* of most chemical species are in the range of ~ 2 x 10^{-6} cm^2/s to ~ 2 x 10^{-5} cm^2/s. Because most D_o values vary from 0.6 x 10^{-5} to 2 x 10^{-5} cm^2/s (Table 2.1), it would suggest that the minimum τ_a value could be as low as 0.1 or sometimes lower. An approximate τ_a for sands may be taken as 0.67 or 2/3, supported by previous literatures. This value is based only on the geometric tortuosity. Although it may not be a bad approximation for sands, the tortuosity factors for clayey soils are often lower due to the effects of viscosity and electrostatic interaction.

2.4.6 Mechanical Dispersion

When contaminant migration is associated with relatively high velocities as in many aquifers, there occurs mixing due to local variations in the flow velocity of water. This mechanism is called mechanical dispersion D_{md}. Although it is totally different from the diffusion process D^*, the two processes are often lumped together as a composite parameter D as previously shown in Equation (2.2). It is convenient to model the mechanical dispersion as a linear function of seepage velocity (Scheiddegger 1954):

$$D_{md} = \alpha\, v \tag{2.4}$$

where α = dispersivity. Hence, Equation (2.2) can be rewritten as:

$$D = D^* + \alpha\, v \tag{2.5}$$

Provided that there are enough (v, D) data points and most of them have D values greater than the typical D^* range, it is possible to determine average α and D^* values by linear regression as shown in Figure 2.4 (left). However, the scatter of data in v-D plot is normally large, so a better alternative is plotting log v-log D as depicted in the same figure. Figure 2.4 (right) will be called hydrodynamic curve from now on.

Perkins and Johnston (1963) conducted tests on homogeneous sands and proposed an empirical equation as follows:

$$D = D^* + 1.75 d_{avg} v \qquad (2.6)$$

where d_{avg} = average grain size of the porous medium. The multiplier $1.75 d_{avg}$ can be realized as α for the sands in their tests.

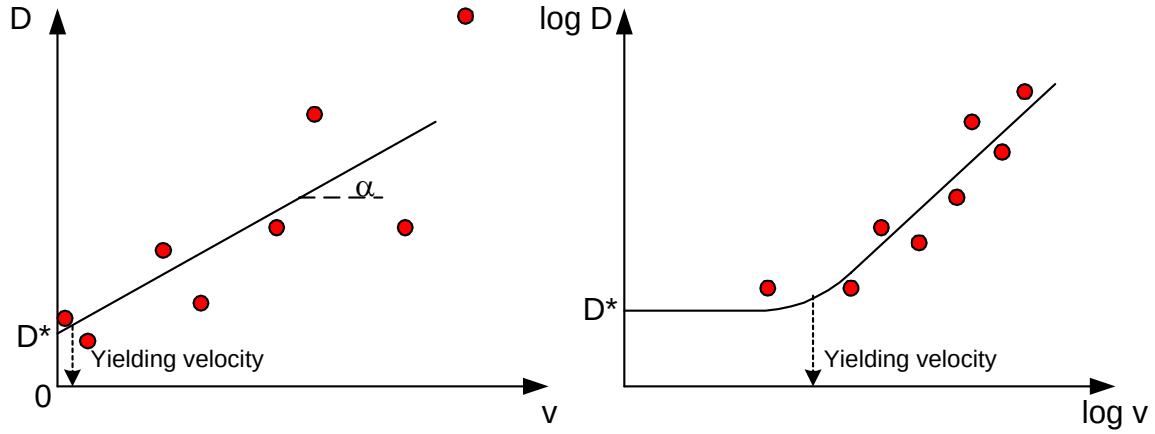

Figure 2.4 Hydrodynamic dispersion coefficient as a function of seepage velocity (not true scale).

By using $\tau_a = 0.67$ and $D_o = 1.5 \times 10^{-5}$ cm^2/s, an average D^* for sands is determined as 1×10^{-5} cm^2/s. If d_{avg} for sands is taken as 0.02 cm, Equation (2.6) becomes:

$$D = 10^{-5} + 0.035v \qquad (2.7)$$

Equation (2.7) may give a good approximation for sands, but the application of Equation (2.6) or (2.7) to silty and clayey soils cannot be warranted. The use of Equation (2.6) for clayey soils can be found in Rowe et al. (1995b) and Reddi and Inyang (2000). Manassero et al. (1997) gave the hydrodynamic curve of Barricalla clay permeated with sodium (Na), potassium (K), and Bromine (Br). The clayey curve and Equation (2.7) are plotted together in Figure 2.5. The two materials do not match each other and have different yielding velocities. For Barricalla clay, Manassero et al. suggested that the yielding velocity is 4×10^{-6} cm/s. The fitting curve of the clay does not have a transition zone between diffusion and mechanical dispersion because the two components are considered separately. The yielding velocity of sands is about 3×10^{-4} cm/s. Figure 2.5 suggests that the hydrodynamic curves of different porous media are not coincident, and Equation (2.6) or (2.7) not be used for other media but sands.

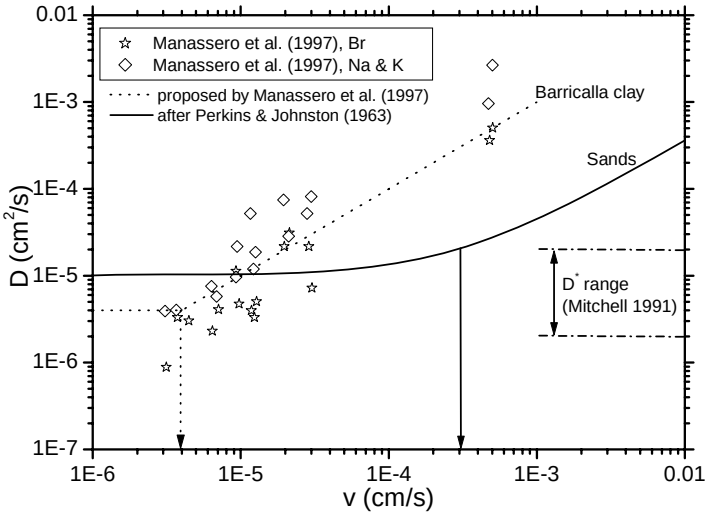

Figure 2.5 Hydrodynamic curves of sands and Barricalla clay.

Normalized or dimensionless hydrodynamic curves are introduced in many literatures [e.g., Perkins and Johnston (1963); Bear (1972); Spitz and Moreno (1996); Yu et al. (1999)]. Normalization is done by dividing D by D_o and multiplying v by d_{avg}/D_o, with corresponding units. The d_{avg} is normally taken as d_{50}. The d_{50} is grain size at 50% finer. The product vd_{avg}/D_o is called Peclet number and symbolized as P here to make no confusion with column Peclet number P_e which will be mentioned later. Figure 2.6 shows the normalized version of sand data.

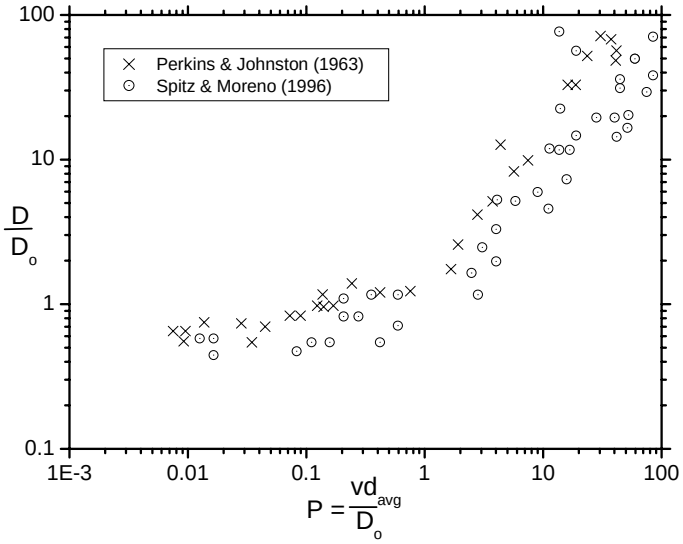

Figure 2.6 Normalized hydrodynamic curve of sandy media.

The data is directly obtained from Perkins and Johnston (1963), and Spitz and Moreno (1996). For the sand normalized hydrodynamic curve, data from Perkins and Johnston seems

to provide upper-bound values, and lower-bound values come from Spitz and Moreno (1996). It is noted that Spitz and Moreno combined data from a number of researches on granular media. Figure 2.6 shows that mechanical dispersion starts prevailing at Peclet number approximately equal to 1. From Equation (2.3), it can be realized that τ_a values of sandy media vary in a narrow range between 0.4 and 1.0. Thus, the average τ_a of 0.67 previously mentioned seems rational. Whether Figure 2.6 can be applied to other media apart from sands or not will be discussed in Chapter 4.

2.4.7 Adsorption

Sorption is a dominant process affecting almost all dissolved species in groundwater. It is the process describing the removal of contaminants from solution. Sorption is a term used to embrace all the processes responsible for the removal: absorption, adsorption, precipitation and ion exchange. Absorption is the process whereby the contaminants are incorporated into the interior of the solid phase. Adsorption is the attraction of the contaminants onto the solid surface. Precipitation is the phenomenon in which the dissolved species in solution are transformed into a solid phase. And, ion exchange is the process in which ions are exchanged between a solution and the solid phase. These phenomena are usually intermingled and interchangeable; however, the important aspect is the removal of the solute from solution. The term adsorption is used in place of sorption in many literatures regarding clayey barriers, and it will be used throughout this research. The process by which a contaminant, originally in solution, becomes distributed between the solution and the solid phase is called partitioning or distribution. As a result of adsorption, reactive solutes (adsorbate) will move more slowly than the groundwater that is transporting them; this effect is called retardation.

Retardation factor R_d in Equation (2.1) typically is determined in the laboratory from the results of column tests or batch equilibrium tests. In most cases, the adsorption of a given solute is often characterized using an adsorption isotherm. The isotherm allows partitioning of the solute between the solid and liquid phases. It is generally obtained by performing the batch testing.

2.4.8 Effective Porosity

In some soils, some of the fluid in the pore space may be immobile due to dead-end pores and/or attraction of fluid molecules to the surface of soil particles (Bear 1972). As a result, the portion of the pore space available for solute transport could be significantly less than the

total pore space. In such cases, an effective porosity n_e should be used instead of the total porosity n to determine the seepage velocity v. Effective porosities on the order of 2 – 100% of the total porosity have been measured in compacted soils [Horton et al. (1985); Liao and Daniel (1989)]. Rowe et al. (1995b) claimed that the effective porosity, with respect to diffusion through saturated clayey barriers of low activity clays is often reasonably estimated on the basis of water content; that is, the effective porosity is essentially the same as the total porosity.

2.4.9 Resident and Flux Concentrations

Equation (2.1) is written in terms of the volume-averaged or resident concentration C_r which is the mass of solute per unit volume of fluid contained in an elementary volume of the system at a given distance. On the other hand, a second type of concentration, known as a flux-averaged or flowing concentration has been defined as the mass of solute passing through a given cross section (i.e., solute mass flux) per unit volume of fluid during an elementary time interval [Kreft and Zuber (1978); van Genuchten and Parker (1984)]. The difference in the definitions will become significant in the study of solute transport by column testing.

2.5 STUDIES ON ADSORPTION AND HYDRODYNAMIC DISPERSION

2.5.1 Batch Testing

Batch testing is used to study the adsorption of a solute. Adsorption is determined by measuring how much of the solute can be adsorbed by a particular material (e.g., clayey soil). The procedure for batch testing consists of mixing (agitating) a known amount of soil and chemical solution in a predetermined mixing ratio for a specified period (normally 24 hours) and at a constant temperature (usually 25° C). The total concentration of the chemical species of interest in the solution is measured before the solution is added to the soil, and the equilibrium concentration is measured after the agitation is completed. The same procedure is repeated several times with different initial concentrations of the solute. The results from the tests are plotted as an adsorption isotherm, or adsorbed concentration q versus equilibrium concentration. The adsorbed concentrations are determined using the following equation:

$$q=\frac{(\text{initial concentration} - \text{equilibrium concentration})\,\text{volume of solution}}{\text{soil mass}} \qquad (2.8)$$

The equilibrium concentration is in fact the resident concentration C_r. In general, adsorption isotherms can be linear, concave nonlinear, or convex nonlinear. Nonlinear adsorption isotherms for soils typically are of the concave type. Linear adsorption is considered as a reasonable approximation for low concentrations of contaminant. The linear model is written as:

$$q = KC_r \tag{2.9}$$

where K = partitioning or distribution coefficient. At high concentrations, adsorption becomes nonlinear, and Freundlich or Langmuir models are generally used because any nonlinear experimental data can be transformed into a linear line. By applying linear regression technique, one can easily determine curve-fitting parameters by reading the slope and intercept of that linear line. Freundlich model can be written as:

$$q = KC_r^{\varepsilon} \tag{2.10}$$

where ε = empirically determined constant. Clearly, Freundlich model represents the power equation, and it reduces to Equation (2.9) for ε = 1. Figure 2.7 shows the shapes of Equations (2.9) and (2.10) together with the transformed plot used to determine parameters.

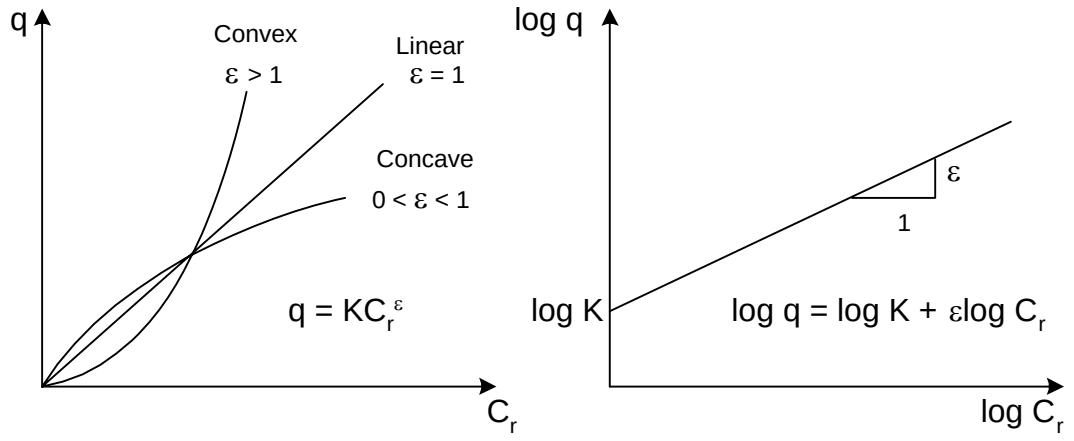

Figure 2.7 Linear and Freundlich adsorption isotherms.

It should be noted that the transformation may not yield good results as compared to direct nonlinear regression. The direct nonlinear regression of the power equation is available in most curve-fitting softwares, so the transformation is unnecessary. The Langmuir isotherm is not described here because it is not always adequate for describing

adsorption processes. The details of Langmuir model can be found in Rowe et al. (1995b) or Fetter (1999).

From the adsorption isotherm, the value of retardation factor R_d can be determined using the relationship:

$$R_d = 1 + \frac{\rho_d}{n}\frac{dq}{dC_r} \tag{2.11}$$

where ρ_d = dry bulk density of the soil. The differential term is the partitioning function which is the change in the adsorbed concentration relative to a change in the equilibrium concentration. This term represents the tangential slope of the adsorption isotherm evaluated at a specific equilibrium concentration. In case of Freundlich model, Equation (2.11) becomes:

$$R_d = 1 + \frac{\rho_d}{n} K \varepsilon C_r^{\varepsilon - 1} \tag{2.12}$$

In many cases, the partitioning function is based on the use of secant lines instead of tangent lines (e.g., in POLLUTE software). The secant line approach is illustrated in Figure 2.8. The retardation factor for Freundlich model is then determined by:

$$R_d = 1 + \frac{\rho_d}{n} K C_r^{\varepsilon - 1} \tag{2.13}$$

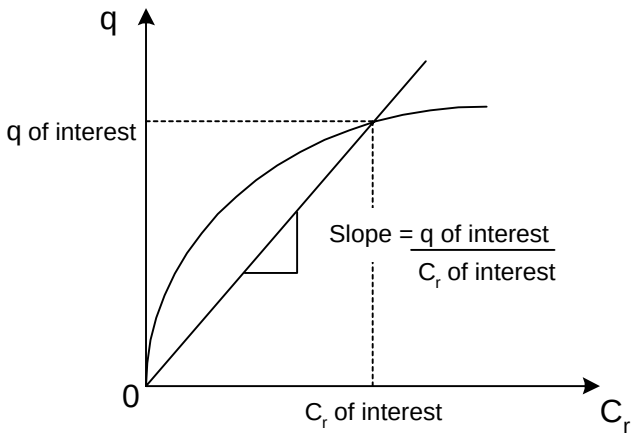

Figure 2.8 Secant formulation for a concave isotherm.

Solid-to-solution ratio is another important factor which influences the degree of adsorption. A 1:4 solid-to-solution ratio (by weight) is recommended by Roy et al. (1991) for batch testing conducted on soils. However, this ratio is equivalent to a water content w_c of 400% which is much higher than the values for natural soils or compacted clays (e.g., $w_c \approx$ 25%). Normally, the more the water content, the higher the adsorption becomes. As an alternative to solve this problem, Manassero et al. (1998) carried out many series of batch testing with various solid-to-solution ratios up to about 1:1 ($w_c \approx 90\%$) and fitted every adsorption data with nonlinear models. It was suggested that an adsorption isotherm at field condition may be obtained by plotting curve-fitting parameters versus solid-to-solution ratios and using extrapolation to the field water content. This approach is shown in Figure 2.9.

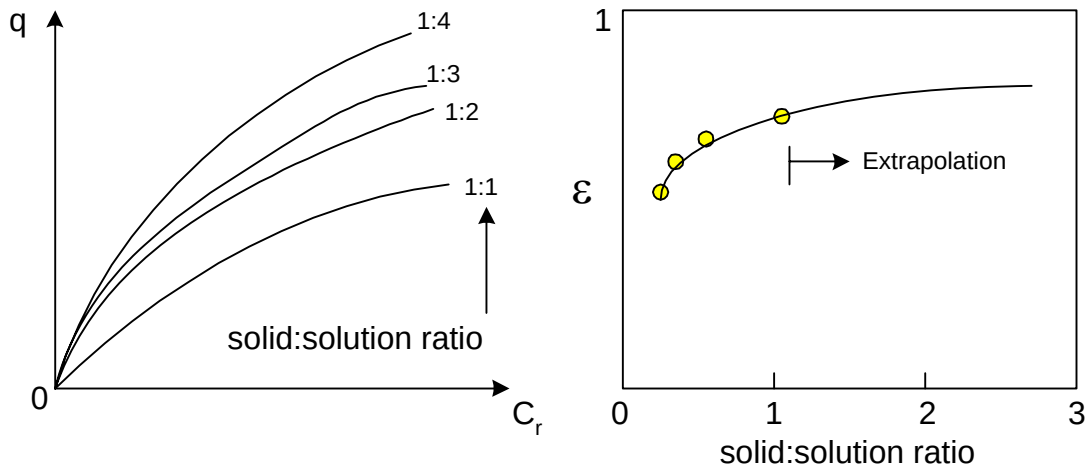

Figure 2.9 Influence of solid:solution ratio on adsorption together with extrapolation technique.

Nevertheless, the question that shaking condition in batch testing really simulates field condition has not been resolved yet. Due to the difficulty in the interpretation of batch testing, pure diffusion and column tests, which are conducted on massive specimens, would preferably provide better choices.

2.5.2 Pure Diffusion Testing

Pure diffusion testing is used to evaluate adsorption and diffusion parameters simultaneously. The test is conducted at zero seepage velocity, so advection is eliminated. The primary objective of the diffusion test is to allow the measurement of D^* and K in Equation (2.9). There are two possible kinds of diffusion testing as shown in Figure 2.10 (Rowe et al. 1988).

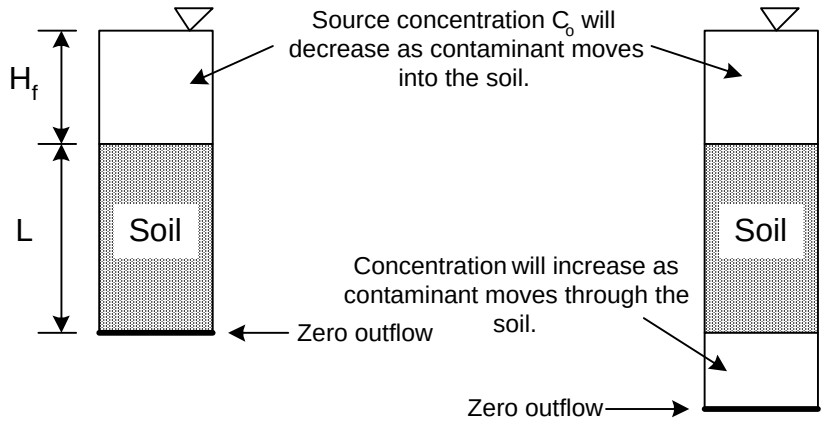

Figure 2.10 Schemes of pure diffusion testing with a finite mass of contaminant source.

Contaminant is allowed to transport from the source reservoir through the soil and, if available, into the collector reservoir (Figure 2.10, right). If no additional contaminant is added to the source reservoir, then the source concentration will decrease with time as contaminant mass diffuses into the soil. The rate of decrease can be controlled by the selection of the height of solution H_f. In the collector reservoir, concentration will increase as contaminant moves through the soil. The rate of decrease in source concentration and increase in collector concentration can be monitored with time. At the end of the test, it is possible to extract pore water at different distances of the sample and determine the concentration profile through the soil sample.

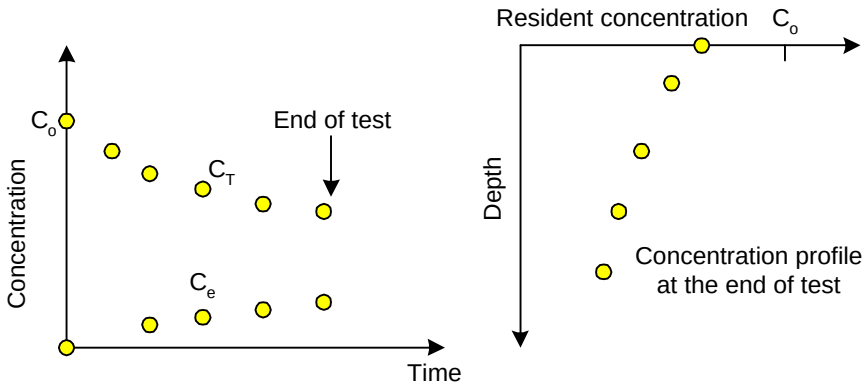

Figure 2.11 Measurement of source and exit concentrations and concentration profile.

Figure 2.11 shows three basic experimental curves from diffusion testing. There may be difficulties in obtaining meaningful concentration profile through the sample due to losses which occur when squeezing the pore water from the sample slices. Thus, it is often necessary to rely on the source and collector concentrations. Figure 2.10 (left) is the easiest

diffusion test which can be performed very quickly, and it is thus used in this research. In diffusion testing, seepage is nil, so Equation (2.1) is reduced to:

$$\left(1+\frac{\rho_d K}{n}\right)\frac{\partial C_r}{\partial t} = D^* \frac{\partial^2 C_r}{\partial x^2} \tag{2.14}$$

Equation (2.14) assumes that adsorption is linear [Equations (2.9) and (2.11)]. By fitting theoretical curves to the observed variation in concentration in the source reservoir and/or the concentration profile, it is then possible to determine the values of D^* and K for the soil and chemical species being considered.

Assuming that the concentration drop in the source reservoir is due only to diffusion through the soil specimen, the boundary condition representing the solute concentration in the source reservoir at any time t, C_T, can be written as (Rowe and Booker 1985):

$$C_T(t) = C_o - \frac{1}{H_f}\int_0^t f_T(t)dt \tag{2.15}$$

where $f_T(t)$ = mass flux of the contaminant into the soil at time t. This diffusive mass flux across the source-sample interface can be related to the solute's concentration gradient across the interface by Fick's first law:

$$f_T(t) = -nD^*\left(\frac{\partial C_r}{\partial x}\right)_T \tag{2.16}$$

For this flux-controlled boundary condition, a semi-analytical solution to Equation (2.14) has been implemented in the computer program POLLUTE (Rowe et al. 1998). This approach permits accurate calculation of concentration in only a few seconds on a microcomputer, so it is well suited for the interpretation of the results of diffusion testing.

The above explanation is for the determination of D^* and K from simple diffusion testing by assuming that adsorption is linear. For real analyses or predictions of practical problems, adsorption can be modeled in POLLUTE as a function of the concentration of contaminant by using an adsorption isotherm obtained from batch testing. The program uses the secant approach in Equation (2.13).

2.5.3 Column Testing

Column testing is conducted at nonzero seepage velocity, and can be used to evaluate adsorption R_d and hydrodynamic dispersion D parameters at the same time. The main advantage is its possibility to simulate field conditions as realistically as possible. Important field conditions that can be simulated are water content, effective stress, and seepage velocity. If seepage is low enough, the hydrodynamic dispersion coefficient D will represent D^* in the typical range of ~ 2 x 10^{-6} cm^2/s to ~ 2 x 10^{-5} cm^2/s (Mitchell 1991). When a calculated D value is more than 2 x 10^{-5} cm^2/s, it is likely to have mechanical dispersion occurring in the test column. The degree of adsorption is also affected by the seepage v.

The parameters R_d and D can be obtained by fitting an analytical solution to concentration data, usually a series of effluent concentrations C_e. Figure 2.12 shows the schematic diagram of flexible-wall column testing performed at a constant seepage v.

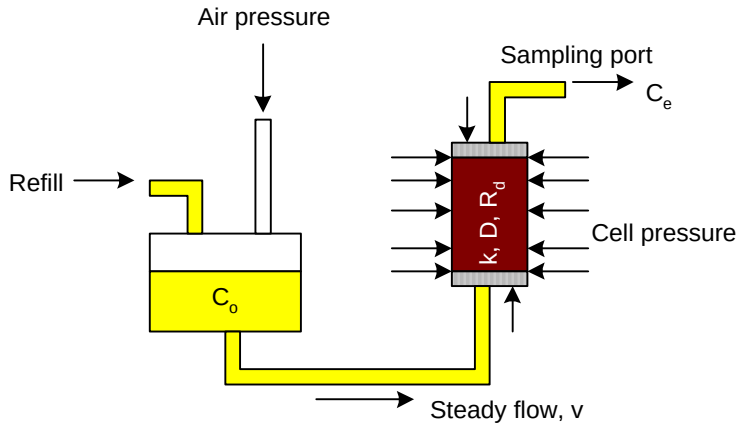

Figure 2.12 Flexible-wall column testing.

The analytical solution is normally dependent on the assumption of constant transport parameters; consequently, the results from column testing may just yield average transport parameters of a solute along a flow path under an induced seepage velocity. When analyzing various sections of a tested column, different distances from the source concentration C_o tend to have varied adsorption and diffusion parameters [Yong et al. (1992); Achari et al. (1997)]. However, the determination of resident concentrations inside the sample is not a simple matter, and is always discouraged. The interpretation of column testing thus relies on C_e.

In fact, there are many analytical solutions which can be used to interpret the results from column testing. In the next section, only two practical solutions have been selected for this research.

2.6 SOLUTE TRANSPORT IN COLUMN TESTING

2.6.1 Breakthrough Curve

In laboratory column testing, flux-type boundary condition introduced by Danckwerts (1953) has been used to conserve mass across the inlet boundary, and is expressed as:

$$(-D\frac{\partial C_r}{\partial x} + vC_r)\Big|_{x=0^+} = vC_o\big|_{x=0^-} \tag{2.17}$$

Because Equation (2.17) leads to zero mass entering the column when seepage velocity is equal to zero, it is only applied to advection-input laboratory testing. The advection-input testing using Equation (2.17) requires that dispersion in the source reservoir is negligible. This can be true by separating the source reservoir and the test column by using a very thin and rather long connecting line (Shackelford and Rowe 1998) such as triaxial system (see Figure 2.13).

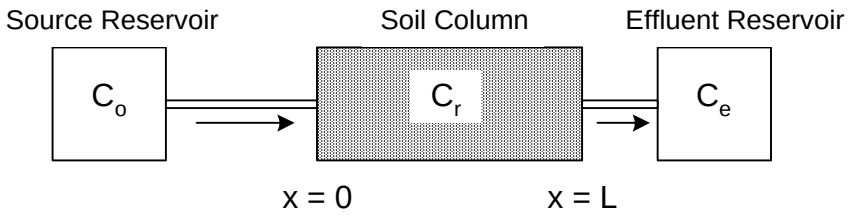

Figure 2.13 Components of column testing.

The initial condition and another boundary condition are Equations (2.18) and (2.19), respectively:

$$C_r(x,0) = 0 \tag{2.18}$$

$$\frac{\partial C_r(\infty,t)}{\partial x} = 0 \tag{2.19}$$

The analytical solution to Equations (2.1), (2.18), (2.17), and (2.19) is referred to Lindstrom et al. (1967) as follows:

$$\frac{C_r(x,t)}{C_o} = \frac{1}{2}\left[\begin{array}{l} \operatorname{erfc}\left(\frac{R_d x - vt}{2\sqrt{DR_d t}}\right) + 2\sqrt{\frac{v^2 t}{\pi DR_d}}.\exp\left(-\frac{(R_d x - vt)^2}{4DR_d t}\right) \\ -\left(1 + \frac{vx}{D} + \frac{v^2 t}{DR_d}\right).\exp\left(\frac{vx}{D}\right)\operatorname{erfc}\left(\frac{R_d x + vt}{2\sqrt{DR_d t}}\right) \end{array}\right] \tag{2.20}$$

where erfc(z) = complementary error function = $1-\frac{2}{\sqrt{\pi}}\sum_{m=0}^{\infty}\frac{(-1)^m z^{2m+1}}{m!(2m+1)}$

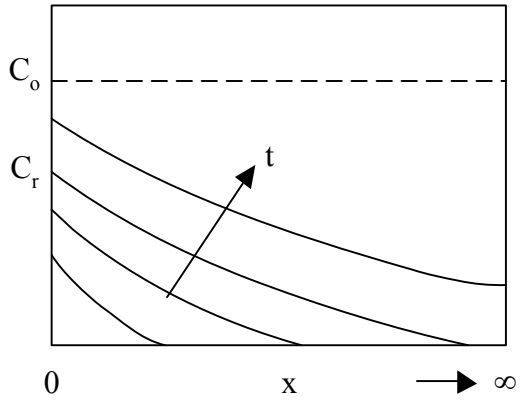

Figure 2.14 Transient resident concentration distributions in semi-infinite domain by Equation (2.20).

Figure 2.14 shows the concentration distributions generated by Equation (2.20). It is seen that concentrations across the inlet boundary are macroscopically discontinuous. When time approaches infinity, the resident concentration inside the column will be equal to C_o (dash line). Equation (2.20) can be used to find R_d and D parameters provided that resident concentration distribution at any time t is known. Nevertheless, this method is not practical, and more attention is paid to the effluent or exit concentration C_e.

Because the column effluent data C_e does not represent resident concentrations, but rather flux-averaged concentrations which mean the mass of solute per unit volume of fluid passing through a given cross-section during a time interval (Kreft and Zuber 1978), transformation is necessary to obtain an equation for effluent concentration (van Genuchten and Parker 1984). The transformation of Equation (2.20) leads to Equation (2.21):

$$\frac{C_e(L,t)}{C_o}=\frac{1}{2}\left[\operatorname{erfc}\left(\frac{R_d L-vt}{2\sqrt{DR_d t}}\right)+\exp\left(\frac{vL}{D}\right)\operatorname{erfc}\left(\frac{R_d L+vt}{2\sqrt{DR_d t}}\right)\right] \tag{2.21}$$

To easily analyze the column effluent data, a dimensionless form of Equation (2.21) can be written as:

$$\frac{C_e}{C_o}=\frac{1}{2}\left[\operatorname{erfc}\left(\frac{R_d-T}{2\sqrt{\frac{R_d T}{P_e}}}\right)+\exp(P_e)\operatorname{erfc}\left(\frac{R_d+T}{2\sqrt{\frac{R_d T}{P_e}}}\right)\right] \tag{2.22}$$

where C_e/C_o = dependent variable; T = independent variable = pore volumes of flow = vt/L; R_d and P_e are coefficients to be determined. After knowing P_e, D then can be calculated, for P_e = column Peclet number = vL/D. The number of pore volumes of flow is the cumulative volume of fluid collected in the effluent from the beginning of the test divided by one pore volume of the column V_v. van Genuchten and Parker (1984) recommended that Equation (2.22) be used to capture effluent breakthrough curves from finite columns on the bases of mass conservation and easy utilization.

In case the test column has initial or background concentration $C_r(x,0) = C_i$, the left hand side of Equation (2.22) can be replaced with:

$$\frac{C_e}{C_o} \rightarrow \frac{C_e - C_i}{C_o - C_i} \tag{2.23}$$

Normally, the parameters R_d and P_e are best calculated by nonlinear regression. Without regression analysis, retardation factor R_d can also be obtained by 2 methods in case of breakthrough curve. Figure 2.15 shows the theoretical curves of Equation (2.22).

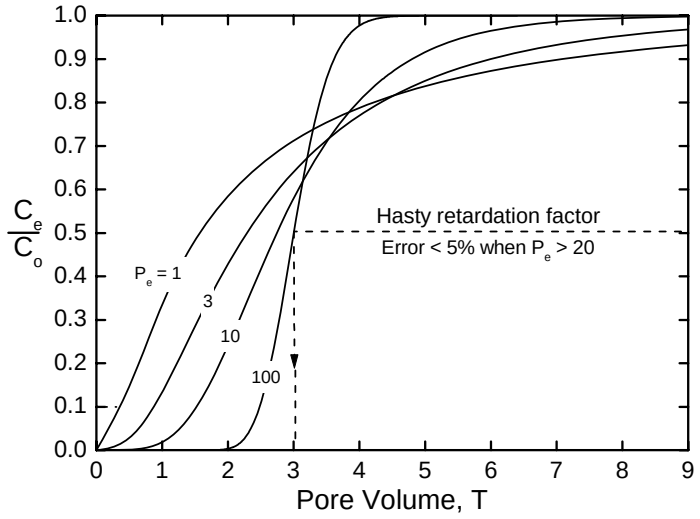

Figure 2.15 Effluent breakthrough curves with $R_d = 3$.

All the four curves in Figure 2.15 have the same retardation factor, valuing 3. Because of the difference in column Peclet numbers, the shapes of the curves become different. At high column Peclet numbers (e.g., more than 20), retardation factor can be obtained at $C_e/C_o = 0.5$ (Freeze and Cherry 1979) with little error. However, this method is not applicable at low column Peclet numbers; moreover, whether column Peclet number is more than 20 or not cannot be judged easily by eyes.

Retardation factor for any column Peclet numbers can be calculated more correctly by the integration of the area above a breakthrough curve from T = 0 to steady-state transport (van Genuchten and Parker 1984).

The remarkable advantage of plotting a breakthrough curve is that it is easy to trace the solute transport inside the test column by eyes. For example, in order to do the regression analysis to find R_d and P_e, the test should be carried out until C_e is equal to $0.7C_o$ or more. The best way is to perform the test until steady-state transport is reached ($C_e = C_o$).

2.6.2 Cumulative Mass Approach

Shackelford (1995) proposed an alternative approach for column testing by considering the cumulative amount of solute mass that enters the effluent reservoir. Firstly, incremental mass ratio (IMR) is determined for each effluent sample:

$$IMR = \frac{C_e}{C_o}\Delta T \tag{2.24}$$

where ΔT = sample volume/V_v. Then, cumulative mass ratio (CMR) is calculated from:

$$CMR = \sum_{i=1}^{m} IMR_i \tag{2.25}$$

where m = the total number of effluent samples collected during the elapsed time t. An analytical model for cumulative mass approach corresponding to Equation (2.22) is:

$$CMR = \frac{R_d}{2P_e}\left[\left(\frac{TP_e}{R_d} - P_e\right)\text{erfc}\left(\frac{R_d - T}{2\sqrt{\frac{TR_d}{P_e}}}\right) + \left(\frac{TP_e}{R_d} + P_e\right)\exp(P_e)\,\text{erfc}\left(\frac{R_d + T}{2\sqrt{\frac{TR_d}{P_e}}}\right)\right] \tag{2.26}$$

As suggested by Shackelford (1995), cumulative mass approach removes the influence of increment in effluent sample volume on the measured concentrations, and effluent sampling is less labor-intensive. Thus, Equation (2.26) is used in regression analyses to determine the parameters R_d and P_e for all the column tests in this research. The regression analyses are carried out with MATHEMATICA.

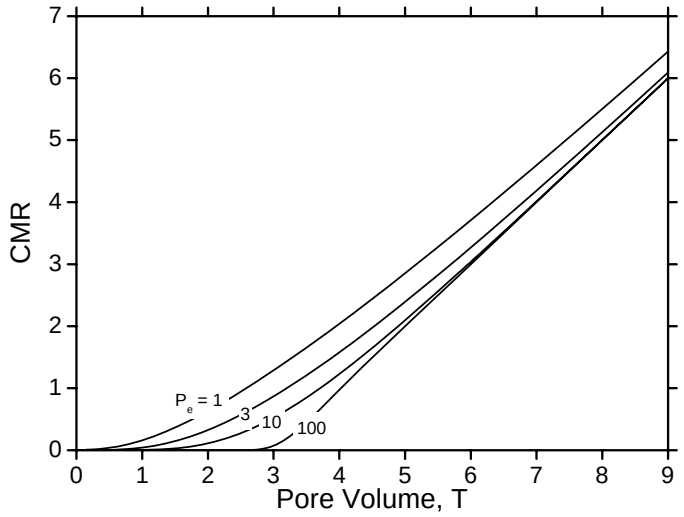

Figure 2.16 CMR curves with R_d = 3.

Figure 2.16 is generated by Equation (2.26) by fixing R_d = 3 and varying P_e. Providing that steady-state transport has been reached, it is possible to find retardation factor by drawing a tangent line from the steady-state transport to x-axis. From Figure 2.16, with T from 0 to 9, only the curves 10 and 100 have reached the steady-state transport. It will take a longer time for low-P_e curves to reach the same condition, so the assessment of retardation factor using the cumulative mass approach may require long durations under low flow rates (leading to low P_e values) since the procedure is based on achieving steady-state transport condition. Besides Figure 2.16, a better plot is (T, T-CMR) as shown in Figure 2.17.

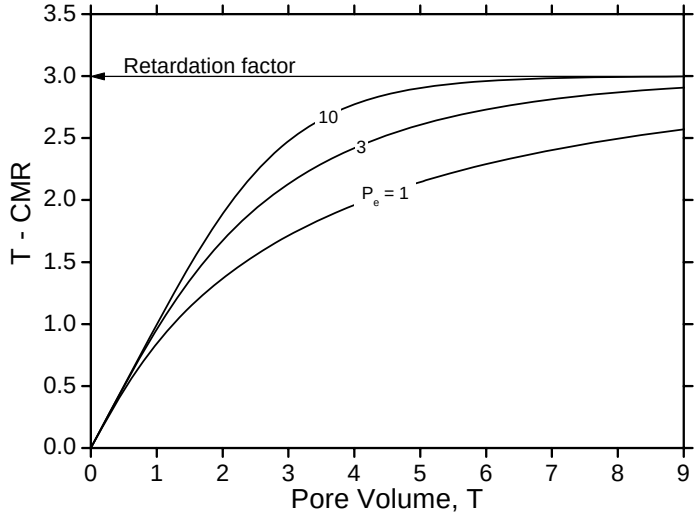

Figure 2.17 T – CMR method in cumulative mass approach.

It should be emphasized that Equations (2.22) and (2.26) theoretically yield the same regressed parameters. However, cumulative mass approach is preferable as discussed above.

2.6.3 Column Peclet Number

In Equations (2.22) and (2.26), there is an important dimensionless parameter called column Peclet number P_e. This parameter is different from Peclet number P in Section 2.4.6. It may be useful to rewrite the definition of P_e here.

$$P_e = \frac{vL}{D} \tag{2.27}$$

Column Peclet number represents the relative contribution of advective transport based on the seepage velocity v to the hydrodynamic dispersive transport based on the value of D. At high column Peclet numbers, advection dominates the solute transport whereas diffusion dominates the transport at low column Peclet numbers. Because v and L are known parameters, the D parameter can be calculated after knowing P_e. If the calculated D value is less than 2 x 10^{-5} cm^2/s (Mitchell 1991), it would suggest that the transport is diffusion-dominated.

Unlike the retardation factor R_d, there has not been a simple method to determine P_e except by means of nonlinear regression.

2.7 CHAPTER SUMMARY

Slurry cutoff walls are often used to isolate polluted areas before remediation work. SB (soil-bentonite) and CB (cement-bentonite) walls are the most typical types of slurry walls used to contain contaminated groundwater.

CB walls are normally constructed by excavating a trench and filling the trench with a supporting liquid prepared from water, bentonite and cement. The trench stabilizing slurry finally hardens in the trench and becomes the backfill material. As in case of compacted clayey liners constructed in landfills, the design of CB walls should deal with: (1) hydraulic conductivity k, and (2) adsorption and hydrodynamic dispersion. The design aspect, hydraulic conductivity, has been considerably studied so far usually by using hydraulic conductivity tests. Most current designs of CB walls are mainly based on only the value of hydraulic conductivity. In contrast, comprehensive studies regarding adsorption and hydrodynamic dispersion have not been provided. Significant factors influencing the adsorption and hydrodynamic dispersion phenomena inside CB mixtures could be curing period, seepage velocity, concentration level, particle size, porosity, and mix design.

Solute transport mechanisms are reviewed including advection, hydrodynamic dispersion, and adsorption. Hydrodynamic dispersion is a combination of effective molecular diffusion and mechanical dispersion. There is a yielding velocity at which mechanical dispersion starts prevailing. It is shown that the yielding velocities of sandy media and Barricalla clay obtained from literatures are different. A detailed dimensionless hydrodynamic curve of sandy media is also given.

Then, the definitions of effective porosity, resident concentration, and flux concentration are explained. Batch testing, diffusion testing, and column testing are shortly reviewed, focusing on their advantages and disadvantages. More details of column testing are subsequently given, for it is the most important experiment in this research. Two analytical solutions for the interpretation of column testing are reviewed; they theoretically yield the same regressed parameters: retardation factor R_d and column Peclet number P_e. After knowing column Peclet number, hydrodynamic dispersion coefficient D can be determined. One of the two solutions, called cumulative mass approach, will be used in the regression of laboratory data in Chapter 4. It is also possible to determine retardation factor without doing regression analysis; however, a simple method to find column Peclet number has not been available.

CHAPTER 3
METHODOLOGY

3.1 COLUMN TESTING AS A BLACK-BOX MODEL

Black-box model, also known as single-element model or mass-balance model, is regarded as a numerical model in its simplest form. Mass fluxes, water and/or contaminant, are balanced over a single element such as an aquifer, and concern goes to the average concentration in the element and its variation with time. In this kind of model, the concentration only depends on time, not on space. Black-box model is normally used for field-scale problems because of its simplicity.

By adopting the above concept, this research considers column testing (Section 2.6) as a black-box model where contaminant flows in and out. Figure 3.1 shows the schematic diagram of column testing as a single-element model.

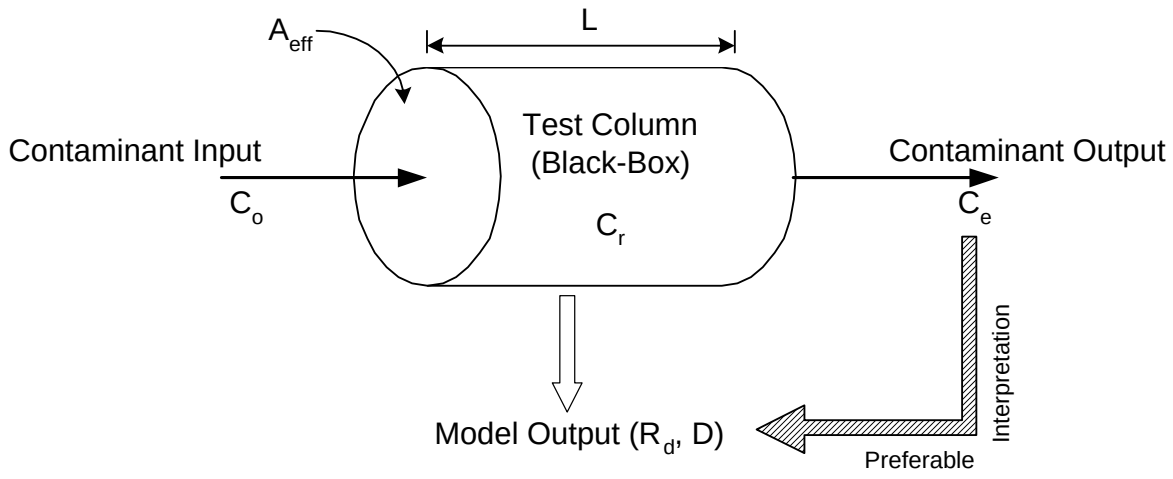

Figure 3.1 Column testing as a black-box model.

From Figure 3.1, contaminant input is a controllable factor governed by Equation (2.17) whereas contaminant output is measurable and can be linked to an output function, either Equation (2.22) or (2.26). The function of the black-box element is called transfer function. The contaminant input is transferred into the contaminant output via the transfer function. In field problems, the transfer function must be calculated based on the observed data of contaminant input and output. In other words, the black-box model is an inverse

problem. Once the transfer function of a field element is obtained, one can predict other contaminant outputs corresponding to different contaminant inputs.

In the laboratory black-box model (Figure 3.1), the transfer function is theoretically available as Equation (2.20), and the output function is resulted from the transformation of the transfer function (van Genuchten and Parker 1984). Both the transfer function and output function can be used to evaluate adsorption R_d and hydrodynamic dispersion D parameters as explained in Section 2.6.1. However, the determination of R_d and D based on the contaminant output is easier and thus preferable.

3.2 MASS COMPONENTS AND REFERENCE CONCENTRATION

When regarding an entire test column as a single element, the total mass M_{total} in the column at any time t is the net flux of mass, which has entered the column:

$$\left(\frac{M_{total}}{A_{eff}}\right)_t = v\int_0^t \left[C_o - C_e(t)\right]dt \qquad (3.1)$$

where A_{eff} = column effective area = V_v/L; and V_v = void volume. Because T = vt/L, L.dT = v.dt

$$\left(\frac{M_{total}}{A_{eff}}\right)_T = L\int_0^T \left[C_o - C_e(T)\right]dT \qquad (3.2)$$

Divide both sides by C_o and rearrange Equation (3.2).

$$(M_{total})_T = V_v C_o \int_0^T \left[1 - \frac{C_e(T)}{C_o}\right]dT \qquad (3.3)$$

The integral term in Equation (3.3) is the area above a breakthrough curve from zero to T. When T is where $C_e = C_o$, this term is equal to R_d (van Genuchten and Parker 1984). Thus, the maximum mass which can be stored in the column is $V_v C_o R_d$. With Equation (3.3), the increasing trend of total mass in the column can be drawn as shown in Figure 3.2. Subsequently, the trends of resident mass M_{pore} and adsorbed mass $M_{adsorbed}$ can be determined by proportion owing to the assumption of constant retardation factor. By mass

conservation, the trend of resident mass can also be formulated by integrating Equation (2.20) with space:

$$(M_{pore})_T = A_{eff}\left[\int_0^L C_r(x,t)dx\right]_T \qquad (3.4)$$

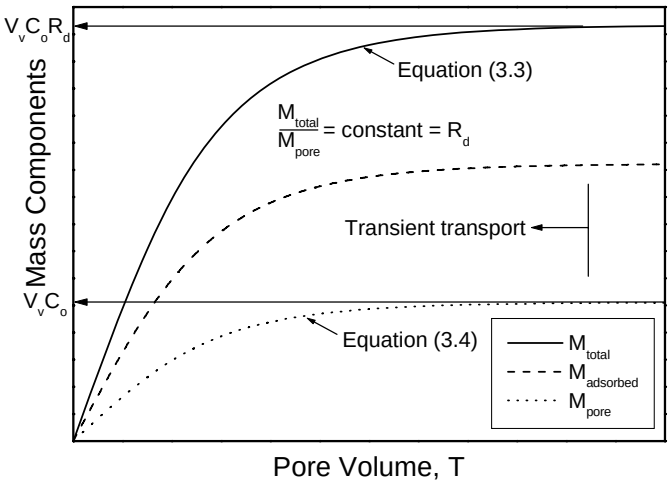

Figure 3.2 Mass components inside a column with $P_e = 5$.

Because the test column is considered as a black box which gives constant retardation factor and hydrodynamic dispersion coefficient, it could be said that those parameters are obtained while the resident concentration is being increased up to the maximum value (C_o). Consequently, the average resident concentration during this increment, or called reference concentration, can be calculated by integrating Equation (3.4) with time:

$$C_R = \frac{A_{eff}}{V_v}.\frac{1}{t_{limit}}.\int_0^{t_{limit}}\int_0^L C_r(x,t)dxdt \qquad (3.5)$$

where C_R = reference concentration. The subscript R means both "Reference" and "Resident". The graphic solution of Equation (3.5) is shown in Figure 3.3, using t_{limit} values to obtain M_{pore} equal to 96%, 97%, 98%, and 99% of the total pore capacity V_vC_o. The 100% line, which is mathematically unavailable, can be obtained by extrapolating the previous 4 lines with parabolic equations. The 100% line can be separated into 2 parts. Two empirical equations are given in Equations (3.6) and (3.7) for practical use. The logistic population model fits the first part, and the latter part agrees well with the power equation.

For $0.1 \leq P_e < 20$

$$\frac{C_R}{C_o} = \frac{1}{1.5 - 0.407e^{-0.082P_e}} \tag{3.6}$$

For $20 \leq P_e \leq 100$

$$\frac{C_R}{C_o} = 0.96P_e^{-0.105} \tag{3.7}$$

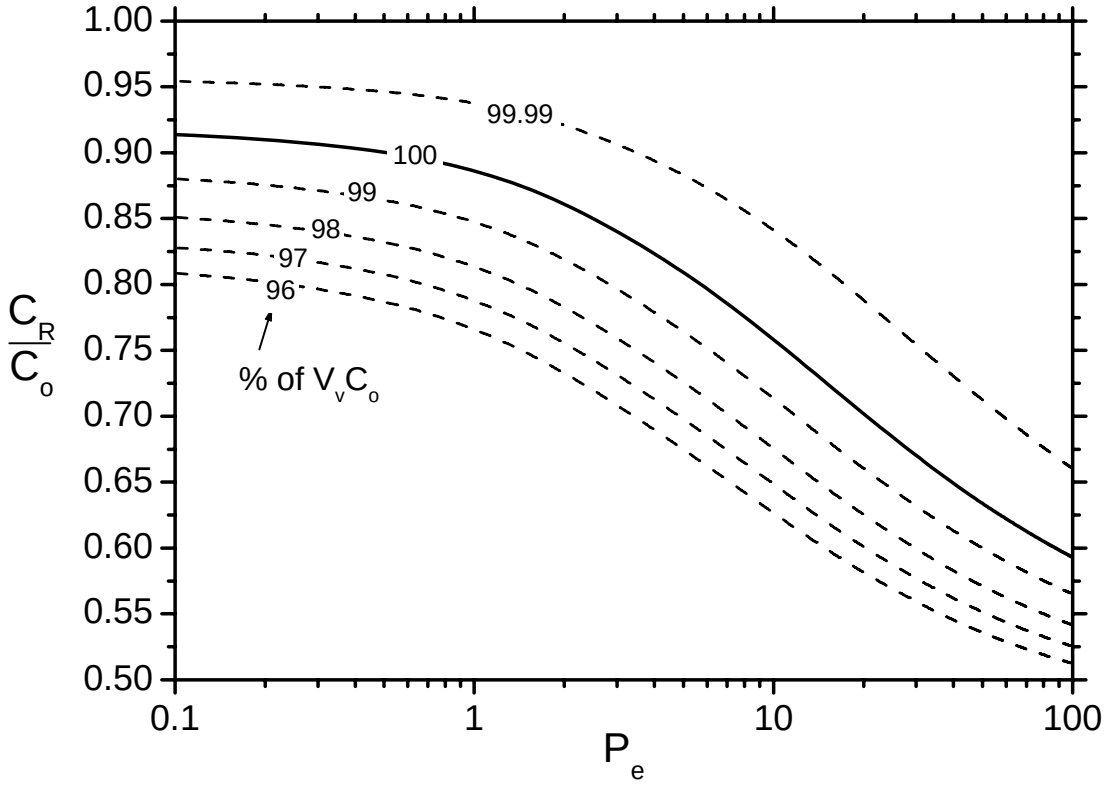

Figure 3.3 Reference concentration timely averaged from total pore capacity.

It could be argued that even though the test is not carried out until the maximum capacity is reached (steady-state transport), constant transport parameters can also be obtained by regression analysis. This research regards the fact that chemical equilibrium between the solid phase and the liquid phase is considered complete only when steady-state transport is achieved; in other words, no more solute is retarded by the column. This consideration imitates the criterion to stop batch testing which requires the complete adsorption of a solute of interest. Thus, even if the column test is stopped before steady-state transport, it is reasonable to calculate its reference concentration based on 100% pore capacity. Two advantages from the proposed approach are: (1) it takes into account the time to reach equilibrium (C_r from 0 to C_o); in contrast, a fixed period (e.g., 24 hours) is used in batch testing (C_r from an initial concentration to a final equilibrium concentration), and (2) an average resident concentration is determined whereas batch testing considers a final resident concentration.

It is seen in Figure 3.3 that neither the value of column source concentration nor half of that represents the reference concentration for a column test. When column Peclet number approaches zero, the reference concentration comes close to the column source concentration, and when column Peclet number increases to infinity, the reference concentration decreases to one half of the source concentration. It will be shown in Chapter 4 that the transport parameters from column testing are related to the level of concentration used in the test.

3.3 INSTANT COLUMN PECLET NUMBER

As mentioned in Section 2.6, retardation factor R_d and column Peclet number P_e are best calculated by nonlinear regression. There are also several methods to determine retardation factor without regression. However, the way to find column Peclet number by simple calculation has not been proposed. Column Peclet number is a very important parameter because hydrodynamic dispersion coefficient D is calculated after knowing this parameter. Obtaining retardation factor by any of the simple methods may not be useful if regression is still needed to find column Peclet number.

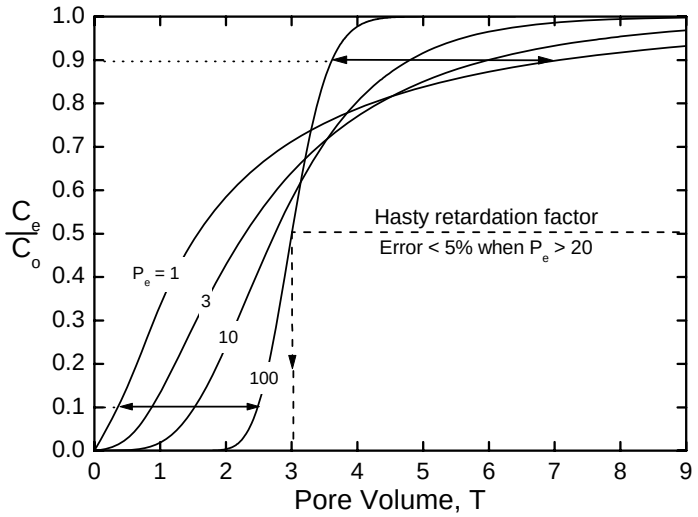

Figure 3.4 Sensitivity of column Peclet number with $R_d = 3$.

Figure 3.4 shows again the theoretical curves of Equation (2.22). All the four curves have the same retardation factor, valuing 3. Because of the difference in column Peclet numbers, the shape of each curve is individual. At high column Peclet numbers (e.g., more than 20), retardation factor can be obtained at $C_e/C_o = 0.5$ (Freeze and Cherry 1979) with marginal error. Nevertheless, at low column Peclet numbers, this method is inapplicable. Retardation factor for any column Peclet numbers can be calculated more correctly by the

integration of the area above a breakthrough curve (van Genuchten and Parker 1984). Unfortunately, this method is not attractive because the integration is needed. Thereafter, Shackelford (1995) suggested that retardation factor is obtained easier by plotting T versus T-CMR, and reading the value at the roof level of the curve (Figure 2.17). It should be noted that the methods by van Genuchten and Parker (1984) and Shackelford (1995) require that steady-state transport be achieved. At this point, it may be concluded that the method by Shackelford seems appropriate to find retardation factor.

Considering Figure 3.4, it is seen that the position of a breakthrough curve depends on retardation factor, but the shape of the curve varies with column Peclet number. After specifying retardation factor, the curvature of the breakthrough curve will result in how much column Peclet number should be. It is evident in the figure that the gaps between a low-P_e curve and a high-P_e curve are large at C_e/C_o equal to 0.1 and 0.9. Thus, these two concentration ratios are considered representative of the variation in column Peclet numbers.

With Equation (2.22), two theoretical charts can be plotted as shown in Figures 3.6 and 3.7. After knowing retardation factor from cumulative mass approach, T values at C_e equal to 10% and 90% of C_o may be obtained from a laboratory breakthrough curve. Two column Peclet numbers can then be determined from the two proposed figures, and the numbers theoretically should be the same. The two column Peclet numbers practically would be different due to any uncertainty in the test; thus, it is better to take an average. Figure 3.5 shows the algorithm to find all the parameters from column testing without regression.

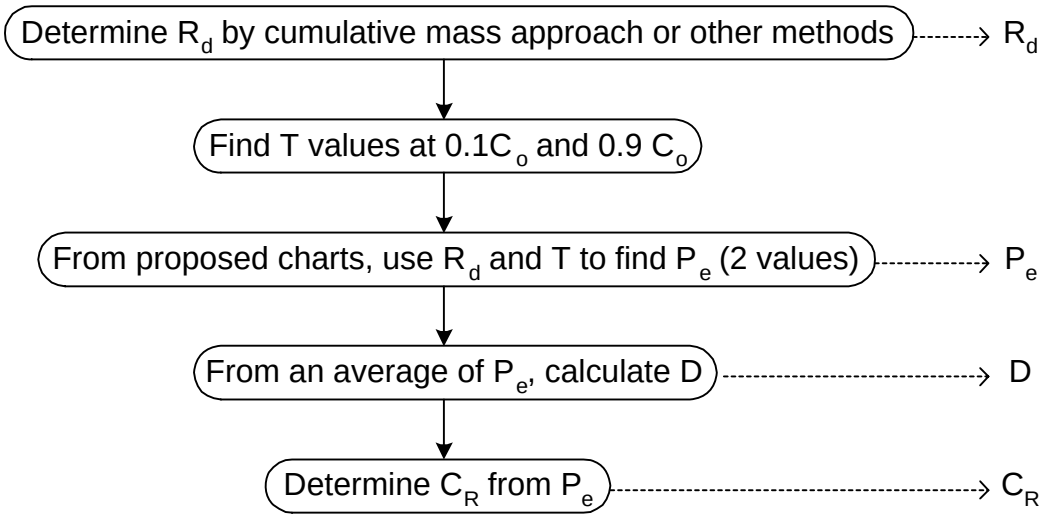

Figure 3.5 Determination of parameters from column testing without regression.

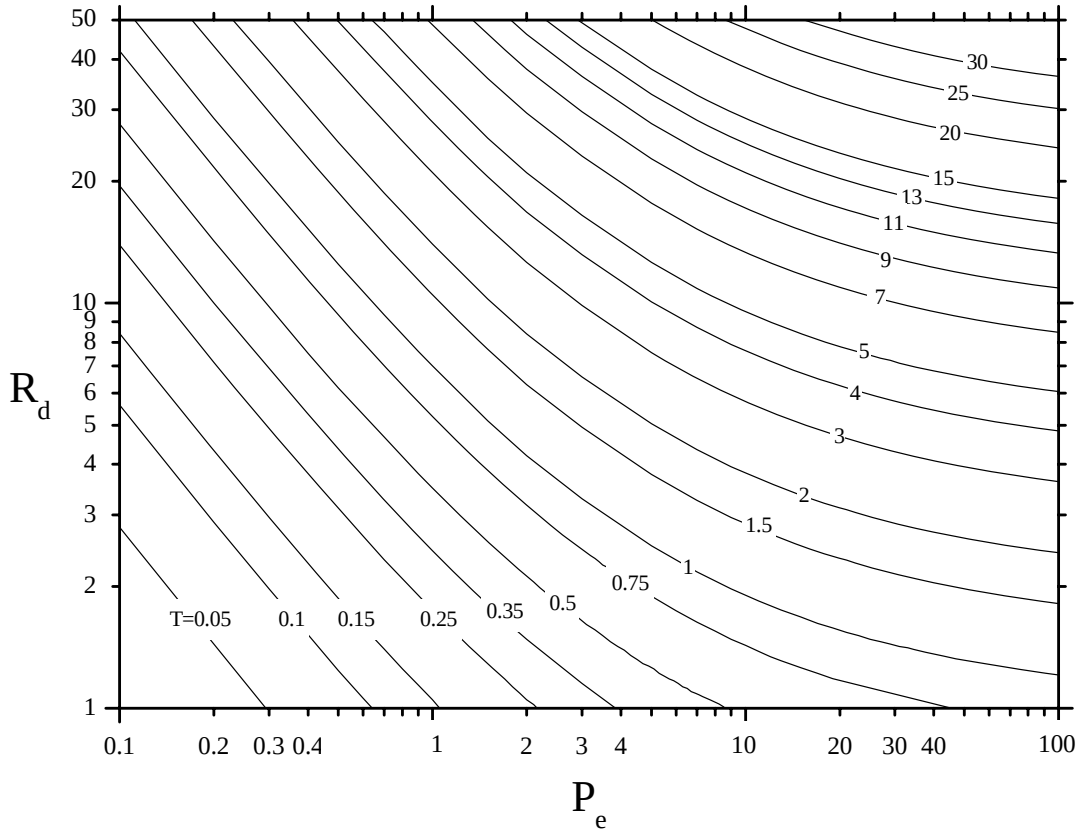

Figure 3.6 Theoretical chart for $C_e = 0.1C_o$.

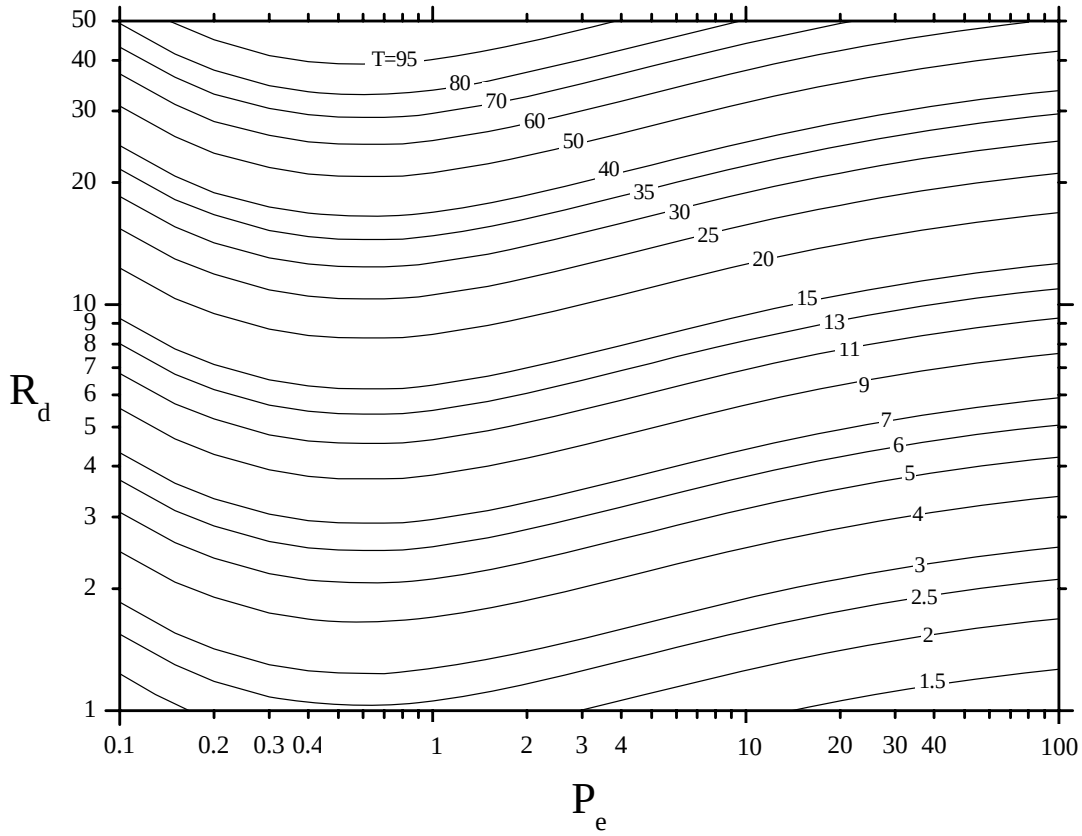

Figure 3.7 Theoretical chart for $C_e = 0.9C_o$.

To verify the approach, a laboratory breakthrough curve is introduced in Figure 3.8. Firstly, retardation of this breakthrough curve is obtained by plotting T versus T-CMR as shown in Figure 3.9. Retardation factor, obtained at the roof level of the curve, is read 1.81. Secondly, T value at $C_e = 0.1C_o$ is read 1.4, and T value at $C_e = 0.9C_o$ is read 2.4.

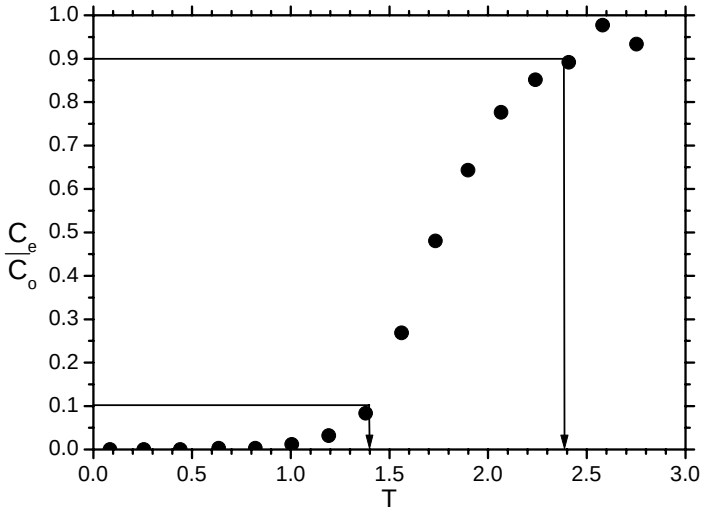

Figure 3.8 Laboratory breakthrough curve.

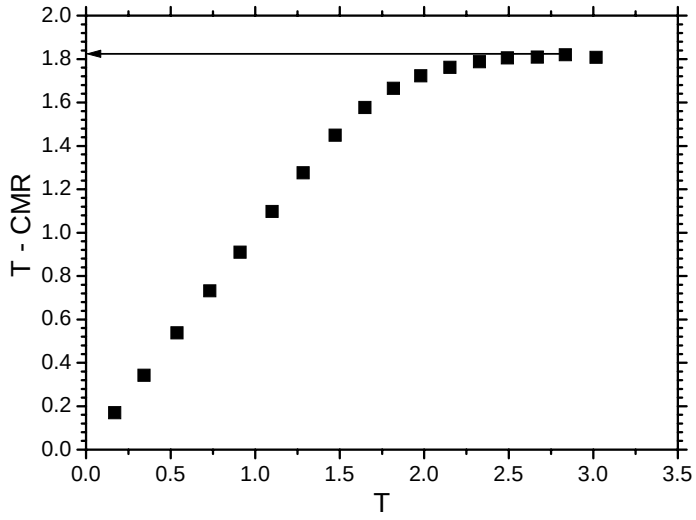

Figure 3.9 Cumulative mass approach: T – CMR method.

From Figure 3.6, with $R_d = 1.81$ and $T = 1.4$, P_e value can be obtained from the chart as 44 (by eyes). From Figure 3.7, with $R_d = 1.81$ and $T = 2.4$, P_e value is obtained as 44 as well. It can be concluded that, without regression, retardation factor R_d is found to be 1.81, and column Peclet number P_e is equal to 44.

The laboratory data was also nonlinearly regressed by using MATHEMATICA. Yet, Equation (2.26) is used instead of Equation (2.22) to increase the precision of the regressed parameters. The regressed R_d is 1.814, and the regressed P_e is 44.68. Thus, error in finding R_d from cumulative mass approach is only 0.22%, and P_e from the proposed method yields error of only 1.52%.

It is important to note that the precision of the proposed method depends on: (1) how accurate retardation is chosen (Figure 3.9), (2) how scattered data points are (Figure 3.8), and (3) how well column Peclet numbers are read from Figures 3.6 and 3.7. Peclet number from the algorithm can be used directly to find hydrodynamic dispersion coefficient, or be considered as an initial value for nonlinear regression in elaborate researches. All the R_d and P_e values in this research are determined by nonlinear regression using MATHEMATICA.

3.4 EXPERIMENTAL APPROACHES

3.4.1 Materials Used

Because this research is intended to study the behaviors of CB mixtures as contaminant barriers, powdered sodium bentonite (B), ordinary Portland cement (OPC) and blastfurnace slag cement (BSC) are utilized to make the CB mixtures. The sodium bentonite is a product of Hojun (ホージュン) Company, Gunma, Japan. The OPC is provided by Sumitomo Osaka Cement (住友大阪セメント) Company, Tokyo, Japan, and Taiheiyo Cement (太平洋セメント) Company, Tokyo, Japan provides the BSC. In addition, a cement retarder used in a part of the research (batch testing) is obtained from Sankyo Chemical (三協化学) Company, Shizuoka, Japan.

3.4.2 Solutions and Measurement Technique

Chemical solutions used throughout the research are 0.1 M (mole/litre) Sodium Chloride (NaCl) obtained from Nacalai Tesque (ナカライテスク) Company, Kyoto, Japan. The original solutions are also diluted by distilled water in order to make various levels of concentrations. Chloride ions are the only ions to be studied. The measurement of chloride concentrations is done by using an ion selective electrode (ISE) from Horiba Company, Kyoto, Japan. Before the measurement, each liquid sample is added with an ionic strength adjusting buffer solution (0.1 M KNO_3). The chloride concentration measurement is performed immediately after the collection of each sample.

3.4.3 Types of Experiments

There are mainly 5 kinds of tests which are conducted in this research. They are column testing, batch testing, diffusion testing, scanning electron microscopy (SEM), and laser diffraction (LD) technique. Among them, column testing is the most important experiment used to study the chloride transport through CB mixtures under various influencing factors. Forty-two column tests, two diffusion tests, and two series of batch tests have been carried out on CB mixtures. SEM is used to investigate the microstructure of bentonite, cements, and CB columns. LD technique is applied to prehydrated CB mixtures to determine their particle size distributions (PSD). Except the results of diffusion testing, all other experimental results are provided in Chapter 4. The results of the two diffusion tests together with theoretical predictions are provided in Chapter 5.

3.4.4 Testing Procedures

Batch Testing

At about 25 °C, two series of batch testing are performed to study chloride adsorption in shaking condition. Each sample in the first series is formulated by mixing 12.5 g of the sodium bentonite (B) with 37.5 g of the slag cement (BSC), and then adding 200 mL NaCl solution of a known concentration. The same is the second series except 1 mL of the cement retarder is added to each slurry. The quantity of the retarder is so small that it does not significantly affect the initial concentration of each slurry. It is noted here that the solid:solution ratio (by weight) is equal to 1:4 which is the largest ratio recommended by Roy et al. (1991) for batch testing conducted on soils. After 24-hour shaking, all the slurries are not solidified even those without the retarder. Then, a portion of each slurry is extracted and centrifuged at 3,000 rpm for 30 minutes. The resultant liquid is analyzed for chloride concentration using the ion selective electrode (ISE).

Column Testing

There are 42 column tests. Each design mix is formulated by first adding a desired amount of the bentonite to distilled water. The bentonite water is agitated in a mechanical mixer at 3,600 rpm for a 20-minute period, and then allowed to hydrate for 24 hours. Thereafter, the mixing is continued by adding the cement of interest to the bentonite water. The CB mixture is then stirred for 20 minutes. The final slurry is carefully poured into a plastic mold inside a 500 mL beaker. Distilled water is poured into the beaker until the water level is

about 1 cm higher than the top of the sample. With the top surface slightly disturbed, this procedure is done to assure the saturation of the sample and to minimize bleeding problem. When the sample is cured to 2 days, the upper part is cut off to eliminate the disturbed top surface, and the shortened sample is again positioned under distilled water. The mold is stored in an environmentally controlled room where the temperature is maintained at about 25 °C. Figure 3.10 shows the procedure of making a columnar CB sample.

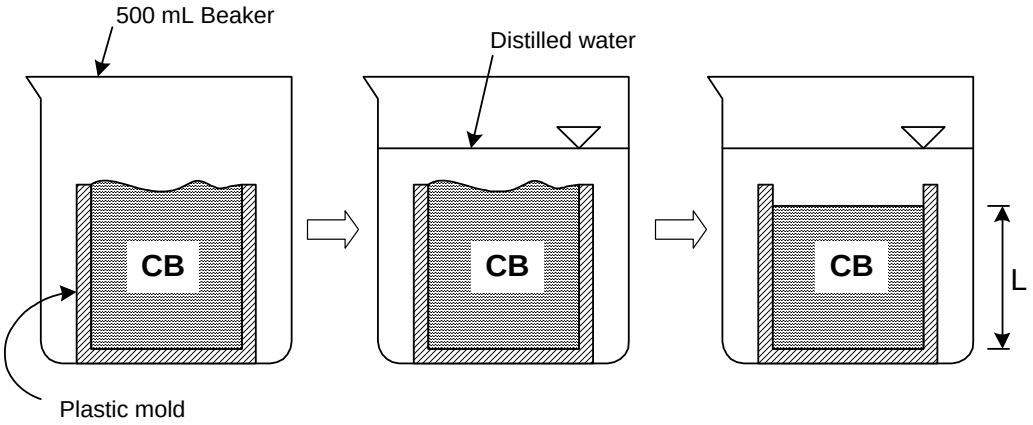

Figure 3.10 Preparation of each CB column.

After curing, each cured sample is removed from its mold. It is placed and wrapped with a membrane in a hydraulic cell (Figure 3.11). Cell pressure then acts to empty a gap between the specimen and the membrane. Distilled water is introduced from a source reservoir into the sample by a hydraulic gradient. After obtaining a steady seepage velocity, the distilled water in the source reservoir is replaced by NaCl solution of a known concentration. Figure 3.11 corresponds with Figure 2.12.

Figure 3.11 Laboratory flexible-wall column testing.

While the solution is flowing through the sample, effluent samples are collected periodically for the measurement of chloride concentrations. Chloride concentrations are measured immediately after sampling by the ion selective electrode (ISE). After the completion of each test, the dry density (ρ_d) and total porosity (n) of the specimen are calculated based on water content lost in a 110°C oven.

Diffusion Testing

Two diffusion tests corresponding to Figure 2.10 (left) are performed at 25 °C. Each diffusion sample is formulated by mixing an amount of the bentonite with a volume of distilled water. The bentonite slurry is agitated in a mechanical mixer at 3,600 rpm for 20 minutes, and then allowed to hydrate for 24 hours. After that, the mixing is continued by adding a desired amount of the slag cement (BSC) to the bentonite water. It should be noted that the solid (bentonite + slag cement):solution (distilled water) ratio (by weight) is 1:4. The CB mixture is then stirred for 20 minutes. The final slurry is carefully poured into a cylinder which has an impermeable base. Distilled water is gently poured into the cylinder until the water level is about 3 cm higher than the top of the sample. A clean flat spoon is used to flatten the disturbed top surface. Each sample is left to cure for 28 days. Figure 3.12 illustrates the way to prepare each diffusion specimen.

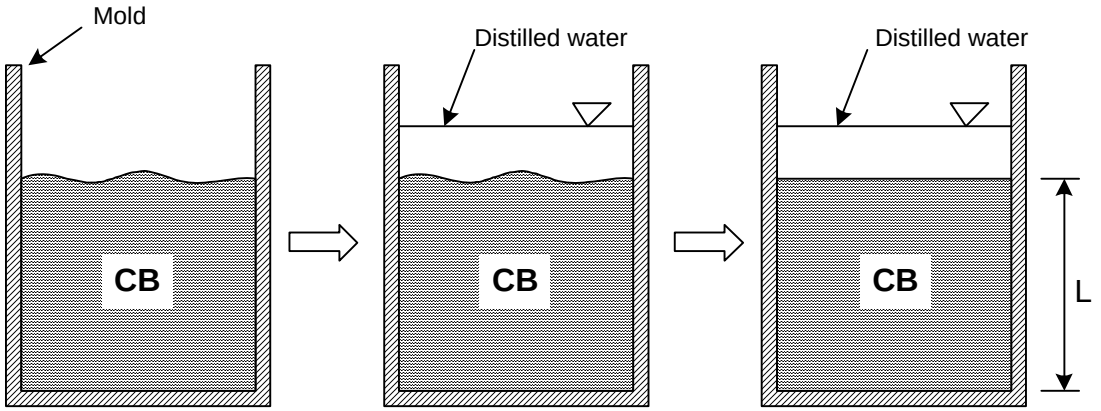

Figure 3.12 Preparation of each CB diffusion specimen.

The first sample is 6.1 cm high, and 8 cm high is the second sample. After curing, the curing water is replaced by NaCl solution of 2,100 mg/L chloride concentration. The heights of the solution are 2.9 and 3 cm, respectively. The concentration drop in each source solution is daily measured for 6 days by the ISE.

Scanning Electron Microscopy (SEM)

A general-purpose SEM machine, JSM-5510LV from JEOL Company, has been utilized in this study. The machine can provide the microscopic images of the sodium bentonite, cements, and cured CB samples. The main objective of using SEM is to study the binding (adsorption) of chloride ions in CB mixtures. The binding of chloride ions in mortars and concretes has been comprehensively studied, but the binding of the same ions in the mixture of bentonite and cement has not been clarified.

The investigation by SEM has simple steps as follows:

1. Coat a small piece of sample in a coating machine.
2. Devacuum the vacuumed SEM machine.
3. Set the sample in a sample chamber.
4. Vacuum the machine again.
5. View an image and adjust contrast and brightness.
6. Capture the image as a digital file.

Laser Diffraction (LD)

This technique relies on the fact that, for light passing through a suspension, the diffraction angle is inversely proportional to the particle size. The laser diffraction (LD) instrument consists of a laser source of known wavelength, a photosensitive detector, and a means of passing sample particles through the laser beam. Normally, the sample particles can be suspended in either liquids or gases, and drawn through the laser beam.

In this research, LD technique is used to determine the particle size distributions (PSD) of prehydrated CB mixtures because the conventional hydrometer analysis for soils is not suitable for cement-based materials that hydrate with time. The PSD curves are obtained at Shimadzu Techno-Research (島津テクノリサーチ) Company, Kyoto, Japan.

3.4.5 Transport Parameters considered in Column Testing

During column testing, hydraulic conductivity k is the first transport parameter that can be evaluated. Knowledge of hydraulic conductivity leads to the determination of a seepage velocity. Under the constant seepage, a solute of interest is introduced into the test column, and subsequently retardation factor R_d and hydrodynamic dispersion coefficient D are resulted from the regression analysis of effluent concentration data. Thus, k, R_d and D are the

three transport parameters to be evaluated in this research. However, attentions are especially paid to adsorption and hydrodynamic dispersion phenomena.

3.4.6 Effect of Effective Porosity

The use of effective porosity n_e instead of total porosity n calculated from water content w_c will increase R_d but keep P_e unchanged in regression analysis. Figure 3.13 illustrates that if n_e is used, the laboratory breakthrough curve will shift to the right, resulting in a new R_d but the same P_e.

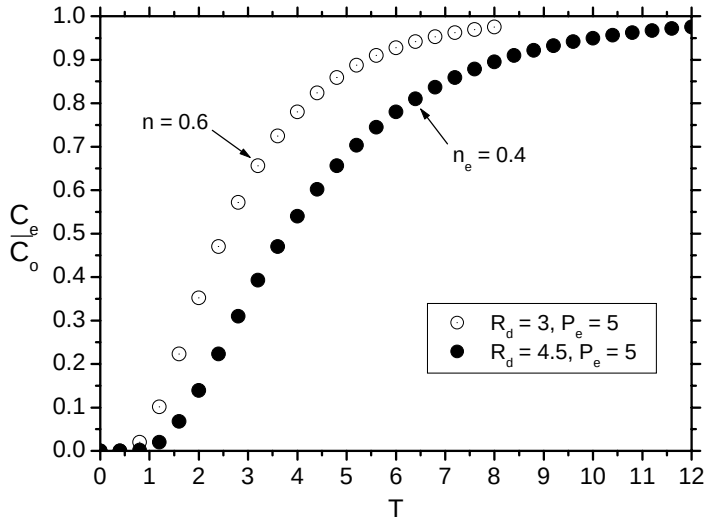

Figure 3.13 Effect of effective porosity.

Despite P_e remaining constant, D will increase due to a new higher seepage value calculated by n_e. It can be proved that both R_d and D parameters will increase by the same factor when n_e is used:

$$(R_d)_{eff} = (R_d)_{total} \cdot \frac{n}{n_e} \tag{3.8}$$

$$(D)_{eff} = (D)_{total} \cdot \frac{n}{n_e} \tag{3.9}$$

By Equations (3.8) and (3.9), the results of R_d and D from total porosity can be changed into the effective parameters without repeating the regression analysis. From Figure 3.13, the R_d of 3 is multiplied by (0.6/0.4), resulting in the effective R_d of 4.5. The effective porosity n_e may be obtained by a mercury intrusion porosimeter (see Fratalocchi et al. 1996), or by cumulative mass approach (see Shackelford 1995).

3.4.7 Effect of Curing

Due to cement hydration process, the hydraulic conductivity k of CB mixtures decreases with curing time. This reduction can appreciably continue for months or years, depending on the type of cement and pore fluid. In this research, it is believed that if hydraulic conductivity changes with time, then adsorption R_d and hydrodynamic dispersion D parameters cannot remain constant as well. The assessment of the hydraulic conductivity of CB materials used for contaminant prevention has been done so far [e.g., Fratalocchi et al. (1996); Fratalocchi and Pasqualini (1998)]; however, comprehensive studies regarding the adsorption and hydrodynamic dispersion as a function of curing time are not available.

Three curing periods 5, 28, and 60 days are chosen for the study of curing effect using column testing. For instance, a CB column is cured under distilled water (Figure 3.10) for a specified period and then permeated with NaCl solution to find k, R_d and D under a constant seepage velocity. And another similar column is cured for a longer period, and permeated with the same solution (concentration) under the same velocity. To attain the same velocity, it is necessary to increase the hydraulic gradient i because the latter sample has a lower k value owing to the longer curing. These two exemplary columns are likely to yield different R_d and D values because of different curing periods.

3.4.8 Effect of Seepage Velocity

The magnitude of seepage has influence on adsorption and hydrodynamic dispersion. Firstly, the moving speed of pore liquid affects chemical reactions between adsorbate (chloride ions) and adsorbent (CB solid phase), and thus influences the degree of adsorption. Second, there is a yielding velocity at which mechanical dispersion starts predominating (Section 2.4.6). Beyond the yielding velocity, the hydrodynamic dispersion coefficient D is increased linearly with seepage velocity in log-log plotting (Figure 2.4). Figure 2.5 has further suggested that the yielding velocities of different porous media may not be unique. Thus, the yielding velocity of CB columns permeated with chloride ions shall be discussed.

In order to study the effect of velocity, columns with the same material and curing period (in other words, the same k) are tested with different velocities. The yielding velocity of CB columns in this research is evaluated by conducting a number of column tests at both low and high seepage velocities, and plotting the hydrodynamic curve (log v, log D) as Figure 2.5. The resultant hydrodynamic curve of CB columns will be compared with those of sands (Perkins and Johnston 1963) and Barricalla clay (Manassero et al. 1997).

3.4.9 Effect of Concentration

The approach developed in Section 3.2 is for studying the effect of concentration used in column testing. After finishing a column test, the resultant R_d and D parameters are related to an average resident concentration, or called reference concentration C_R, by either Equation (3.6) or (3.7). The concentration-dependent behaviors of parameters R_d and D can be demonstrated by performing a series of column tests with different source concentrations C_o on the same material under the same velocity v and column length L.

In Chapter 4, the result of concentration-dependent adsorption from a series of column tests performed at the comparatively lowest seepage is compared with the results from the two series of batch testing mentioned in Section 3.4.4. The results of both adsorption and hydrodynamic dispersion at other velocities are also plotted as a function of C_R. The effect of concentration on the D parameter, which frequently has been disregarded in practical applications, will be drawn into attention. The applicability of concentration-dependent parameters derived from column testing using the proposed approach is substantiated in Chapter 5 where the results of the two diffusion tests (Section 3.4.4) are predicted by POLLUTE software.

3.4.10 Effect of Mean Particle Size

As mentioned in Section 2.4.6, the mean particle size d_{avg} or d_{50} is generally used to make the dimensionless or normalized hydrodynamic curve of porous media. The normalized hydrodynamic curve of sands is introduced in Figure 2.6 by combining the data from Perkins and Johnston (1963) and Spitz and Moreno (1996). Whether Figure 2.6 is applicable to clayey soils or CB mixtures or not is illustrated in Chapter 4. The normalized hydrodynamic curve of Barricalla clay together with the normalized curve of CB mixtures from this research will be combined with Figure 2.6. The values of D_o are obtained from Table 2.1, and the d_{50} values of CB mixes come from the LD technique.

3.4.11 Effect of Porosity Change

Researches dealing with the relationship between void ratio e (or porosity) and hydraulic conductivity k are available for clays and geosynthetic clay liners [e.g., Mesri and Olson (1971); Fernandez and Quigley (1985); Petrov et al. (1997)]. Yet, the effect of porosity change on the transport parameters of CB mixtures has not been investigated. This research attempts to study not only k, but also R_d and D of CB material when subjected to consolidation.

Five CB columns (out of 42 column tests) are specially designed to study the effect of porosity change. Each of which is made by pressing the top of an immersed sample (Figure 3.10, middle) with a porous disk until a desired length is obtained. This procedure is done immediately after having poured distilled water into the beaker which contains the sample mold. The initial lengths of the samples before pressing are varied and less than 5 cm. Four of these special columns are used to study hydraulic conductivity, and the fifth sample is for the studies of hydraulic conductivity, adsorption and hydrodynamic dispersion.

3.4.12 Effect of Mix Designing

The use of blastfurnace slag (BS) to replace a certain amount of ordinary Portland cement (OPC) is known to decrease the hydraulic conductivity of CB mixtures. According to Dhir et al. (1996) and Luo et al. (2003), BS helps in increasing chloride binding capacity and decreasing chloride diffusion coefficient in concrete. However, the influence of BS on adsorption and hydrodynamic dispersion in CB mixtures has been unknown. It is in Chapter 4 where discussion on the effect of BS on chloride binding and dispersion in CB mixes is provided. In addition, it will also be shown that the quantity of sodium bentonite used in mix designing also has strong influence on the hydraulic conductivity of hardened CB mixtures.

3.4.13 Study of Chloride Binding

Chloride ions are the only ions to be focused in this research. The binding or adsorption of chloride in CB mixtures has not been particularly investigated. This research uses scanning electron microscopy (SEM) to examine the microstructure of CB columns which have and have not been permeated with NaCl solution. The results from SEM are compared with previous literatures concerning the binding of chloride in mortars and concretes.

3.5 SEMI-ANALYTICAL APPROACH

3.5.1 POLLUTE

In many applications, the movement of contaminants is fundamentally in one direction, and can be predicted using the one-dimensional advection-hydrodynamic dispersion equation as Equation (2.1). POLLUTE (Rowe et al. 1998, Figure 3.14) is a computer program that implements a solution to the one-dimensional advection-hydrodynamic dispersion equation for a layered deposit of finite or infinite extent. Using this solution, POLLUTE calculates the concentrations of a contaminant at specified times and distances.

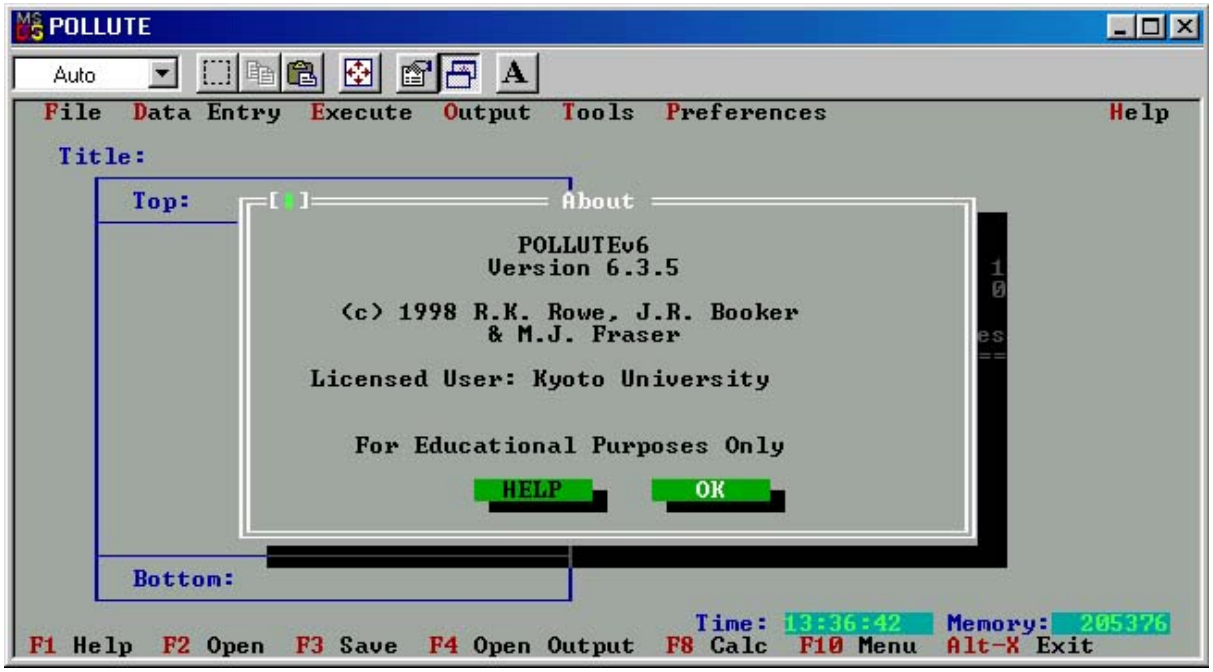

Figure 3.14 Introductory screen of POLLUTE version 6.3.5.

Unlike finite element and finite difference methods, POLLUTE does not require the use of a "time-marching" procedure. POLLUTE uses a finite-layer (semi-analytical) formulation that provides numerically accurate results while requiring relatively little computational and data input effort. Basically, the concentration of contaminant can be directly determined at any specified time without calculating the concentration at earlier times.

Some important features of the program are listed as follows:

1. The deposit may be subdivided into individual layers, with different parameters for each layer.
2. Depletion of the source with time can be modeled, or the source can have a constant concentration with time.
3. The bottom of the deposit can be impermeable, permeable, infinite, or have a constant concentration.
4. The effect of chemical reactions on a reactive solute may be considered; using either linear adsorption, Freundlich nonlinear adsorption (Equation 2.13), or Langmuir nonlinear adsorption.
5. An initial concentration profile with depth may be input.

In Chapter 5, some theoretical predictions on the laboratory results of the two diffusion tests (Section 3.4.4) are carried out by POLLUTE. The program solves Equation (2.1) subject to boundary conditions at the top and bottom of the soil deposit being modeled. There are three possible top boundaries; these are zero flux, constant concentration, and finite mass. The finite mass top boundary for diffusion testing is simplified to Equation (2.15). The bottom boundary may be either zero flux, constant concentration, fixed outflow, or infinite thickness. Because each diffusion test has an impermeable base (Figure 2.10, left), the flux across the bottom boundary is zero. Figure 3.15 shows the graphical user interface of POLLUTE during the analysis of a diffusion test.

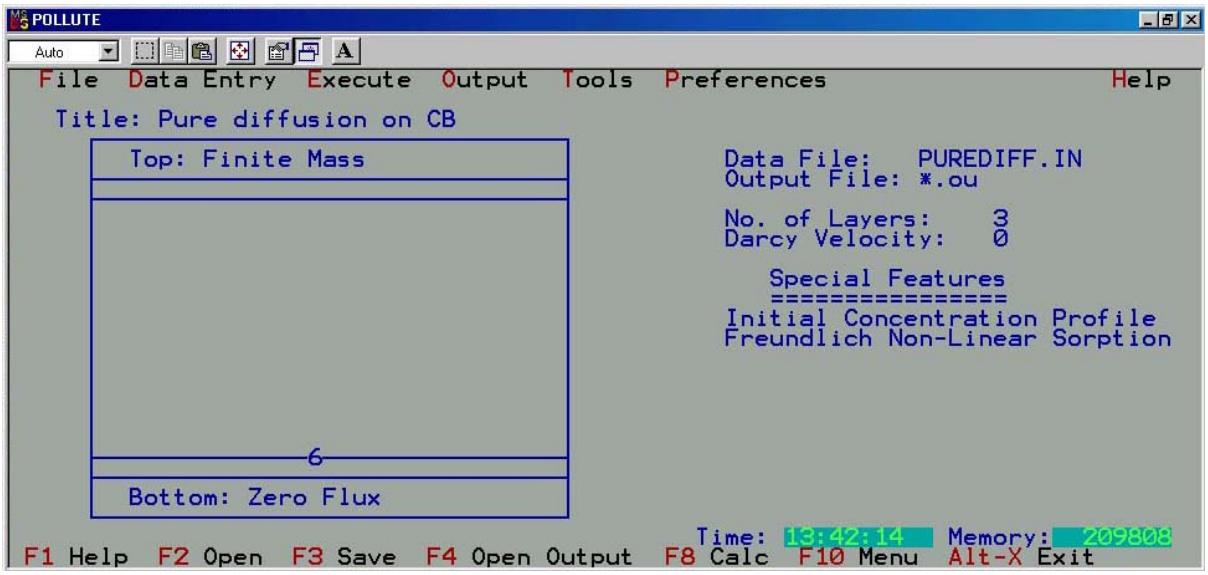

Figure 3.15 Analysis of diffusion testing by POLLUTE.

3.5.2 Prediction of Diffusion Testing by Parameters from Column Testing

Provided that column testing is performed at a sufficiently low velocity, the resulting hydrodynamic dispersion coefficient D will be equal to D^* in the range of ~ 2 x 10^{-6} cm^2/s to ~ 2 x 10^{-5} cm^2/s (Mitchell 1991). If it is further assumed that the degree of adsorption at the low velocity (no mechanical dispersion) is exactly or almost the same as that at zero velocity, then the results from column testing can be applied to diffusion testing of the same material.

Figure 3.16 illustrates that similar parameters can be obtained from both diffusion and column testing. This implies that it should be able to predict the results of diffusion testing by parameters from column testing conducted at low seepage. In Chapter 5, the concentration-dependent parameters R_d and D^*, which are resulted from a series of column

tests performed at a low velocity, are used to predict the drops of source concentrations in two diffusion tests. The theoretical predictions are generated using POLLUTE.

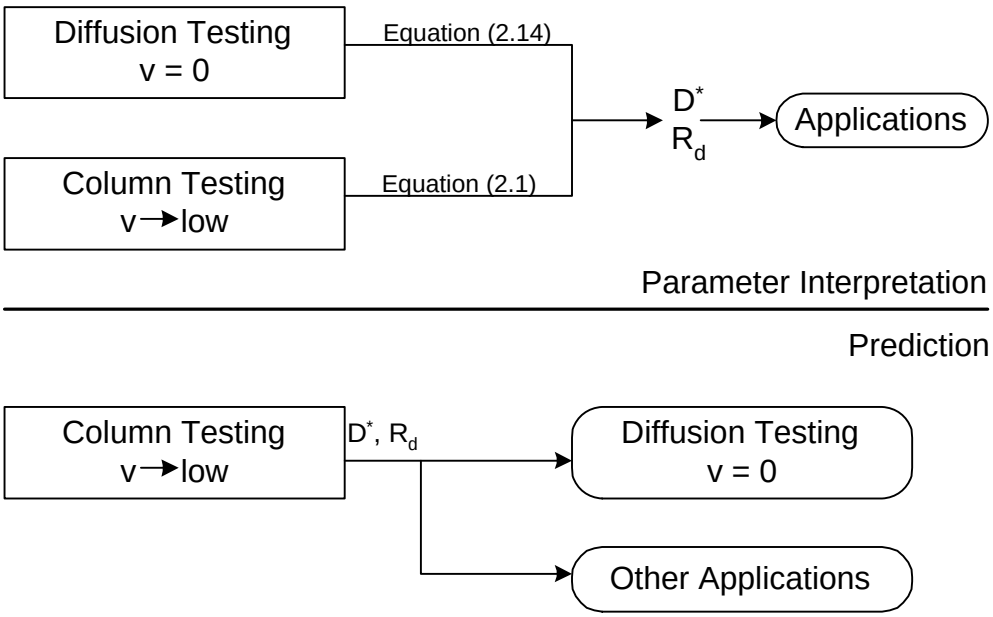

Figure 3.16 Interpretation and application of transport parameters.

3.6 CHAPTER SUMMARY

This chapter starts by considering column testing as a black-box model which yields lumped retardation factor R_d and hydrodynamic dispersion coefficient D. The analytical solution by Lindstrom et al. (1967), which describes resident concentration C_r distribution with space x and time t inside the column, is considered as transfer function. The first integration of the transfer function with space changes the column into a black-box or single-element model. Then, the second integration with time from the beginning to steady-state transport ($C_e = C_o$) can yield the timely-averaged resident concentration, called reference concentration C_R, which is a function of column Peclet number P_e. The two parameters, R_d and D, interpreted from column testing shall be related to this C_R. The concept of C_R will be used in Chapter 4 where a number of column test results are presented. At this point, the first objective of this research, to develop an approach to understand solute transport in view of concentration levels, has been fulfilled.

Then, a simple algorithm to find P_e without nonlinear regression is proposed. Column Peclet number P_e is somewhat a very important parameter, for hydrodynamic dispersion coefficient D and reference concentration C_R are calculated after knowing this dimensionless

parameter. Two inflection points of the breakthrough curve at 10% and 90% of source concentration C_o are considered representative of the variation in P_e, and thus two theoretical charts corresponding to those two points are proposed to find P_e. Consequently, the second research objective, to simplify the interpretation of column testing, is accomplished.

Next, the chapter describes experimental approaches used in this research. Experimental results are not shown in this Chapter but in Chapter 4. Sodium bentonite (B), ordinary Portland cement (OPC), and blastfurnace slag cement (BSC) are used to make CB mixtures. Sodium Chloride (NaCl) solutions are used throughout the research, and chloride ions are the only ions to be focused. The measurement of chloride concentrations is possible by using an ion selective electrode (ISE).

Five kinds of experiments are explained in details, namely column testing, batch testing, diffusion testing, scanning electron microscopy (SEM), and laser diffraction (LD) technique. Two series of batch tests, without and with cement retarder, are performed to study chloride adsorption to the mixtures of bentonite and BSC. Two diffusion tests are conducted on 28-day cured CB specimens made from bentonite and BSC. SEM is used to see the microscopic images of bentonite and cements and to study the binding (adsorption) of chloride ions in CB columns. LD technique is for the determination of particle size distributions (PSD) of prehydrated CB mixtures. There are 42 column tests, and the columns are prepared from the combination of bentonite and either BSC or OPC. Hydraulic conductivity k, retardation factor R_d and hydrodynamic dispersion coefficient D are the three transport parameters to be evaluated by column testing. However, attentions are specially paid to the R_d and D parameters.

The effect of effective porosity n_e on R_d and D is explained, following by the explanation of six factors which are believed to influence the transport of chloride ions through CB mixtures: curing, seepage, concentration, average particle size, porosity change, and mix designing.

The semi-analytical method by POLLUTE software (Rowe et al. 1998) is shortly described. The software is capable of analyzing laboratory diffusion testing; therefore, it is used as a tool in this research. It is explained that if column testing is conducted under diffusion-dominated condition or relatively low seepage, the results from the test can be used to predict the results of diffusion testing of the same material. The predictions of the two diffusion tests in this research are done by POLLUTE and shown in Chapter 5.

CHAPTER 4
RESULTS AND DISCUSSIONS

4.1 PROPERTIES OF BENTONITE

Table 4.1 shows some properties of the sodium bentonite (named 穂高印) used in this research. Sodium bentonite is not itself a mineral name, but more correctly, it is a swelling clay composed primarily of the mineral montmorillonite. It may be inferred that the quantity of montmorillonite is 64.9% by considering the true clay size of less than 2 μm.

Table 4.1 Properties of sodium bentonite

Property	Value
Moisture content	6.4%
Density	0.39 g/cm^3
Swelling index	17.3 ml/2g
Degree of swelling	6.1 g/g
pH	10.4
size < 53 μm	98.7%
< 5 μm	74.5%
< 2 μm (clay)	64.9%
< 1 μm	53.2%

According to Japanese specification, the water content must be less than 10%. The density should be in between 0.35 and 0.5 g/cm^3. The swelling index must fall in the range of 17 to 22 ml/2g; the degree of swelling should be in between 5 and 8 g/g. And the pH using 2% dispersion liquid must be in the range of 9.5 to 10.8. The percent retain on the 53 μm mesh is 1.3% less than the specification of 10%. Figures 4.1 and 4.2 show the shapes and sizes of the bentonite particles seen by SEM.

4.2 PROPERTIES OF CEMENTS

The chemical compositions and physical properties of ordinary Portland cement (OPC) and blastfurnace slag cement (BSC) are given in Table 4.2. The manufacturer of BSC informed that the cement was made by blending 58% (by mass) OPC and 42% blastfurnace slag (BS). This mixing apparently decreases CaO content but increases SiO_2 and Al_2O_3 in the final product compared with OPC. Figures 4.3 and 4.4 show the SEM images of OPC, and seen in Figures 4.5 and 4.6 are the SEM images of BSC.

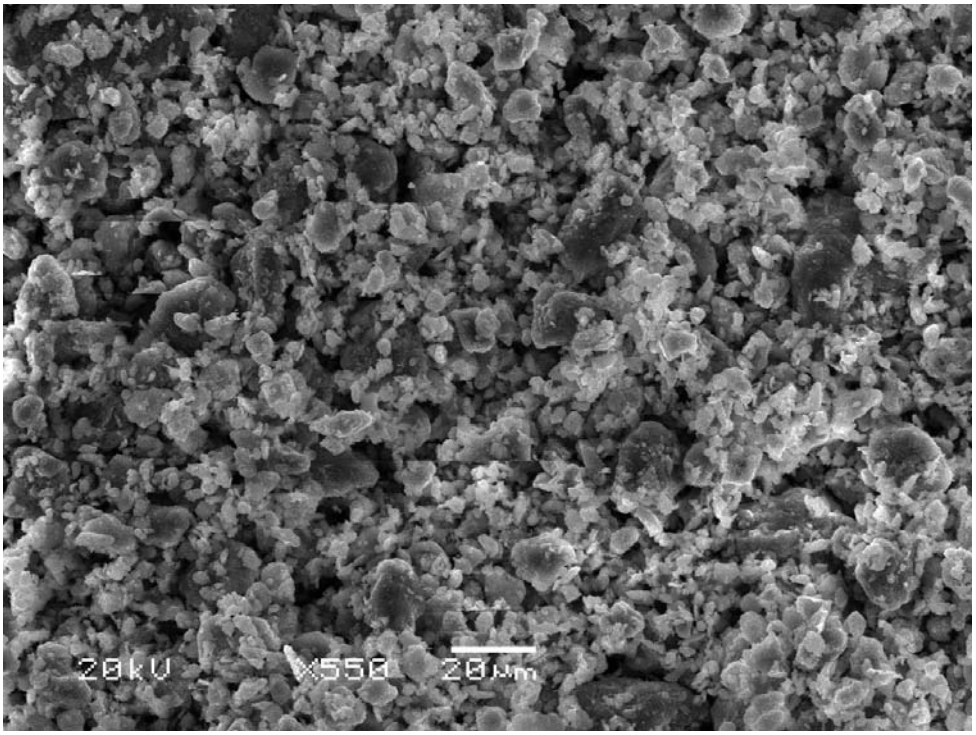

Figure 4.1 SEM image of sodium bentonite at 550-time enlargement.

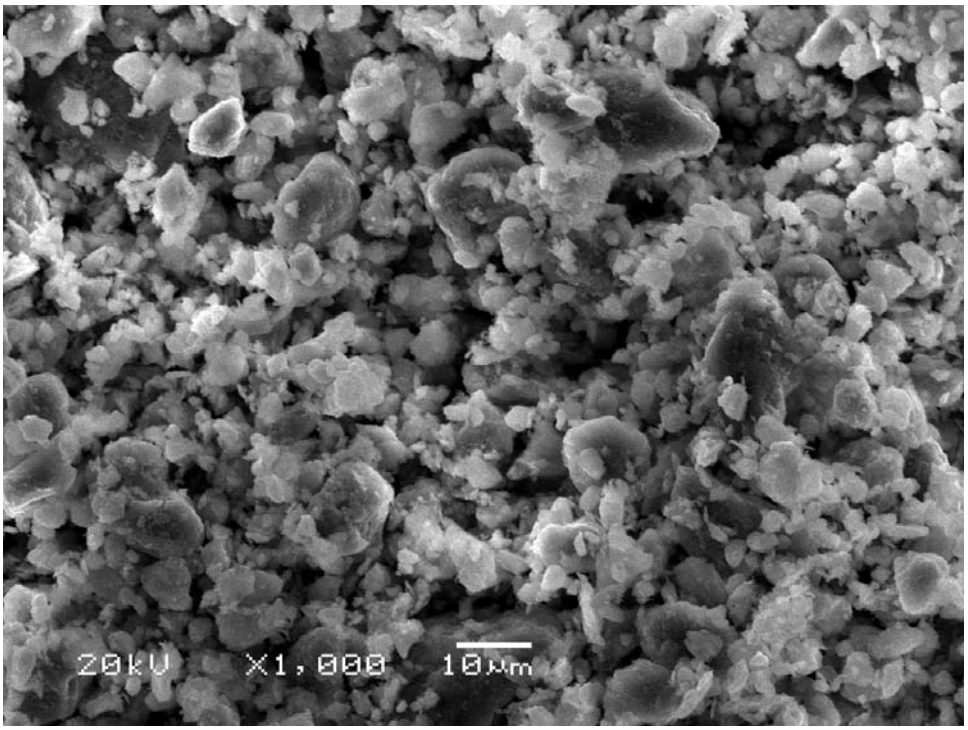

Figure 4.2 SEM image of sodium bentonite at 1000-time enlargement.

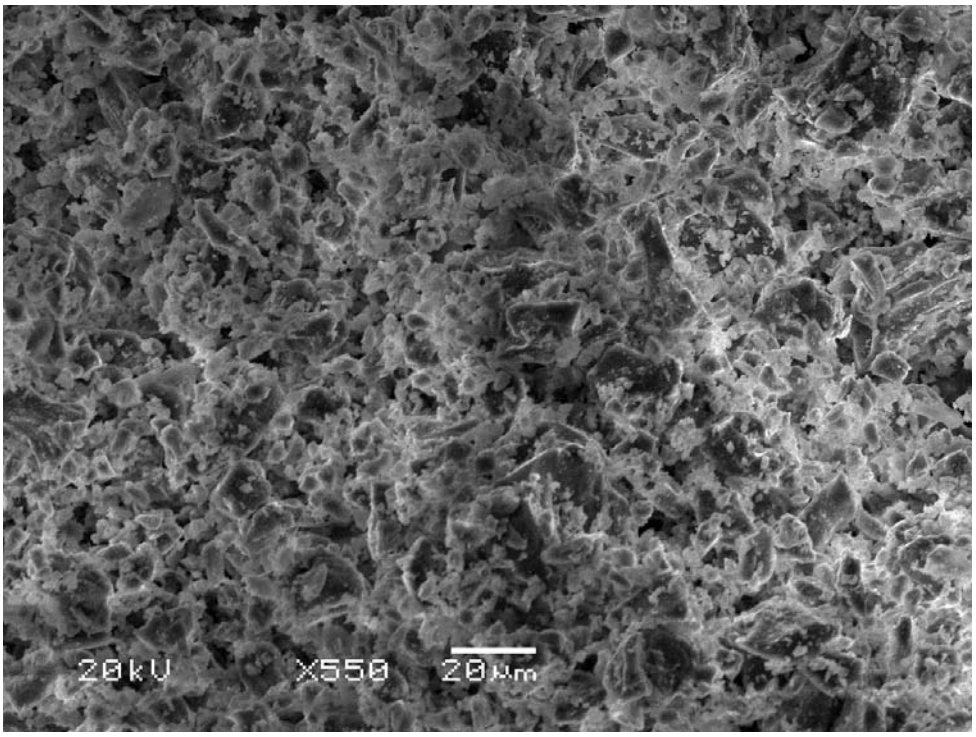

Figure 4.3 SEM image of OPC at 550-time enlargement.

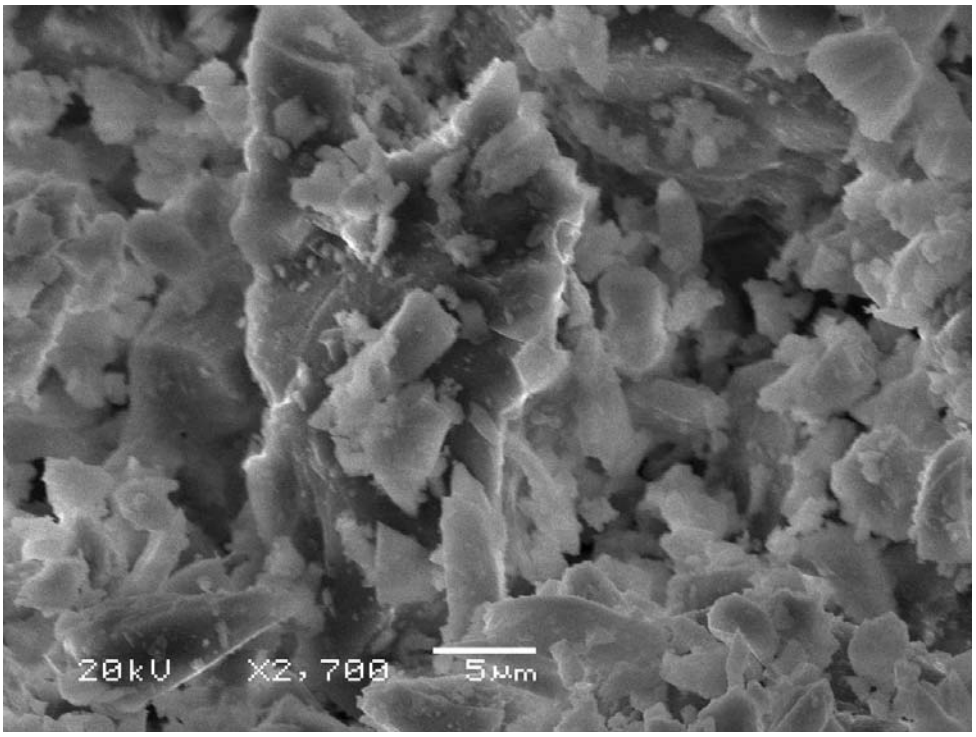

Figure 4.4 SEM image of OPC at 2700-time enlargement.

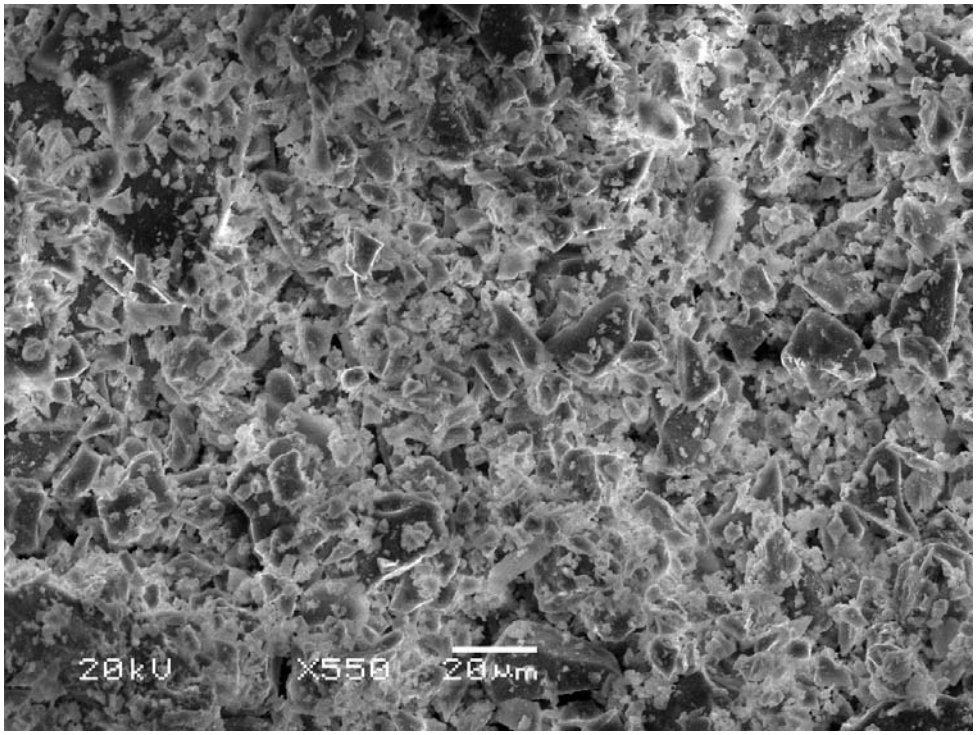

Figure 4.5 SEM image of BSC at 550-time enlargement.

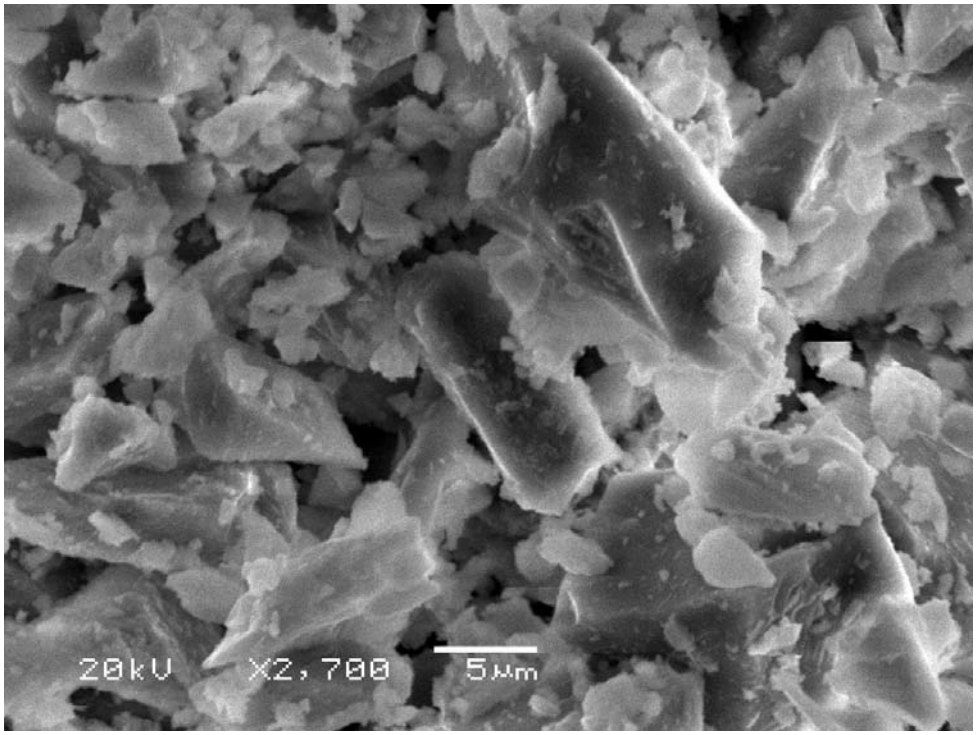

Figure 4.6 SEM image of BSC at 2700-time enlargement.

There are insignificant chloride contents in both cements. These chloride contents may partially induce background chloride concentrations in test specimens; however, their effect on the test results is slight due to comparatively high concentration NaCl solutions used in the tests.

Table 4.2 Chemical compositions and physical properties of OPC and BSC

Composition/Property	OPC	BSC
Silicon dioxide (SiO_2=S)	22%	26%
Aluminum trioxide (Al_2O_3=A)	5.5%	8.4%
Ferric trioxide (Fe_2O_3=F)	3%	2.1%
Calcium oxide (CaO=C)	64.2%	54.8%
Magnesium oxide (MgO)	1.5%	3.2%
Sulfur trioxide (SO_3)	2%	1.7%
Chloride (Cl)	0.007%	0.006%
C_3S[a]	47.2%	--
C_2S[a]	27.5%	--
C_3A[a]	9.5%	--
C_4AF[a]	9.1%	--
density (g/cm^3)	3.15	3.04
specific surface (cm^2/g)	3300	3800
water content (%)	27.5	28.9

[a]Calculation based on ASTM C150-81

4.3 MIX DESIGNS

There are three CB mix designs with their proportions shown in Table 4.3. Laser diffraction (LD) technique was used to determine the particle size distribution (PSD) of each mix design. Figure 4.7 shows the PSD curves of the three mixtures together with that of sodium bentonite.

Table 4.3 CB mix designs

Characteristic	Mix 1	Mix 2	Mix 3
Distilled water	80%	80%	80%
Sodium bentonite	5%	5%	10%
Cement	15% BSC	15% OPC	10% OPC
d_{50} (μm)[a]	13.4	14.0	10.6

[a]Obtained from laser diffraction technique

The mean particle size at 50% finer (d_{50}) of each CB mixture is also expressed in Table 4.3. Mix 3 has the lowest d_{50} value due to that fact that its bentonite content is higher than the other mixes. Mix 1 is the most important mixture since the majority of the column tests in the research have been performed on this mix design. Also, batch and diffusion testing described in Section 3.4.4 are all carried out with mix 1.

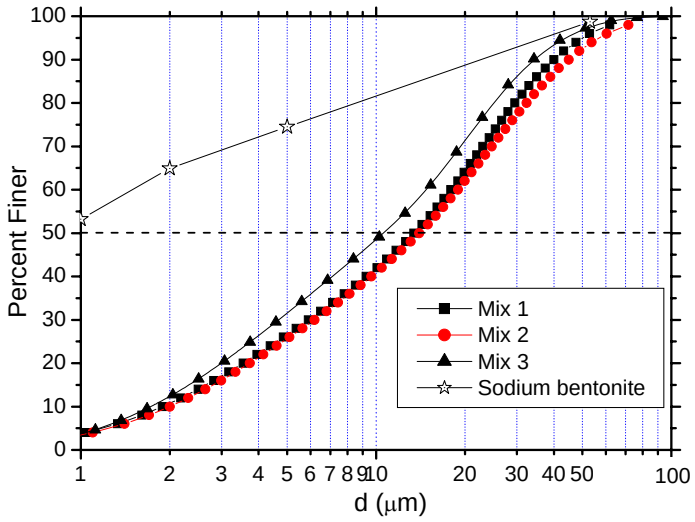

Figure 4.7 PSD curves of materials used.

4.4 EXPERIMENTAL RESULTS

4.4.1 Batch Testing

According to Section 3.4.4, the results of the two series of batch testing, without and with the cement retarder, are shown in Figure 4.8. Every single sample was agitated for 24 hours.

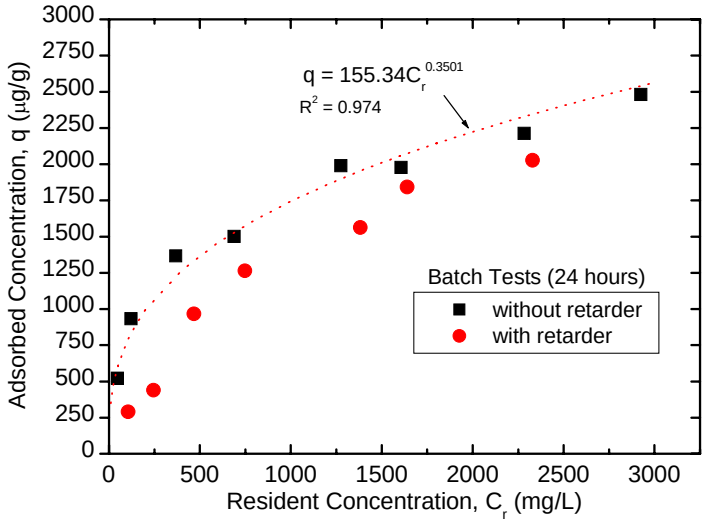

Figure 4.8 Adsorption isotherms from batch testing.

The results from the tests without the retarder agree well with Freundlich adsorption model (Equation 2.10) as shown in the figure. The degree of adsorption, as implied by the slope of the isotherm, tends to decrease when resident concentration increases. The second series also has the same inclination. This special series was done to study the effect of cement retarder which is frequently used in slurry wall construction. It is seen that the

additive lessens the degree of adsorption, especially at the low concentration level. In fact, even though the retarder was not used in the first series, the slurries in this series were not hardened, at least within the shaking period of 24 hours. This suggests that the cement hydration process was not working, or hardly working under the dynamic condition of batch testing for soils. It is known that the properties of CB materials also depend on the hydration of cement with pore fluid. Because the hydration did not work to harden any of the slurries, the two adsorption isotherms deduced from conventional batch testing may not give meaningful information for the design.

More realistic batch testing for cement-based materials may be referred to Tang and Nilsson (1993). The researchers mixed cement paste samples, cured them for a long period, ground the hardened samples into power, and then immersed the powered samples in solutions of different chloride concentrations. At the end of an immersion period, the equilibrium chloride concentration of each solution was determined. The study of Tang and Nilsson (1993) actually represents a kind of static batch testing which is different from conventional batch testing for soils conducted under agitation (Roy et al. 1991). This approach seems more appropriate for cement-based materials, for the samples are well cured before the introduction of solutions.

In addition, the order of mixing is also an important factor that controls the properties of CB materials (Fam and Santamarina 1996). Batch testing for soils uses the dry-mixing method; likewise in this research, the bentonite and cement had been mixed together before a solution was introduced. This method does not accord with the real construction of slurry walls which requires the full hydration of bentonite before any cement is added. On the other hand, column testing represents the wet-mixing method by prehydrating the bentonite and then adding cement. Thus, column testing has an advantage over batch testing in terms of mixing order.

4.4.2 Column Testing

Due to the fact that the properties of CB materials change with curing time, long-term column testing may not yield meaningful results regarding adsorption and hydrodynamic dispersion. In this research, it is convinced that if hydraulic conductivity changes, then adsorption and hydrodynamic dispersion parameters cannot remain constant as well. Therefore, most of the test columns were specially designed to have high permeability in order to complete the tests before any significant change in permeability would have occurred. Table 4.4 summarizes all the parameters from column testing.

Table 4.4 Summary of parameters from column testing

Test	Group	L (cm)	k (cm/s)	Porosity	v (cm/s)	C_o[a] (mg/L)	R_d	P_e	D (cm^2/s)	C_R (mg/L)
1	1SC5_v1	5	5.6×10^{-5}	0.909	6.2×10^{-4}	133.3	2.63	25.3	1.22×10^{-4}	91.1
2			5.6×10^{-5}	0.908	6.2×10^{-4}	332.5	2.20	30.03	1.03×10^{-4}	223.3
3			6.1×10^{-5}	0.909	6.7×10^{-4}	1030.5	1.61	45.06	7.45×10^{-5}	663.2
4			6.1×10^{-5}	0.908	6.7×10^{-4}	3518	1.33	103.12	3.26×10^{-5}	2075.7
5	1SC5_v2	5	5.6×10^{-5}	0.906	1.4×10^{-3}	149.3	2.77	25.03	2.72×10^{-4}	102.2
6			5.8×10^{-5}	0.900	1.4×10^{-3}	316.5	1.81	59.64	1.20×10^{-4}	197.8
7			5.2×10^{-5}	0.902	1.3×10^{-3}	1024.5	1.49	114.87	5.56×10^{-5}	597.7
8			5.4×10^{-5}	0.908	1.3×10^{-3}	3516	1.25	86.14	7.63×10^{-5}	2114.1
9	1SC28_v1	5	1.8×10^{-5}	0.896	4.0×10^{-5}	148.1	2.55	24.81	8.04×10^{-6}	101.5
10			1.8×10^{-5}	0.898	3.9×10^{-5}	318.8	2.18	32.30	6.11×10^{-6}	212.5
11			1.6×10^{-5}	0.893	3.5×10^{-5}	1034.9	1.37	80.37	2.17×10^{-6}	626.8
12			1.6×10^{-5}	0.895	3.5×10^{-5}	3522.7	1.18	65.14	2.71×10^{-6}	2181.2
13	1SC28_v2	5	1.7×10^{-5}	0.905	2.1×10^{-4}	147.3	1.71	60.26	1.71×10^{-5}	91.9
14			1.7×10^{-5}	0.890	2.2×10^{-4}	304.5	1.56	76.49	1.41×10^{-5}	185.4
15			1.5×10^{-5}	0.897	2.2×10^{-4}	1012.5	1.34	56.49	1.94×10^{-5}	636.4
16			1.3×10^{-5}	0.899	2.0×10^{-4}	3437	1.14	164.46	5.99×10^{-6}	1930.9
17	1SC28_v3	5	2.0×10^{-5}	0.908	5.0×10^{-4}	151.3	2.29	56.82	4.36×10^{-5}	95.0
18			2.8×10^{-5}	0.909	6.8×10^{-4}	320.5	1.93	58.58	5.79×10^{-5}	200.7
19			2.6×10^{-5}	0.904	6.4×10^{-4}	1024.5	1.53	75.99	4.19×10^{-5}	624.2
20			2.3×10^{-5}	0.895	5.1×10^{-4}	3509	1.30	114.08	2.24×10^{-5}	2048.6
21	1SC28_v4	5	2.3×10^{-5}	0.923	1.2×10^{-3}	322.5	1.81	44.68	1.36×10^{-4}	207.7
22			2.5×10^{-5}	0.898	1.4×10^{-3}	3472	1.25	138.36	4.89×10^{-5}	1986.3
23	1SC60_v1	5	9.9×10^{-6}	0.900	6.3×10^{-4}	142.3	1.21	49.15	6.38×10^{-5}	90.7
24			1.3×10^{-5}	0.906	6.0×10^{-4}	305.5	1.41	83.49	3.56×10^{-5}	184.3
25			1.3×10^{-5}	0.906	5.9×10^{-4}	1015.5	1.27	130.68	2.26×10^{-5}	584.5
26			1.5×10^{-5}	0.911	6.6×10^{-4}	3516	1.22	99.50	3.31×10^{-5}	2082.3
27	1SC60_v2	5	9.3×10^{-6}	0.900	1.3×10^{-3}	331.5	1.28	113.77	5.56×10^{-5}	193.6
28			9.2×10^{-6}	0.897	1.3×10^{-3}	3474.1	1.16	111.9	5.59×10^{-5}	2032.3
29	2PC28_v1	5	3.5×10^{-5}	0.886	5.5×10^{-4}	169.3	2.46	35.7	7.72×10^{-5}	111.6
30			2.8×10^{-5}	0.892	4.3×10^{-4}	334.5	2.05	56.54	3.84×10^{-5}	210.2
31			3.6×10^{-5}	0.898	5.6×10^{-4}	1041.5	1.52	64.74	4.33×10^{-5}	645.3
32			3.2×10^{-5}	0.893	5.1×10^{-4}	3521	1.28	116.57	2.18×10^{-5}	2050.9
33	2PC28_v2	5	3.3×10^{-5}	0.900	1.3×10^{-3}	336.1	1.91	110.39	5.83×10^{-5}	196.9
34			3.4×10^{-5}	0.894	1.3×10^{-3}	1046.5	1.47	86.91	7.59×10^{-5}	628.6
35			3.1×10^{-5}	0.894	1.2×10^{-3}	3490.6	1.31	92.2	6.67×10^{-5}	2083.9
36	3PC28_v1	3	4.5×10^{-7}	0.882	2.8×10^{-4}	346.7	1.18	27.76	2.98×10^{-5}	234.8
37			3.7×10^{-7}	0.895	2.1×10^{-4}	3517.4	1.12	50.78	1.22×10^{-5}	2235.6
38	2PC28_n	2.37	8.0×10^{-8}	0.819	-	-	-	-	-	-
39		2.71	4.0×10^{-7}	0.834	-	-	-	-	-	-
40		3.06	3.3×10^{-7}	0.855	-	-	-	-	-	-
41		3.39	1.7×10^{-7}	0.868	-	-	-	-	-	-
42	1SC28_n	3.35	1.1×10^{-6}	0.887	1.9×10^{-4}	1029.8	1.03	15.98	4.03×10^{-5}	740.7

[a]Chloride source concentrations, already corrected for background concentrations

Note: From the second column, prefix 1, 2, or 3 = mix 1, 2 or 3. SC = blastfurnace slag cement. PC = ordinary Portland cement. 5, 28 or 60 = 5, 28 or 60 days curing. v? = seepage velocity no. ?. n = study on porosity

In Table 4.4, all the test columns have a diameter of 6 cm. Columns 36 and 37, with comparatively low k values, were made shorter than columns 1 to 35 in order to minimize test durations. Columns 38 to 42 were specially designed to study the effect of porosity change on CB transport parameters (Section 3.4.11). It should be emphasized that the typical hydraulic conductivity of CB mixtures, without special additives, varies from 10^{-5} to 10^{-7} cm/s (Fratalocchi et al. 1996). Most columns in the table have k values above the range.

The confining stress is another important factor that influences the hydraulic conductivity of CB mixtures. Manassero et al. (1995) reported that, for confining stress ranging from 100 kPa to 10 MPa applied on 28-day cured CB samples, the hydraulic conductivity varied between 5×10^{-6} and 5×10^{-8} cm/s. From Table 4.4, most of the tests were conducted at 30 kPa confining stress. The maximum confining stress of 200 kPa was applied to only columns 36 and 37. It was observed that there was no significant change in hydraulic conductivity during any tests. This observation is confirmed by data from Shackelford and Jefferis (2000) which showed no significant drop in the hydraulic conductivity of highly-permeable CB samples at low pore volumes of flow under a confining stress of 30 kPa.

Effluent Breakthrough Curve

In Table 4.4, forty-two tests are divided into various groups. Grouping is done by considering mix design, curing time, hydraulic conductivity k, and seepage velocity v, respectively. Except group 2PC28_n and column 42, at least 2 levels of chloride source concentrations C_o were studied in each group. Most of the groups were investigated with 4 levels of source concentration. The parameters R_d and P_e were obtained from regression analyses using cumulative mass approach (Section 2.6.2). After obtaining P_e, the D parameter resulted from Equation (2.27). The reference concentration C_R for each test was calculated by either Equation (3.6) or (3.7). Although some column Peclet numbers in the table are more than 100, it is assumed that Equation (3.7) is still applicable, for the maximum P_e value is 164.46, leading to $C_R = 0.56C_o$, which is still reasonable ($> 0.50C_o$).

Figures 4.9 to 4.19 show the effluent breakthrough curves of chloride ions at different source concentrations. Cumulative mass approach like Figures 2.15 and 2.16 are not shown because the breakthrough curve rather provides a more vivid picture of solute migration from the beginning to the end of the test. Theoretical curves in Figures 4.9 to 4.19 are generated by Equation (2.22) using R_d and D from cumulative mass approach.

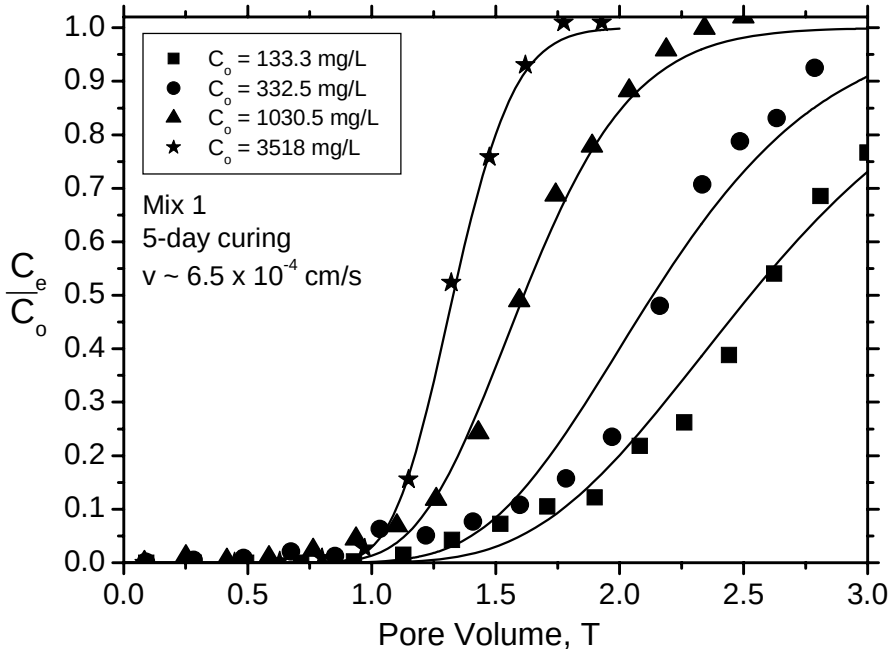

Figure 4.9 Breakthrough curves of 1SC5_v1.

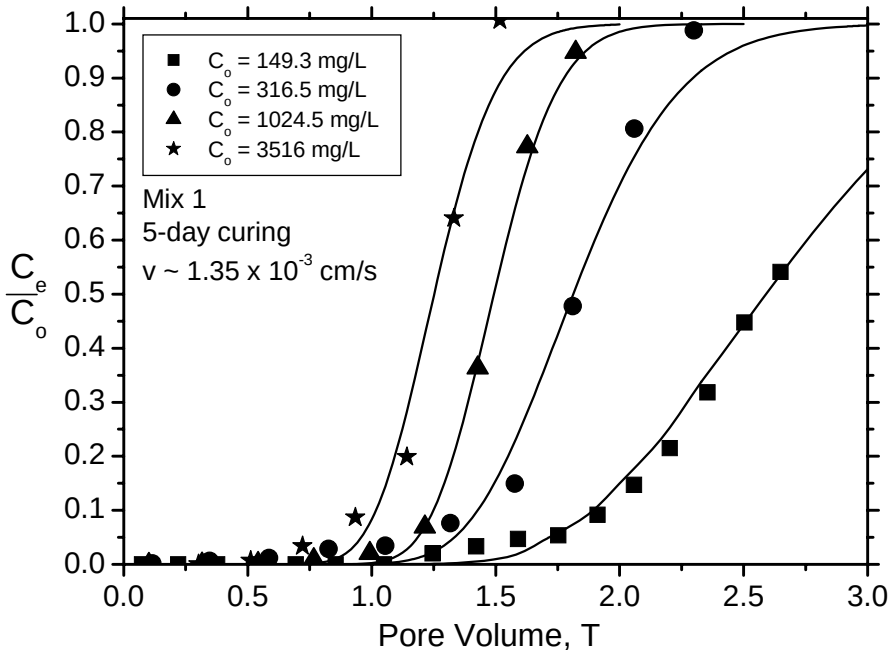

Figure 4.10 Breakthrough curves of 1SC5_v2.

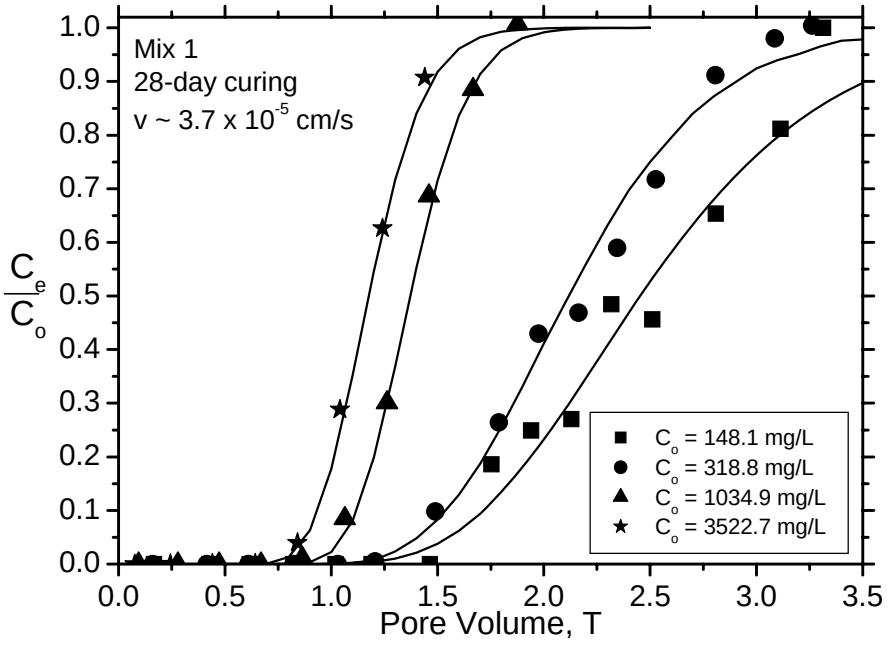

Figure 4.11 Breakthrough curves of 1SC28_v1.

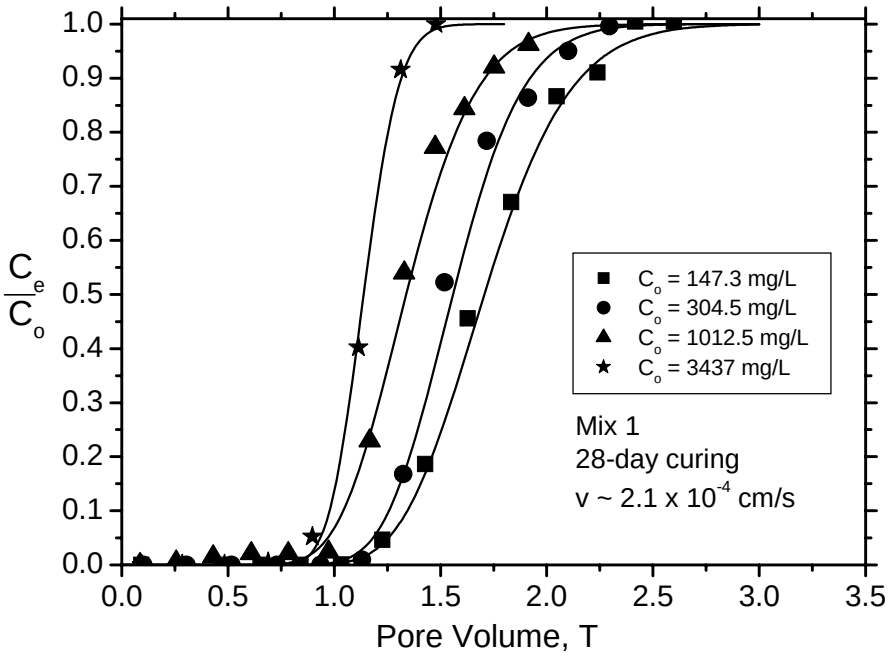

Figure 4.12 Breakthrough curves of 1SC28_v2.

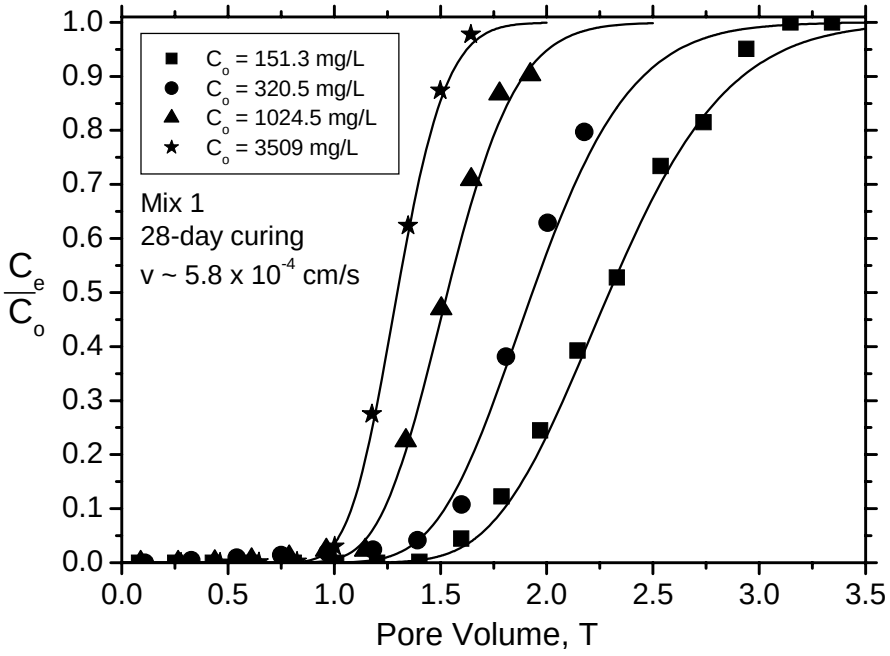

Figure 4.13 Breakthrough curves of 1SC28_v3.

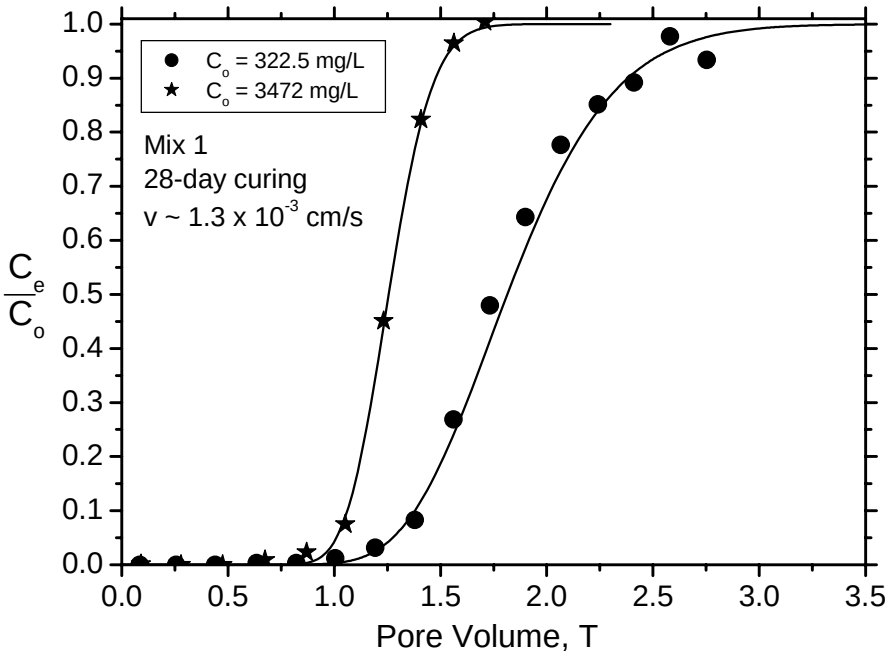

Figure 4.14 Breakthrough curves of 1SC28_v4.

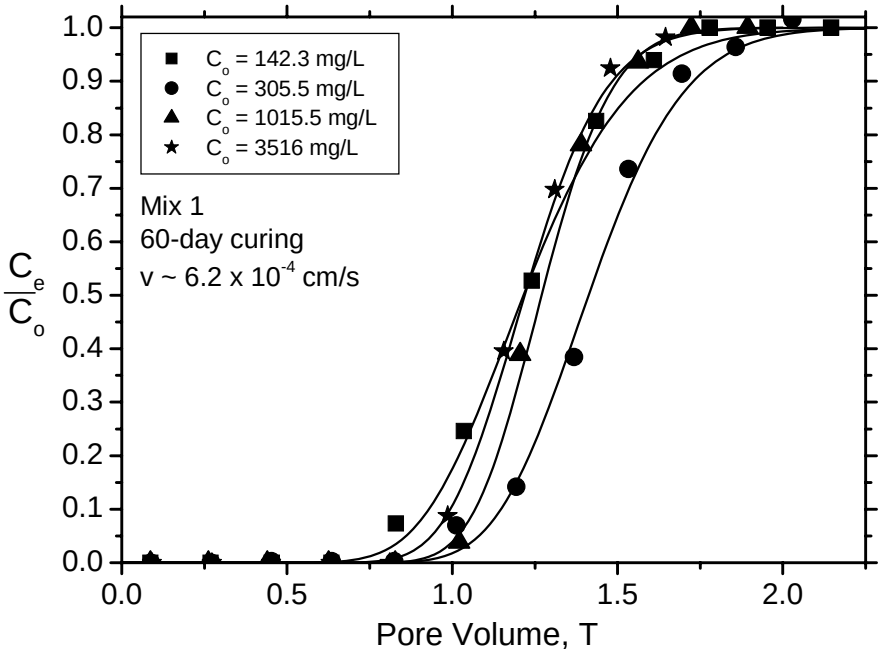

Figure 4.15 Breakthrough curves of 1SC60_v1.

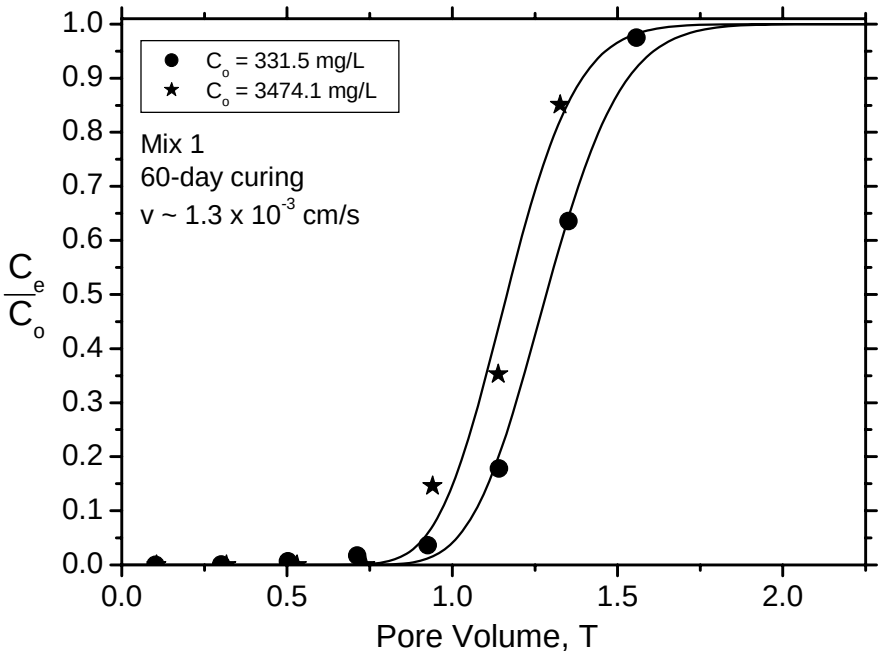

Figure 4.16 Breakthrough curves of 1SC60_v2.

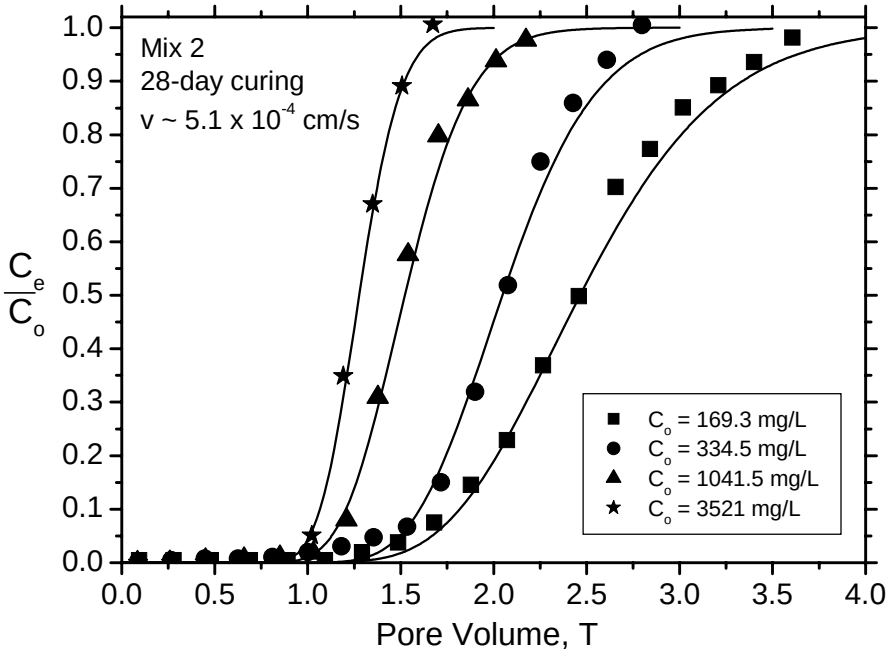

Figure 4.17 Breakthrough curves of 2PC28_v1.

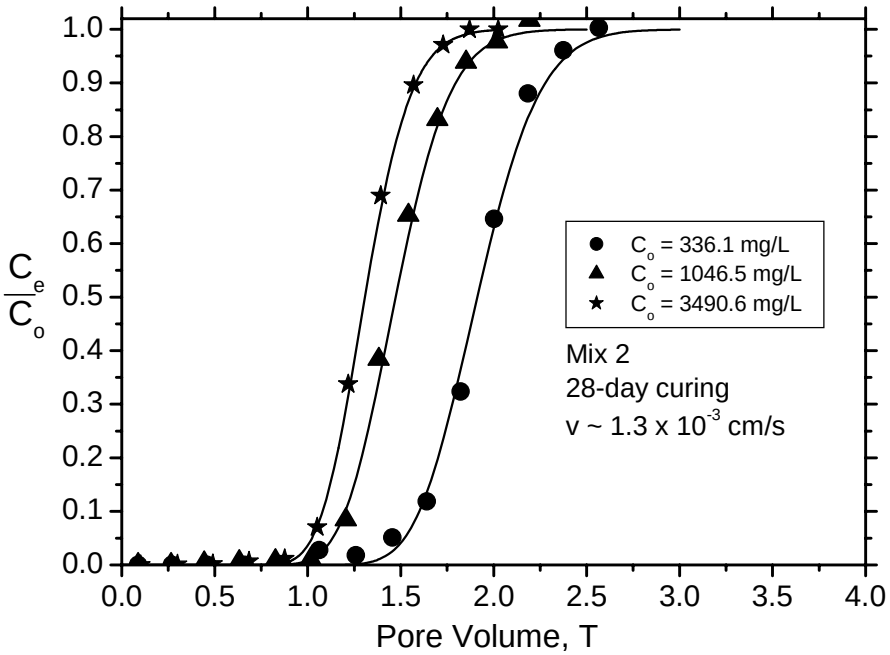

Figure 4.18 Breakthrough curves of 2PC28_v2.

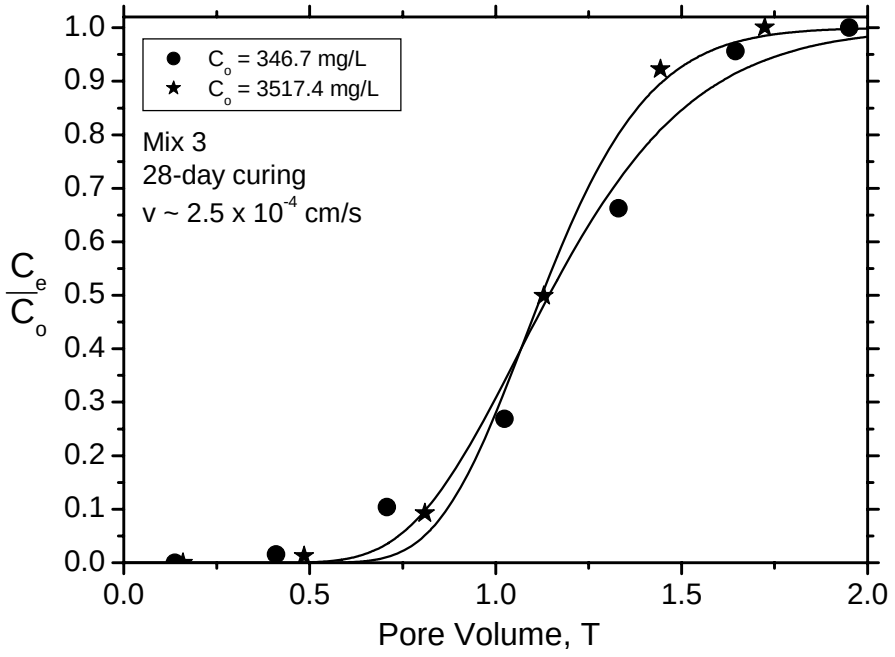

Figure 4.19 Breakthrough curves of 3PC28_v1.

4.5 EFFECT OF EFFECTIVE POROSITY IN COLUMN TESTING

According to Section 3.4.6, the use of effective porosity n_e instead of total porosity n from water content can increase both R_d and D parameters interpreted from column testing by the factor n/n_e. The average total porosity in Table 4.4, excluding columns 38 to 42, is about 0.9. If an average effective porosity is assumed to be 0.8 (see Fratalocchi et al. 1996), then the R_d and D values will increase by about 12.5%. This slight increase is considered insignificant in this research, and more attentions are paid to the trends of transport parameters, under diverse selected factors.

4.6 COLUMN TESTING AT LOW SEEPAGE

4.6.1 Column Adsorption Isotherm versus Batch Isotherms

Seen in Table 4.4, group 1SC28_v1 (Figure 4.11) has the lowest average seepage velocity of about 3.7×10^{-5} cm/s. It is noticeable that all the D values in this group fall in the typical range of D^* (Mitchell 1991), with the maximum value of 8.04×10^{-6} cm^2/s. Thus, this group is believed to be diffusion-dominated. It will also be confirmed in Section 4.12 that the magnitude of seepage in 1SC28_v1 did not allow mechanical dispersion to occur. The next

step is to construct a column adsorption isotherm in this diffusion-dominated condition, and compare the column isotherm with the isotherms from batch testing in Section 4.4.1.

With the same material and curing period and approximately the same k and v, the varied R_d values in 1SC28_v1 can be explained in terms of resident concentrations that increased inside the samples. The R_d values are seen decreasing when reference concentration increases. This behavior is similar to a number of literatures on batch testing which show that R_d decreases with increasing concentration, for a concave adsorption isotherm (Figure 2.8). The average dry density ρ_d from the four samples is 0.265 g/cm^3, and the average total porosity is about 0.9. By adopting Freundlich model in the form of Equation (2.12), Freundlich parameters K and ε were obtained by nonlinear regression of (C_R, R_d) data. The resultant column adsorption isotherm, or perhaps called adsorption characteristic (see Yong et al. 1992), is shown in Figure 4.20, together with the results from batch testing.

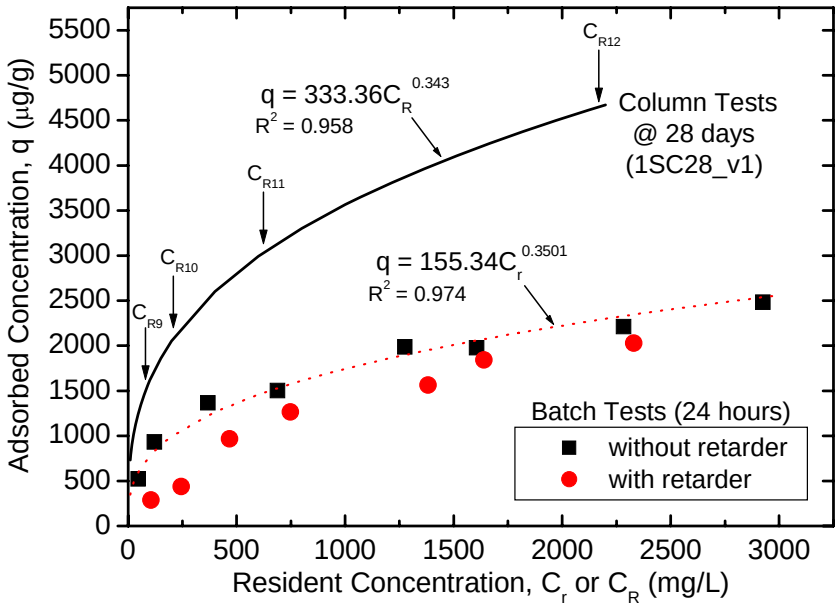

Figure 4.20 Adsorption isotherms from column testing and batch testing.

The coefficient of determination is as good as 0.958. The column adsorption isotherm at 28 days gives higher R_d values as seen by the slope of the solid curve. Even though the solid:solution ratios in the batch tests and 1SC28_v1 were equal, the difference in the isotherms obviously comes from the different conditions of the tests. Easy speaking, column tests were conducted after curing the samples whereas batch testing did not allow curing under shaking condition. Due to static curing process, the properties of CB columns

gradually change as time goes by. It is discussed in Sections 4.7 and 4.10 that parameters k, D and R_d are not constant with time.

The column adsorption isotherm in Figure 4.20 will be applied to two diffusion tests of the same material (mix 1, 28 days curing) in Chapter 5. This is to provide more evidence regarding the applicability of the adsorption isotherm developed from the proposed method.

4.6.2 Concentration-Dependent Diffusion and Tortuosity

In Figure 4.11, columns 9 and 10 which were tested at comparatively low concentration levels have more spreading breakthrough curves, leading to higher values of D seen in Table 4.4. In contrast, columns 11 and 12 with higher source concentrations show less spreading curves and thus lower D values. The values of D^* of most chemical species are in the range of ~ 2 x 10^{-6} cm^2/s to ~ 2 x 10^{-5} cm^2/s (Mitchell 1991). All the D values in 1SC28_v1 fall in this range, so it would suggest that the seepage velocities used were low enough that mechanical dispersion did not occur. It is confirmed in Section 4.12 that mechanical dispersion is inert at v approximately below 1 x 10^{-4} cm/s.

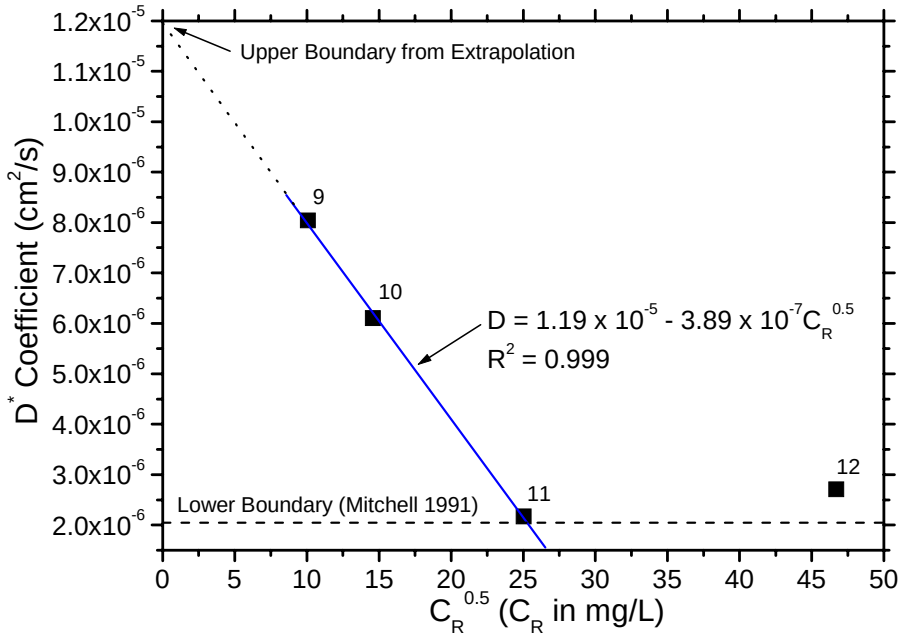

Figure 4.21 Effective diffusion coefficient versus reference concentration.

The effect of ion concentration on diffusion through clay was studied by Achari et al. (1997). The researchers showed that the effective diffusion coefficient D^* of an ionic solution through a clay bed declines linearly with the square root of resident concentration, for a specific concentration range. Also, Chatterji (1999) illustrated that the diffusion

coefficient of chloride ions in cement mortar specimens decreases with the square root of concentration. Both studies are steady-state diffusion experiments. In this research, because the combination of bentonite and cement are experimented, the diffusion phenomenon would be substantiated by the previous two researches. Despite the fact that column testing is a transient-state experiment, the D (or D^*) values in 1SC28_v1 also decrease linearly with the square root of C_R up to the root of 626.8 mg/L, with a high determination coefficient of 0.999 (Figure 4.21).

That column 12 has its D^* value slightly greater than column 11 is attributed to two reasons. First, because breakthrough curves at high P_e values, between 50 and 100, have little difference in shape, slight difference from data coordinates can result in a different regressed P_e value. Second, the lower boundary reported by Mitchell (1991) may suggest that a D^* value rarely goes below 2×10^{-6} cm^2/s. From Figure 4.21, a D^* value at infinite dilution can be obtained by extrapolating the straight line in the figure to the y-axis (Achari et al. 1997). This y-intercept, valuing 1.19×10^{-5} cm^2/s, represents an upper boundary for the D^* coefficient of chloride in this study. It can be observed that the upper bound value is also in the typical range of D^* i.e., less than 2×10^{-5} cm^2/s.

It should be noted that Achari et al. (1997) defined the D^* coefficient as a function of resident concentration by using a "local-value" approach. They separated each clay sample into segments, measured the resident concentration in each segment, and calculated the corresponding effective diffusion coefficient. In this research, because column testing is considered as a single-element model which yields averaged transport parameters, the method to relate those parameters to an averaged resident concentration would be considered as a "global-value" approach. The single-element or global-value approach has been substantiated clearly by Figures 4.20 and 4.21 in which the determination coefficients are very satisfactory.

In Section 2.4.5, it is said that apparent tortuosity factor τ_a can be considered as a ratio of D^* over D_o. Because Figure 4.21 represents D^* values, τ_a values can be obtained by dividing y-axis by the D_o of chloride which is 2.03×10^{-5} cm^2/s (Table 2.1). Figure 4.22 shows the transformed version of Figure 4.21. The maximum τ_a at infinite dilution is 0.59, and τ_a decreases linearly with increasing concentration and approaches a steady value of about 0.12. In other words, tortuosity is a function of concentration. The effect of concentration on tortuosity would be regarded as the combination of fluidity factor and electrostatic interaction factor (see Rowe et al. 1995b).

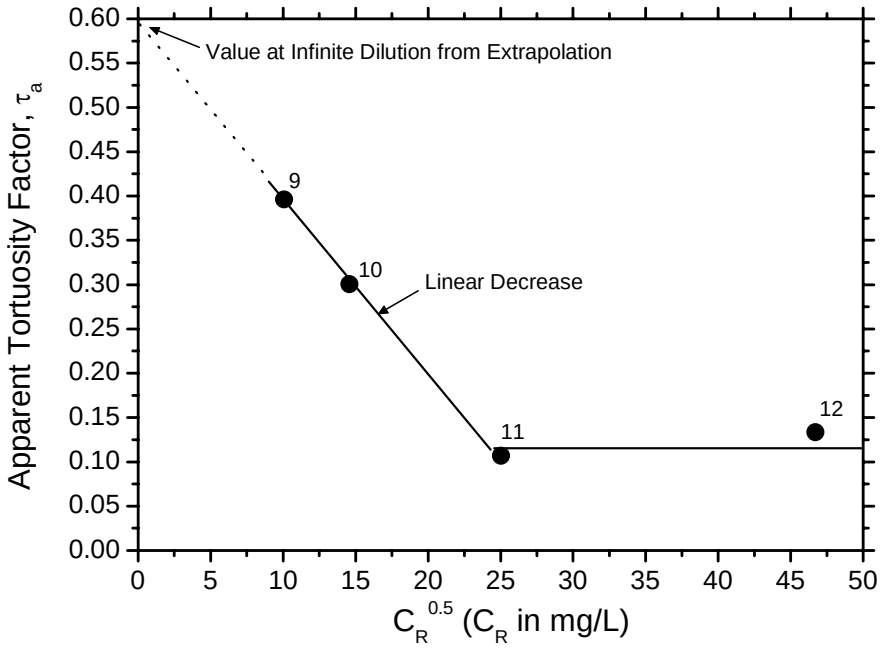

Figure 4.22 Apparent tortuosity factor as a function of concentration.

4.7 EFFECTS OF CURING, MIX DESIGN, AND CONCENTRATION ON HYDRAULIC CONDUCTIVITY

Figure 4.23 shows the relationship between hydraulic conductivity and curing time. There are 37 data points corresponding to columns 1 to 37. It should be noted that each data point represents one column test at a specific time. For example, column 18 was cured under distilled water for 28 days and then permeated with NaCl solution to find k, R_d and D under a seepage velocity of 6.8 x 10^{-4} cm/s.

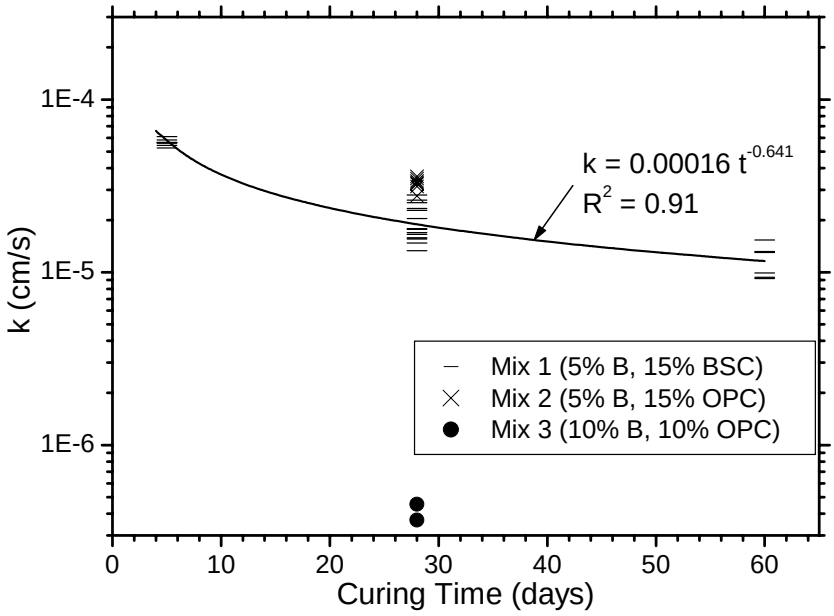

Figure 4.23 Hydraulic conductivity of CB mixtures versus curing time.

During any tests, it was observed that k values before and after injecting NaCl into the test system were more or less identical. The k values during the permeation of NaCl solution showed negligible variation from the beginning to the end of the test. This suggests that no significant modification in pore structures occurred during the NaCl permeation. As a result, each k value in Figure 4.23 is an average of marginally-varied k values during the permeation of NaCl solution.

In the study of Suryavanshi et al. (1995a), the addition of NaCl to OPC mortars decreased the accessible pore volumes observed by SEM. There are two reasons that could explain the difference between their research and this research. Firstly, in their research, NaCl was added to the mortars at the time of mixing, so the reaction between NaCl and the mortars started from the mixing and continued with the curing of the mortars. The longer reaction could effectively change the pore structures of the mortars. Second, in this research, the reaction between NaCl and CB in each test occurred under a seepage velocity. This dynamic condition lessens chemical activities, especially adsorption, in the specimen. This will be discussed in Section 4.8.

At 28 days curing, mix 2 gives slightly higher k values than mix 1. Because both mixes have the same water content and bentonite content, the lower k values in mix 1 are visibly due to the existence of blastfurnace slag (BS). When comparing mixes 2 and 3, a drop in k values by about 100 times is mainly attributed to an increase in bentonite content. A drop in OPC content would slightly affect the k values, but effectively change the rate of reduction in them (see Fratalocchi and Pasqualini 1998).

Considering mix 1, there are noticeable variations in k values at 28 and 60 days curing. This firstly could be due to the sample preparation process. Second, it was observed that columns that were molded latter had lower k values compared with those molded earlier. It would suggest that there was slight prehydration of the cement and/or bentonite caused by moisture in the air despite the careful storage of both materials in entirely covered boxes. Nevertheless, the reduction in k values with time of mix 1 is fairly fitted by power law though the data points are from separate column tests. The permeability reduction is mainly due to carbonation reaction. This reaction is described in Section 4.10.

4.8 EFFECT OF VELOCITY ON ADSORPTION AND HYDRODYNAMIC DISPERSION

In order to study the effect of seepage velocity, columns with the same age and approximately the same k are plotted together as depicted in Figures 4.24 and 4.25.

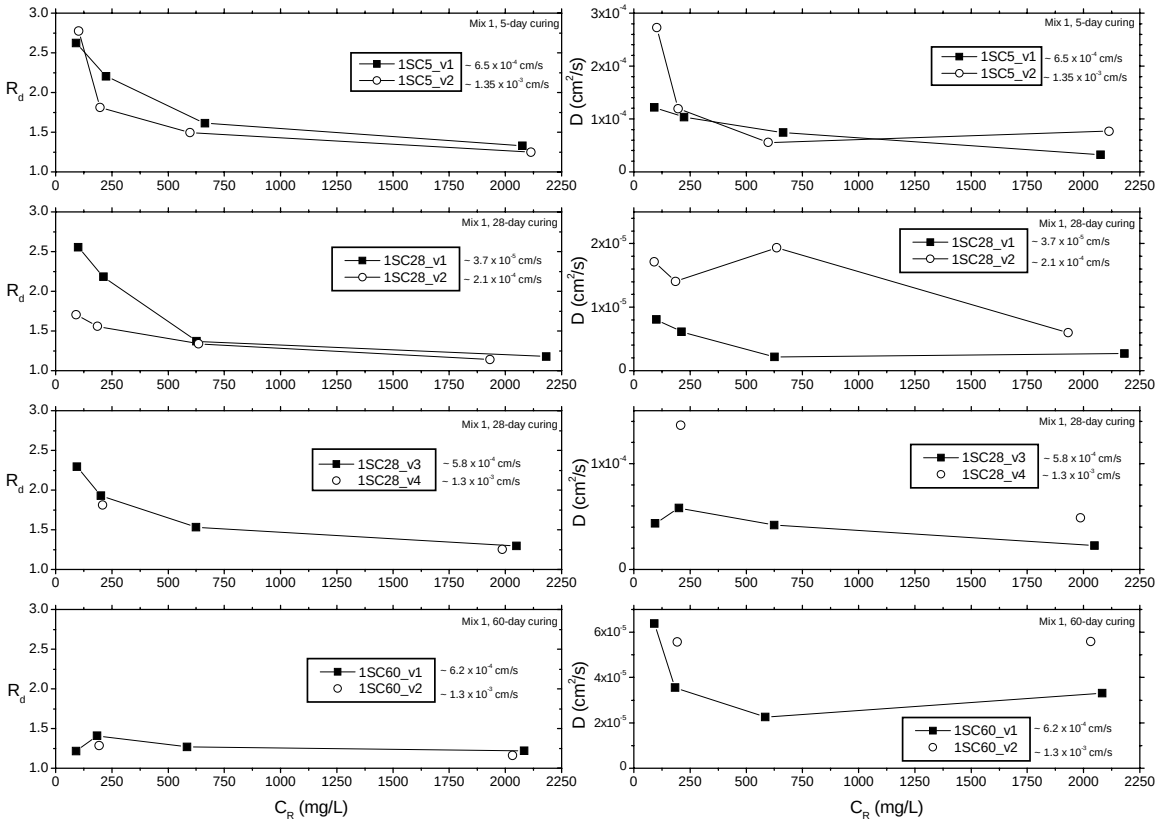

Figure 4.24 Effects of seepage velocity and concentration on R_d and D; mix 1.

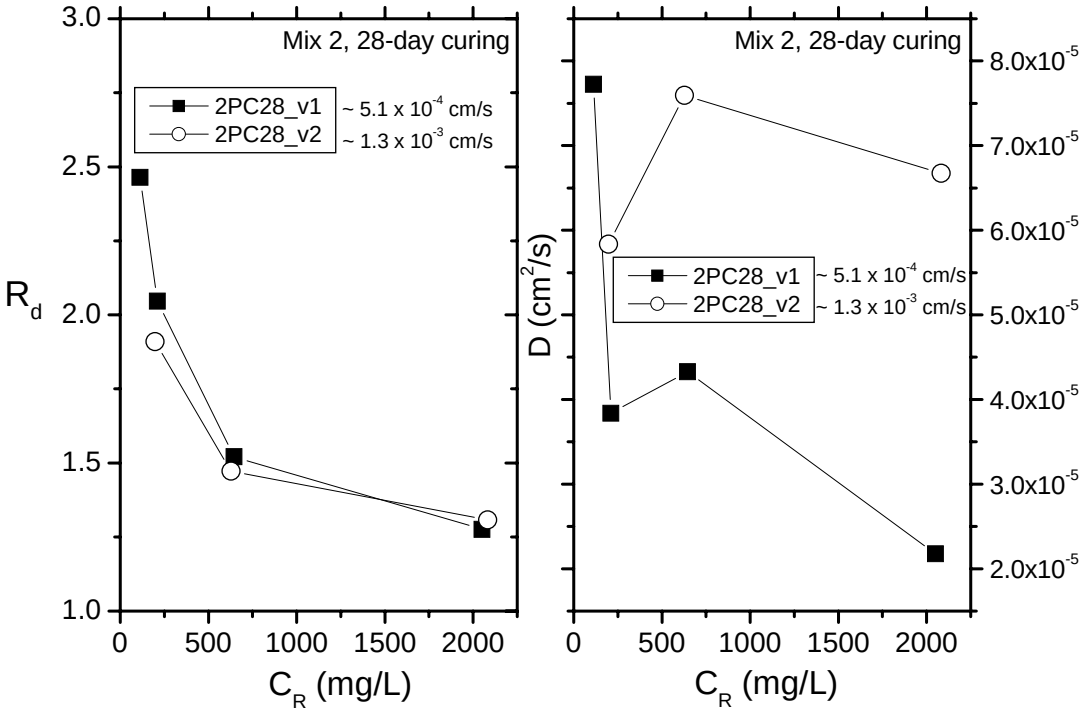

Figure 4.25 Effects of seepage velocity and concentration on R_d and D; mix 2.

Groups 1SC28_v1 and 1SC28_v2 are not plotted with groups 1SC28_v3 and 1SC28_v4 despite the same age because the former groups have lower k values probably due to the reasons discussed in Section 4.7.

The effect of velocity is observable in vertical direction, not horizontal direction. Figures 4.24 and 4.25 clearly show that when v increases, R_d naturally decreases due to the shortened reaction time between chloride and CB. This phenomenon is in accordance with many literatures concerning solute transport through clayey barriers. Comparing 1SC28_v2 with 1SC28_v3, although 1SC28_v2 has lower average seepage, its R_d values appear lower than those of 1SC28_v3. It is evident that the lower R_d values in 1SC28_v2 are attributed to lower k values. Mentioned in Section 4.7, the lower k values are probably due to the prehydration of cement and/or bentonite. As well known that chloride is nonreactive to clayey soils, the adsorption of chloride ions is owing to the cement phase (Suryavanshi et al. 1996). Consequently, the lower adsorption in 1SC28_v2 would rather come from the prehydration of cement with air moisture. The more the cement hydration, the lower the adsorption of chloride. This point will be discussed again in Section 4.11.

For hydrodynamic dispersion, Figures 4.24 and 4.25 illustrate that, at the same concentration level, when v increases, D also tends to increase. Only D values at about 625 mg/L in the uppermost right graph of Figure 4.24 are in inverse trend, probably due to the scatter in concentration data. It is well known that the increase in D parameter with seepage is because of mechanical dispersion (Section 2.4.6). Most seepage velocities used in Figures 4.24 and 4.25 are beyond the yielding velocity at which the mechanical dispersion starts prevailing. The effect of increasing v on D will be discussed in Section 4.12.

4.9 EFFECT OF CONCENTRATION ON ADSORPTION AND HYDRODYNAMIC DISPERSION

The effect of concentration on R_d and D must be investigated at the same velocity. Seen in Figures 4.24 and 4.25 are generally the drops in R_d and D when C_R increases. Higher adsorption rate at low concentration level corresponds with many literatures on batch testing; that is, when concentration increases, adsorption rate decreases due to the concave adsorption isotherm.

Delagrave et al. (1997) studied the chloride binding capacity of diverse hydrated cement paste systems. The researchers adopted the procedure developed by Tang and Nilsson (1993) by mixing paste samples, curing them for a long period, grinding the hardened specimens into powder, and then immersing the powered samples in solutions of different

chloride concentrations. At the end of immersion period, the equilibrium chloride concentration of each solution was determined. By this static batch testing, it was concluded that the binding of chloride with hydrated cement products is concentration-dependent and can be represented best by Freundlich concave isotherm. It is shown herein that even though column testing is different from batch testing in terms of procedure and interpretation, the nonlinear adsorption behavior does exist in column testing when relating R_d to C_R. In Section 4.6.1, the column adsorption isotherm in diffusion-dominated condition (1SC28_v1) can also be fitted to Freundlich model. The (C_R, R_d) data points of other groups in Table 4.4 could also be transformed into isotherms if needed.

Hydrodynamic dispersion also decreases when concentration increases. One could say without any complicated theory that, under high concentration, solute particles interfere one another and thus proceed slower. In Section 4.6.2, The D values of 1SC28_v1 are found decreasing linearly with increasing concentration under diffusion-dominated condition. From Table 4.4, except 1SC28_v1, 1SC28_v2 and column 37, all other columns have D values higher than the typical range of D^*. This suggests that mechanical dispersion occurred in the majority of the tests. Nevertheless, it will be clarified in Section 4.12 that only group 1SC28_v1 is believed to be purely diffusion-dominated. Figures 4.24 and 4.25 reveal that under mechanical dispersion the D parameter also depends on concentration level. All the groups apart from 1SC28_v1 show the decrease in D when C_R increases. Noticeable fluctuations of D are seen in groups 1SC28_v2, 1SC28_v3, 2PC28_v1 and 2PC28_v2. The fluctuation in 1SC28_v2 would rather come from the scatter in concentration data than from seepage velocities. Appearing low, the first D value in 1SC28_v3 and the second D value in 2PC28_v1 would be owing to the lowest seepage velocities when compared with other columns in the same groups. The first low D value in 2PC28_v2 may have come from the sensitivity of regression in the high-P_e range.

In short, it could be said that at the same velocity, different concentrations used in column testing lead to different D and R_d values. The higher concentration is used, the less adsorption and hydrodynamic dispersion become.

4.10 EFFECT OF CURING ON ADSORPTION AND HYDRODYNAMIC DISPERSION

Figure 4.26 shows the effect of curing at the same velocities. The upper graphs have an average seepage velocity of about 6×10^{-4} cm/s, and the lower ones have an average velocity of about 1.3×10^{-3} cm/s. Curing effect can be seen in vertical direction.

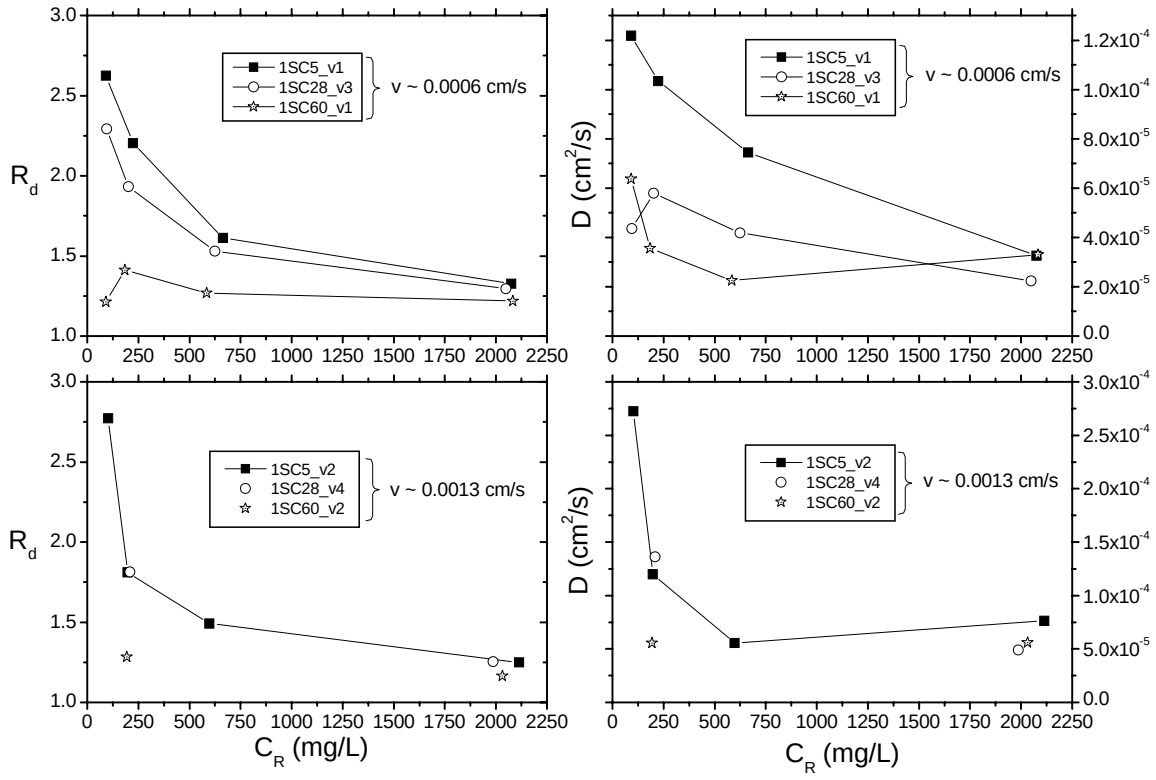

Figure 4.26 Effect of curing on R_d and D; mix 1.

It is seen that, at the same velocity, R_d and D values are lowered when curing time increases. Drops in both parameters are remarkable at low concentration levels, but slight at high concentrations. The degree of chloride adsorption decreases because the reaction between chloride ions and cement phase becomes less at longer curing periods. The chloride binding mechanism will be discussed in Section 4.11.

For hydrodynamic dispersion, the decreases in D values with time should be related to the pore structure of CB material. It is well known that CB pore structure gradually changes by cement hydration (see Fratalocchi et al. 1996). Chemical reactions such as carbonation do make the pore structure denser; therefore, this firstly contributes to the permeability reduction in Figure 4.23, and secondly the denser pore structure makes the transport of chloride ions more difficult. Calcium oxide CaO or lime is a major component in cements (Table 4.2). At room temperature, when lime is mixed with water, it forms calcium hydroxide $Ca(OH)_2$ called slaked lime.

$$CaO\ (s) + H_2O\ (l) \rightarrow Ca(OH)_2\ (s) \qquad (4.1)$$

The reaction of $Ca(OH)_2$ with carbon dioxide CO_2 in the pore liquid results in the deposition of calcium carbonate $CaCO_3$ in the pores. This reaction is known as carbonation.

$$Ca(OH)_2\ (s) + CO_2\ (g) \rightarrow CaCO_3\ (s) + H_2O\ (l) \qquad (4.2)$$

The carbonation reaction may require months or years to be completed. In the mean time, if there is the leaching of CaO from the cement (e.g., by seepage), this mechanism would be expected to diminish the carbonation and thus change the rate of reduction in permeability and hydrodynamic dispersion. In this research, because the column tests were performed in short durations, the leaching of CaO and/or other cement hydrated products are supposed to be negligible. Consequently, the reductions in both hydraulic conductivity and hydrodynamic dispersion with curing time may be mainly attributed to the degree of carbonation in the CB columns.

It should be noted again that the parameters in Figure 4.26 were obtained by using total porosities. The total porosities from water contents are almost the same despite different curing periods. If real effective porosities were used in Figure 4.26, the graphs would shift up slightly. For example, if effective porosities are assumed to be 0.85 and 0.7 at 5-day and 60-day curing, respectively, R_d and D values at 5-day curing will increase by 5.88% and those values at 60-day curing will increase by 28.57%. These increases (not shown) do not change the conclusion from the figure that adsorption and hydrodynamic dispersion reduce by curing time.

4.11 CHLORIDE BINDING IN CEMENT-BENTONITE MIXTURES

In general, chloride ions are nonreactive to clays. It should be cement phase that is responsible for chloride binding. In the study of chloride binding in mortars containing NaCl added during mixing (internal binding), Suryavanshi et al. (1996) found that the majority of chloride ions are bound by adsorption mechanism (~85%), and a fraction of them are bound by anion-exchange mechanism (~15%). Both mechanisms form a chloro-complex, $C_3A.CaCl_2.10H_2O$, or called Friedel's salt which is the result of reaction between chloride and C_3A at room temperature. Besides Friedel's salt, the reaction between chloride and C_4AF also forms another chloro-complex, $C_3F.CaCl_2.10H_2O$ whose crystalline phase is iso-structural to Friedel's salt (Suryavanshi et al. 1995b).

In addition, the studies of external chloride binding (specimens first cured and then immersed in solutions) give a conclusion that the total amount of bound chlorides is related to

the total aluminate content, C_3A and C_4AF (Delagrave et al. 1997). In this research, chloride binding is considered external because the CB specimens had been cured before the permeation of NaCl solution.

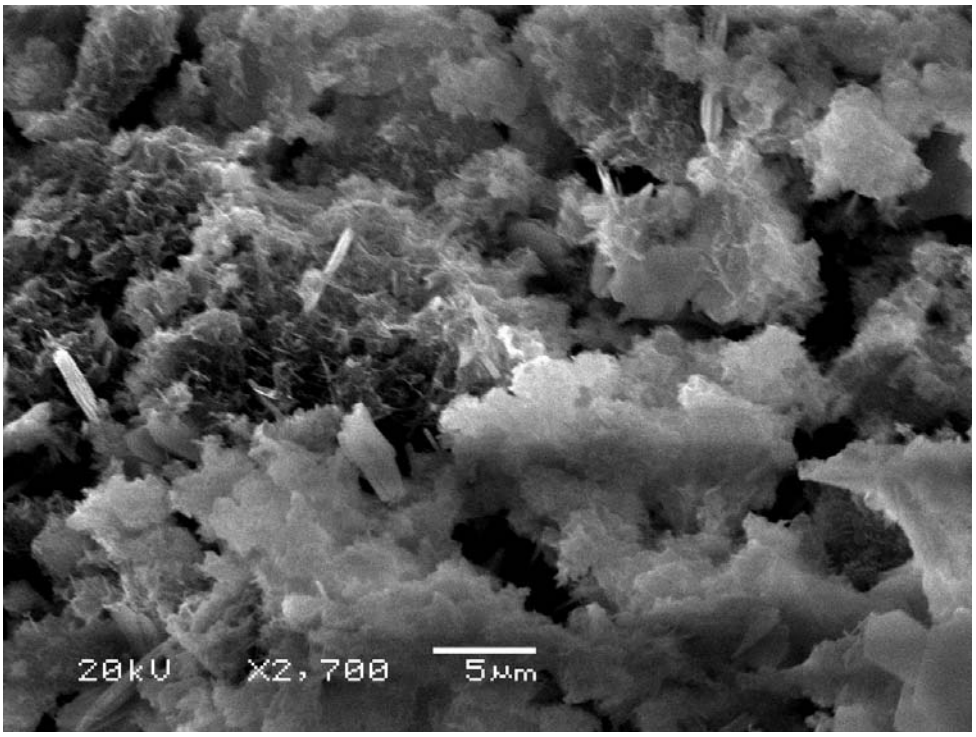

Figure 4.27 SEM image of pre-permeation column at 2700-time enlargement.

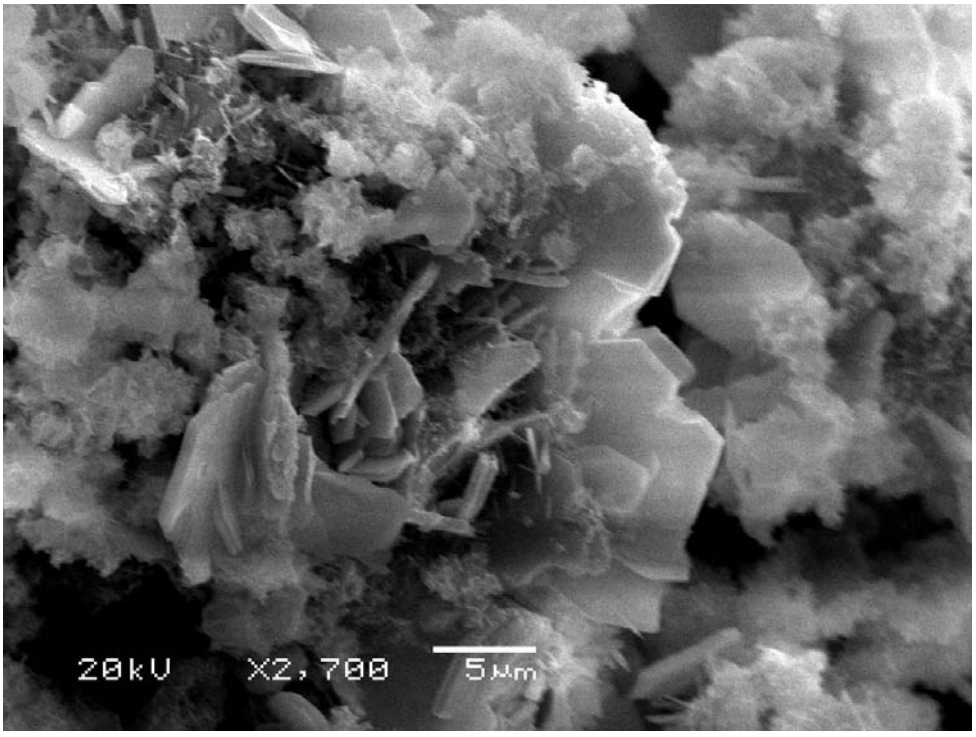

Figure 4.28 SEM image of post-permeation column 11 at 2700-time enlargement.

Figure 4.27 shows the SEM image of a CB column made from mix 1 and cured for 28 days. The picture was taken after curing and drying without the permeation of chloride ions. Figure 4.28 is the SEM image of the oven-dried column 11 taken after the permeation of NaCl solution. These two pictures are compared to see the change in CB microstructure after the attack of chloride. Clearly seen by SEM is the formation of many hexagonal slices in various sizes in Figure 4.28 in contrast with Figure 4.27. There are also some needle structures seen scattering in Figure 4.28. The needle structures are believed to be ettringite which is the product of reaction between C_3A and sulphates in the mix before the permeation of chloride ions. The large hexagonal slices in both figures could be $Ca(OH)_2$ which is formed when CaO reacts with water. The smaller ones may be considered as Friedel's salt or other chloro-complexes. However, they are likely to be Friedel's salt because BSC generally produces this salt more than other products, under the presence of chloride ions [Dhir et al. (1996); Luo et al. (2003)]. It is due to the fact that the addition of BS into OPC results in the high aluminate content cement BSC as seen in Table 4.2. The shape of Friedel's salt accords with Luo et al. (2003) who studied the internal chloride binding in cement mortars by SEM.

In Figure 4.26, adsorption or the formation of Friedel's salt decreases with curing time. The curing of CB mixtures involves the carbonation of $Ca(OH)_2$ to form $CaCO_3$, and this reaction decreases pH value. When pH falls, the formation of Friedel's salt is less, and there will be more free chloride ions in pore solution, corresponding to the study of Page and Vennesland (1983).

4.12 HYDRODYNAMIC CURVE

In Section 2.4.6, Figure 2.6 shows the hydrodynamic curves of Barricalla clay (Manassero et al. 1997) and homogeneous sands (Perkins and Johnston 1963). Figure 4.29 below shows the hydrodynamic curve of CB mixtures from this research together with the previous two curves. The three curves do not match one another and have different yielding velocities. For CB curve, the yielding velocity is approximately 1×10^{-4} cm/s. After yielding, D values increase linearly with velocity in the log-log plot. If Equation (2.5) is used in the linear regression of CB data points in a linear plot, the resultant equation can be drawn as the dash line in Figure 4.29. The equation from linear regression does not seem to fit to the data points plotted in the log-log scale. However, a better fitting curve, seen as a solid line, can be drawn by adjusting parameters D^* and α by eyes. Figure 4.29 emphasizes that the hydrodynamic curves of different porous media are not coincident.

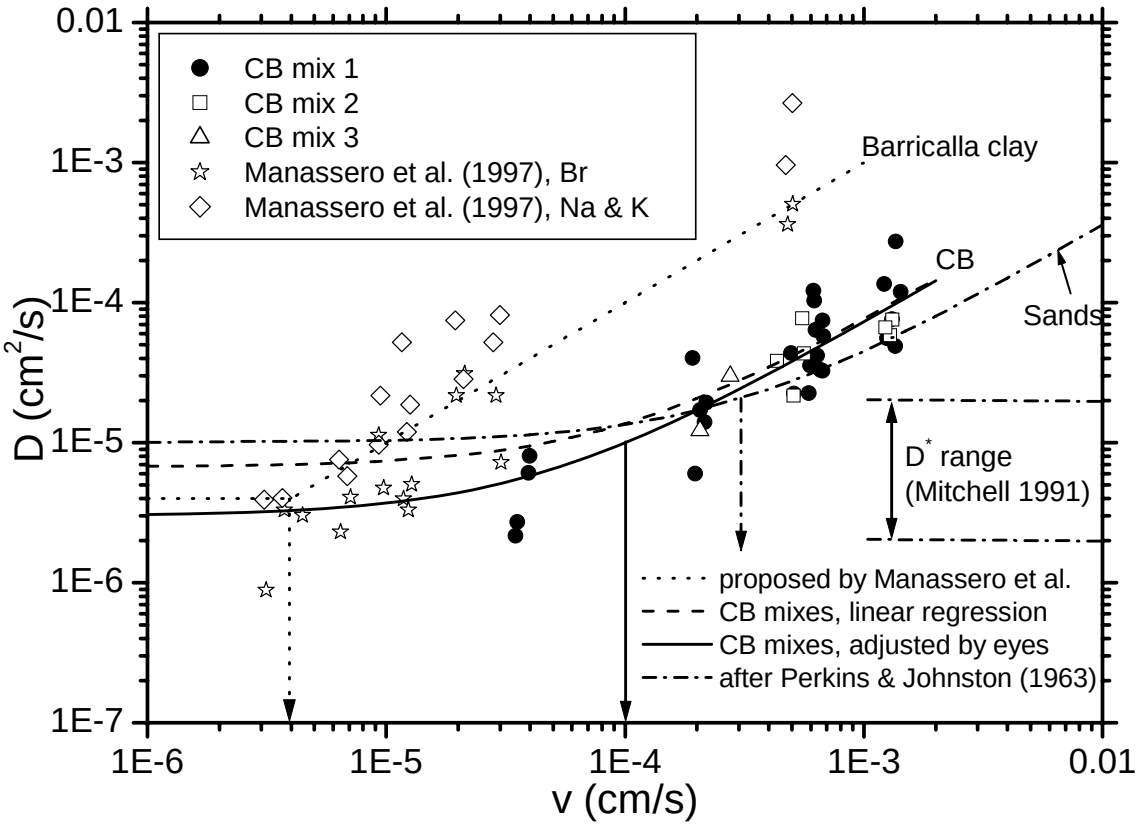

Figure 4.29 Hydrodynamic curves of CB mixes, Barricalla clay and sands.

For example, at v = 1 x 10^{-4} cm/s, there is no mechanical dispersion in case of sands; however, it is about to prevail in CB, and it is prevailing in Barricalla clay. Therefore, data from Perkins and Johnston (1963) shall not be used for other media but sands. It does not mean that the yielding velocity of any clayey soils must be 4 x 10^{-6} cm/s, for this value is obtained from only Barricalla clay. In fact, the shape and position of a hydrodynamic curve should depend on the nature of its medium and fluid used. In Figure 4.29, although the positions of the curves are different, the curves from different porous media appear parallel to one another after their yielding. Thus, it would be a good idea to perform a few column tests on a porous medium of interest at high seepage velocities to obtain D values more than the D^* range, and then draw a line from those values parallel to the lines in Figure 4.29 towards the D^* range. The intersection of the drawn line and the D^* range would approximate the yielding velocity of the medium.

It is explained in Section 4.9 that, at the same velocity, D parameter tends to decrease when increasing the source concentration used in column testing, and any D value can be related to its reference concentration C_R. The concept of C_R is utilized again here to explain the data scatter in CB hydrodynamic curve and perhaps in other curves as well. A low C_R

value gives a high D value, and a high C_R does the opposite. Thus, the variation of D values in Figure 4.29 is evidently generated by various concentrations.

4.13 EFFECT OF MEAN PARTICLE SIZE ON HYDRODYNAMIC CURVE

Figure 2.6 in Section 2.4.6 gives the normalized hydrodynamic curve of sand data collected from Perkins and Johnston (1963) and Spitz and Moreno (1996). With the adoption of empirical approach by Hiby (1959), the average curve drawn in Figure 4.30 can be formulated as follows:

$$\frac{D}{D_o} = 0.67 + \frac{1.5P}{1 + 2.2\sqrt{\frac{1}{P}}} \tag{4.3}$$

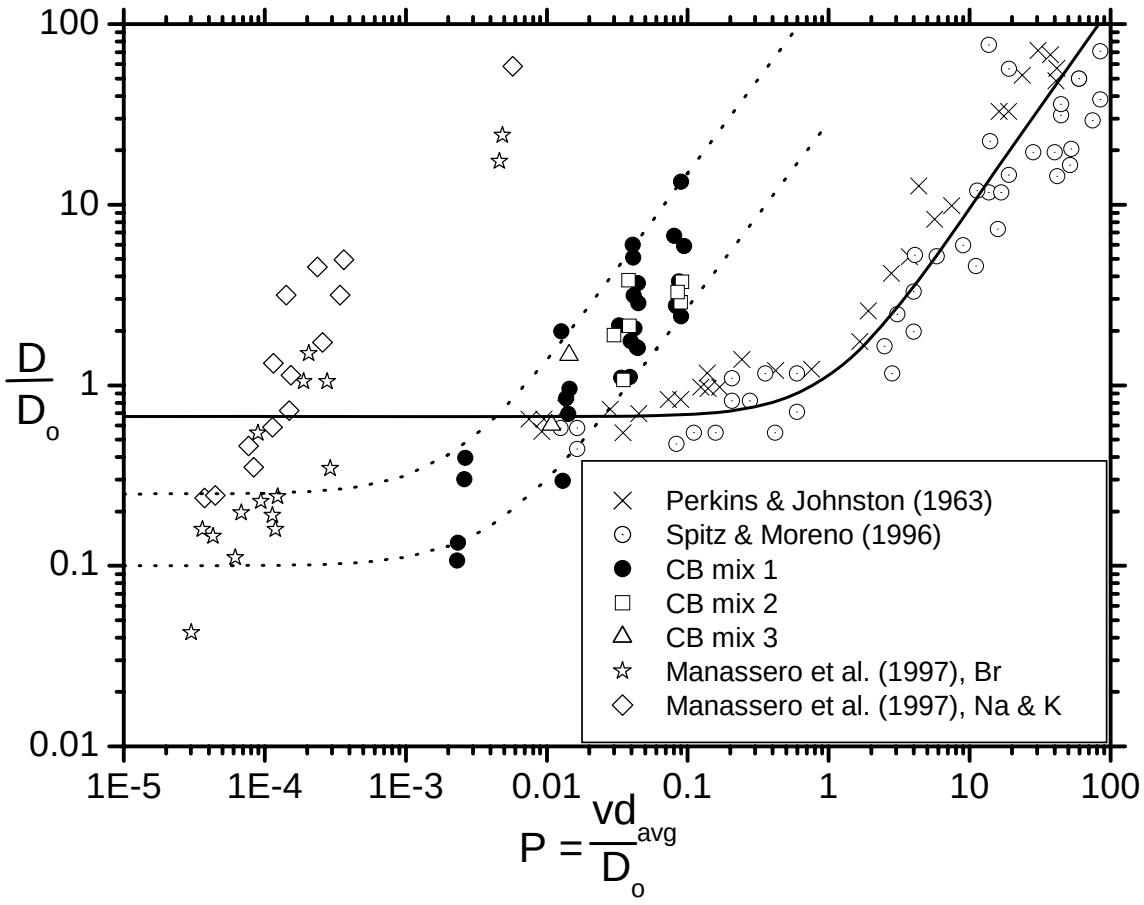

Figure 4.30 Normalized hydrodynamic curves of CB mixes, Barricalla clay and sands.

The value 0.67 is an approximate tortuosity factor τ_a for sands as seen at y-axis. Data from the selected literatures clearly shows that variation in τ_a is somewhat narrow in case of sands. For Barricalla clay, d_{avg} is assumed to be 2 μm which is the maximum clayey size in the unified soil classification system. From Table 2.1, D_o for bromine is 2.08 x 10^{-5} cm^2/s, and an average D_o of 1.65 x 10^{-5} cm^2/s is used for sodium and potassium. The resultant dimensionless hydrodynamic curve of Barricalla clay appears far away from sands. If the correct d_{avg} (< 2 μm) were used, the curve of the clay would shift a bit more to the left. This confirms that: (1) the selected clay data and sand data cannot be matched, and (2) d_{50} which is normally used as d_{avg} may not be an appropriate parameter in the normalization.

If the sand normalized curve or Equation (4.3) is assumed applicable for clayey soils, there could be error in finding D. For example, Barricalla clay with d_{50} = 1 μm is tested with a chemical with D_o = 1.5 x 10^{-5} cm^2/s at v = 1 x 10^{-4} cm/s. Peclet number P is then equal to 6.67 x 10^{-4}. From Figure 4.30, D = 0.67 x 1.5 x 10^{-5} = 1 x 10^{-5} cm^2/s. However, it is seen in Figure 4.29 that, at v = 1 x 10^{-4} cm/s, the correct D is about 1 x 10^{-4} cm^2/s. Fortunately, seepage velocities in practical applications such as clayey barriers are relatively low (e.g., less than 10^{-7} cm/s), so mechanical dispersion is always inactive.

For CB mixes, D_o for chloride is 2.03 x 10^{-5} cm^2/s (Table 2.1). The mean particle size d_{50} of each mix was obtained from laser diffraction (LD) technique as shown in Table 4.3. Due to cement hydration process, the real average size d_{avg} is likely to become bigger whereas pore structure is to be denser (Halamickova and Detwiler 1995). The decrease in porosity increases the values of v and D (see Section 3.4.6). Therefore, real d_{avg}, v, and D values would be higher than those values in Figure 4.30, and the real normalized hydrodynamic curve of CB mixes could shift a bit upwards and also more to the right. The CB curve in the figure lies between Barricalla clay and sand curves mainly because of the average original sizes of CB (10.6 to 14.0 μm) and partially due to the range of v values (Figure 4.29). The CB band (dotted lines) generated by varied concentrations also seems to be parallel to the clay and sand data in the normalized version.

Figure 4.30 emphasizes that hydrodynamic dispersion phenomena in different porous media are not coincident, and the normalization technique currently used cannot unite them. Therefore, applying the normalized hydrodynamic curve of sand data to other porous media could be fallacious. The normalized curve of sands can be found in many textbooks such as Bear (1972), Yong et al. (1992), Spitz and Moreno (1996), and Fetter (1999).

4.14 EFFECT OF POROSITY CHANGE ON TRANSPORT PARAMETERS

Columns 38 to 41 were designed to study the effect of porosity change on hydraulic conductivity. The column were consolidated immediately after molding to obtain different porosities, and then cured for 28 days before hydraulic conductivity tests. The column lengths do not have direct relationship with their total porosities owing to unequal initial lengths before consolidation. The maximum confining pressure was 110 kPa in column 38. Figure 4.31 shows the results of columns 38 to 41, together with columns 29 to 35. By trial and error, the best straight line was obtained in e-log k plotting, with a determination coefficient R^2 of 0.87. Hydraulic conductivity of mix 2 at 28 days is seen decreasing fairly with void ratio. This trend is not to be surprised.

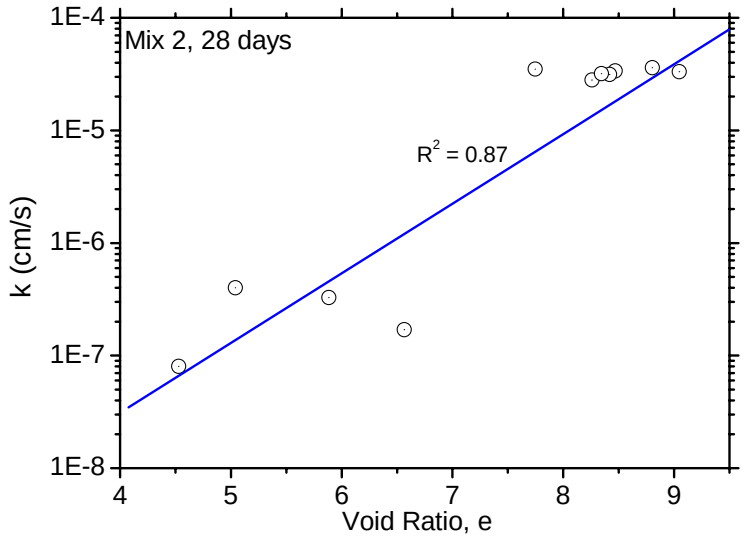

Figure 4.31 Hydraulic conductivity versus void ratio, using water content.

Column 42 was also consolidated to change its porosity. This column not only was studied on k, but R_d and D were also investigated. Column 42 is compared with column 15 because they have the same original material (mix 1), curing time, and approximately the same seepage velocity and source concentration. It is seen in Table 4.4 that, the drop in porosity leads to a lower k value, a lower R_d, but a higher D. The lowered k is predictable. The decrease in R_d is corresponding with the study by Delagrave et al. (1997) which showed by X-ray diffraction that the binding of chloride in hydrated cement samples decreases with water/cement ratio. This suggests that the chloride binding in CB materials is partly controlled by the accessibility of chloride ions to adsorption sites. The more water content, the more the adsorption of chloride ions becomes.

For hydrodynamic dispersion, the reduction in porosity should have decreased the dispersion of chloride ions. The increase in D would rather be attributed to the different lengths of the two samples. Because of the same porous media that sandwiched the samples, chloride ions in the system with the shorter sample (3.35 cm) may have been likely to disperse more than those in the long-sample (5 cm) system.

4.15 EFFECT OF BLASTFURNACE SLAG ON ADSORPTION AND HYDRODYNAMIC DISPERSION

Because mixes 1 and 2 have the same material proportions, they can be compared to see the effect of blastfurnace slag (BS) regarding adsorption and hydrodynamic dispersion. According to Dhir et al. (1996) and Luo et al. (2003), BS helps in increasing chloride binding capacity and decreasing chloride diffusion coefficient in concrete. From Table 4.4, column pairs of 29-17, 32-20, 33-21 and 35-22 are used to make comparisons.

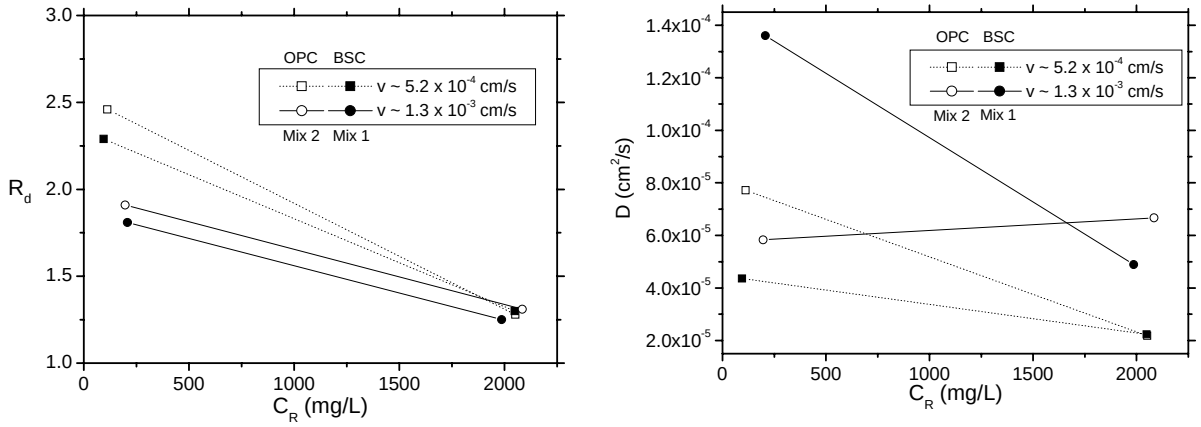

Figure 4.32 Effect of blastfurnace slag on R_d and D.

Figure 4.32 shows the effect of slag on adsorption and hydrodynamic dispersion at low and high concentrations. The slag effect is observable in vertical direction. The black symbols refer to mix 1 made from BSC. The pair 32-20 has negligible differences in R_d and D values, the pairs 29-17 and 35-22 show decreases in both R_d and D, and the pair 33-21 has decreased R_d but increased D.

Therefore, the effect of BS on adsorption and hydrodynamic dispersion is unclear for the CB mixtures in this research. This could be because of the difference in pore structures between concrete and CB. CB mixtures normally have much higher water content and less solid content than concrete. If the solid content is increased, the effect of BS may become

evident. Other important factors could be seepage velocity, bentonite and the role of sodium ions. The column pairs under comparisons have seepage velocities more than the yielding velocity. If low seepage is used, BS would do its job in diffusion-dominated condition. Also, bentonite may react with cations such as sodium ions and thus influence the ionic charge neutrality in the pore solution. The roles of bentonite and sodium ions probably have some influence on the adsorption degree of chloride ions.

4.16 CHAPTER SUMMARY

This chapter aims to achieve the third research objective, to study solute transport through CB mixtures by taking many factors into account. The properties of bentonite and two cements used in this research are tabulated, and the SEM images of the materials are given. There are three CB mix designs, and LD technique is used to determine their PSD curves. Mix 1 made from bentonite and BSC is the most important mixture because the majority of column tests have been performed on this mix, and also batch tests and diffusion tests are all carried out with mix 1. This chapter shows all the experimental results except those of the diffusion tests which are postponed to Chapter 5.

Laboratory results of batch and column testing are shown consecutively. There are two adsorption isotherms from batch testing, and 37 breakthrough curves from column testing. From a series of column tests at the lowest seepage (diffusion-dominated), column adsorption isotherm is constructed and then compared with the batch isotherms. Diffusion coefficient and apparent tortuosity factor are also linked with concentration.

The effects of curing, mix design and concentration on hydraulic conductivity k are discussed at the same time. The effects of velocity and concentration on retardation factor R_d and hydrodynamic dispersion coefficient D are plotted together. The effect of curing on R_d and D is investigated at two velocities. Chloride binding in CB mixtures is clarified by SEM, and compared with other researches. The hydrodynamic curve of CB mixtures is plotted together with those of Barricalla clay and sands; subsequently, the normalized hydrodynamic curves of CB mixtures, Barricalla clay and sands are presented and discussed. Then, the effect of porosity change on k, R_d and D is explained. Finally, the influence of blastfurnace slag on R_d and D is evaluated at two velocities.

CHAPTER 5
PRACTICAL DESIGN AND ANALYSIS

5.1 DESIGN WITH CONSTANT PARAMETERS

In Section 3.3, Figures 3.6 and 3.7 are proposed to use for the determination of column Peclet number P_e. Aside from the finding of column Peclet number, Figures 3.6 and 3.7 are also useful in the design. Because the figures come from Equation (2.21) which mimics an analytical solution provided by Lapidus and Amundson (1952) [as explained by van Genuchten and Parker (1984)]. The solution in 1952 is written as:

$$\frac{C_r(x,t)}{C_o} = \frac{1}{2}\left[\operatorname{erfc}\left(\frac{R_d x - vt}{2\sqrt{DR_d t}}\right) + \exp\left(\frac{vx}{D}\right)\operatorname{erfc}\left(\frac{R_d x + vt}{2\sqrt{DR_d t}}\right) \right] \tag{5.1}$$

Equation (5.1) works on a semi-infinite domain ($0 \leqslant x < \infty$) and is subject to initial and boundary conditions as follows:

$$C_r(x,0) = 0 \tag{2.18}$$

$$C_r(0,t) = C_o \tag{5.2}$$

$$\frac{\partial C_r(\infty,t)}{\partial x} = 0 \tag{2.19}$$

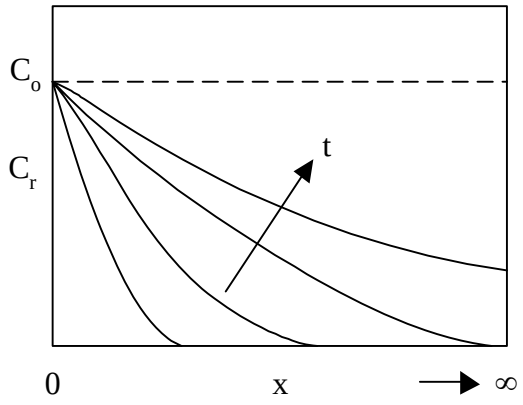

Figure 5.1 Transient resident concentration distributions in semi-infinite domain by Equation (5.1).

Equation (5.2) indicates that concentration is continuous across the inlet boundary, and this situation usually is not possible in practice because mass balance requirement is not satisfied (van Genuchten and Parker 1984). However, for a conservative design, Equation (5.1) may be invoked (e.g., Rabideau and Khandelwal 1998). General distribution curves of Equation (5.1) are shown in Figure 5.1.

The left hand side of Equation (5.1) is seen different from Equation (2.21) with regard to the types of concentrations (see Section 2.4.9). By substituting x = L, Equation (5.1) becomes:

$$\frac{C_r(L,t)}{C_o} = \frac{1}{2}\left[\operatorname{erfc}\left(\frac{R_d L - vt}{2\sqrt{DR_d t}}\right) + \exp\left(\frac{vL}{D}\right)\operatorname{erfc}\left(\frac{R_d L + vt}{2\sqrt{DR_d t}}\right) \right] \tag{5.3}$$

Equation (5.3) mimics Equation (2.21); therefore, it can also be written in the dimensionless form as Equation (2.22):

$$\frac{C_r}{C_o} = \frac{1}{2}\left[\operatorname{erfc}\left(\frac{R_d - T}{2\sqrt{\frac{R_d T}{P_e}}}\right) + \exp(P_e)\operatorname{erfc}\left(\frac{R_d + T}{2\sqrt{\frac{R_d T}{P_e}}}\right) \right] \tag{5.4}$$

The similarity between Equation (2.22) and Equation (5.4) suggests that Figures 3.6 and 3.7 can be used corresponding to Equation (5.4) in terms of resident concentration and the fixed concentration inlet boundary Equation (5.2). Three possible applications of Figures 3.6 and 3.7 in the design are: (1) knowing R_d, v, L and D, time t when $C_r = 0.1C_o$ or $0.9C_o$ (at x = L) can be determined, (2) with known v, L and D, if a design time t is specified, a desired R_d can be evaluated, and (3) with known R_d, v, and D, when time is fixed, it is possible to trial for a corresponding L. Figure 3.6 would represent a conservative design that a resident concentration at the end of a liner is limited to 10% of a specified source concentration, and Figure 3.7 rather provides an economical design in such a way that the liner capacity is nearly exhausted. Care must be paid to the use of Figure 3.7 because the tail water environment would be contaminated to a high degree when $C_r(L,t) = 0.9C_o$. It should be noted that Figures 3.6 and 3.7 provide relatively quick but detailed solutions for two specific cases. A more generalized design method may be referred to Shackelford (1990).

Figure 5.2 illustrates the possible application of Figures 3.6 and 3.7 to a single-layer vertical barrier. The three possible real applications are demonstrated in Sections 5.1.1, 5.1.2, and 5.1.3.

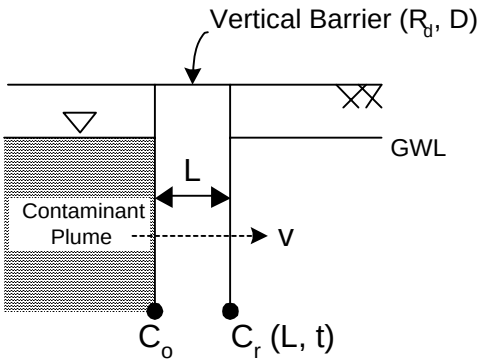

Figure 5.2 Schematic diagram of one-layer design.

Hydraulic conductivity testing is normally conducted to evaluate the k value of the barrier material. With k known, seepage velocity v in the field can be evaluated by the knowledge of hydraulic gradient and porosity. The R_d and D parameters could be determined by laboratory diffusion testing (v = 0) when seepage in the field is rather low. If seepage is quite high, laboratory column testing (v > 0) is preferable because adsorption also depends on the speed of pore fluid (Section 4.8). The level of concentration used in diffusion or column testing ought to be in harmony with the concentration level in the field.

For CB barriers, time is an additional factor in the design. The parameters k, R_d and D must be obtained based on the real functioning time of the barrier. Obtaining such parameters at a short curing period (e.g., 28 days) could raise an argument because the properties of the barrier may not have been stable. Chapter 4 shows that the k, R_d and D parameters do not keep constant at 28 days.

5.1.1 Time Evaluation

For example of the first application, a vertical barrier, 70-cm wide, is to be conservatively designed for $C_r(L,t) = 0.1C_o$. Seepage velocity v in the field is 5×10^{-7} cm/s, R_d and D are determined as 10 and 7×10^{-6} cm^2/s, respectively. Thus, the Peclet number P_e of this problem is 5. With R_d and P_e, the corresponding T can be read from Figure 3.6 as about 4. Figure 5.3 illustrates the use of Figure 3.6 for the first application. As a result, the time required for the design is 17.7 years.

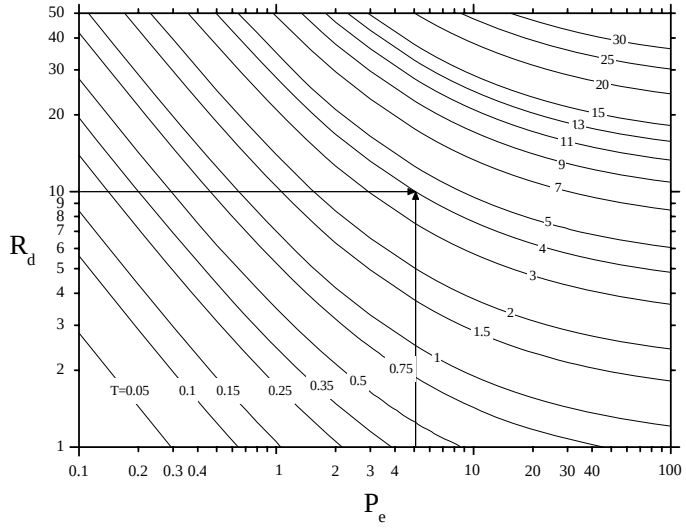

Figure 5.3 Time evaluation for $C_r = 0.1C_o$.

5.1.2 Selection of Retardation Factor

For instance, a slurry wall, 80-cm wide, is to be conservatively designed for $C_r(L,t) = 0.1C_o$. Seepage velocity v in the field is 1 x 10^{-7} cm/s, and D is known as 1.6 x 10^{-6} cm^2/s. The barrier is required to reach $C_r(L,t) = 0.1C_o$ in 50 years. Thus, the Peclet number P_e of this problem is 5, and T is equal to 2. From Figure 3.6, the required R_d should be 5. Figure 5.4 depicts the determination of R_d from this example.

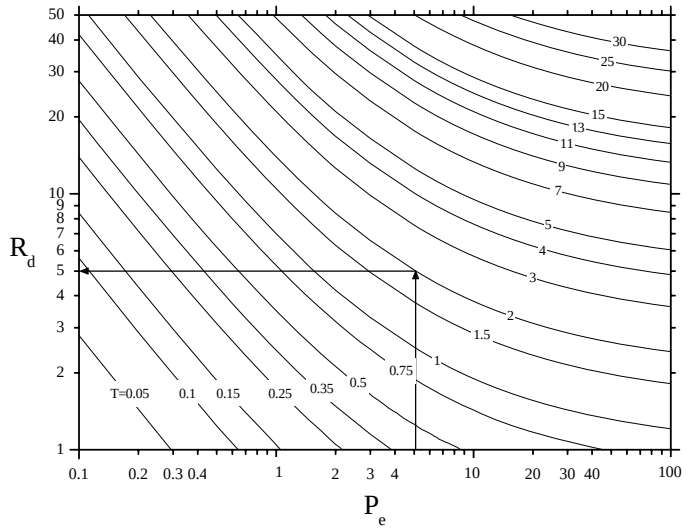

Figure 5.4 Selection of R_d for $C_r = 0.1C_o$.

5.1.3 Design of Barrier Length

For example of the third application, seepage velocity v in the field is 1.9 x 10^{-7} cm/s; R_d and D are determined as 5 and 2.3 x 10^{-6} cm^2/s, respectively. If a vertical barrier is designed to

reach $C_r(L,t) = 0.1C_o$ in 20 years, from trial and error in Figure 3.6, a design length of 60 cm would be obtained with $P_e = 5$ and $T = 2$, approximately. Figure 5.5 illustrates the way to obtain L in this example. Because $T = vt/L$ and $P_e = vL/D$, the parameter L can be written as:

$$L = 120/T \tag{5.5}$$

$$L = 12P_e \tag{5.6}$$

By equating the above equations, the equation for trial and error looks like:

$$T.P_e = 10 \tag{5.7}$$

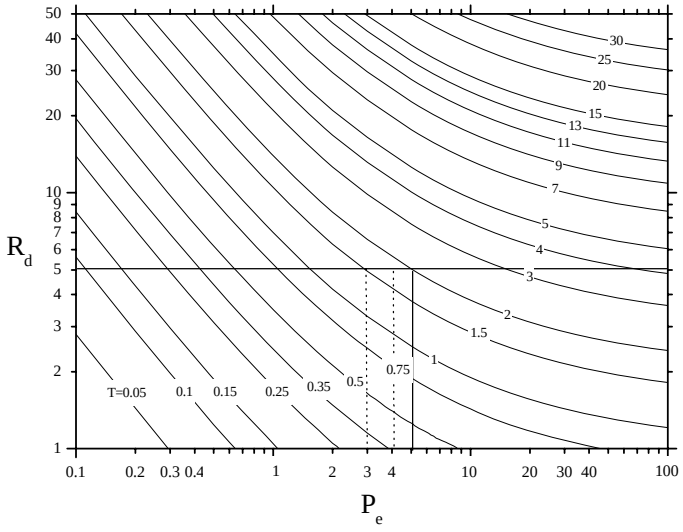

Figure 5.5 Design of barrier length for $C_r = 0.1C_o$.

5.2 ANALYSIS USING CONCENTRATION-DEPENDENT PARAMETERS

Section 5.1 proposes some design methods of one-layer barrier system on the basis of constant parameters. The use of constant parameters for the design may be acceptable because the design does not need as much accuracy as the analysis. However, this thesis has also described an approach to relate the transport parameters R_d and D from column testing to a reference concentration C_R (Section 3.2). The soundness of the approach is substantiated again here after it is in Section 4.6.

5.2.1 Flow Chart to Obtain Parameters

Figure 5.6 summarizes the procedure to obtain concentration-dependent parameters from column testing by the proposed method.

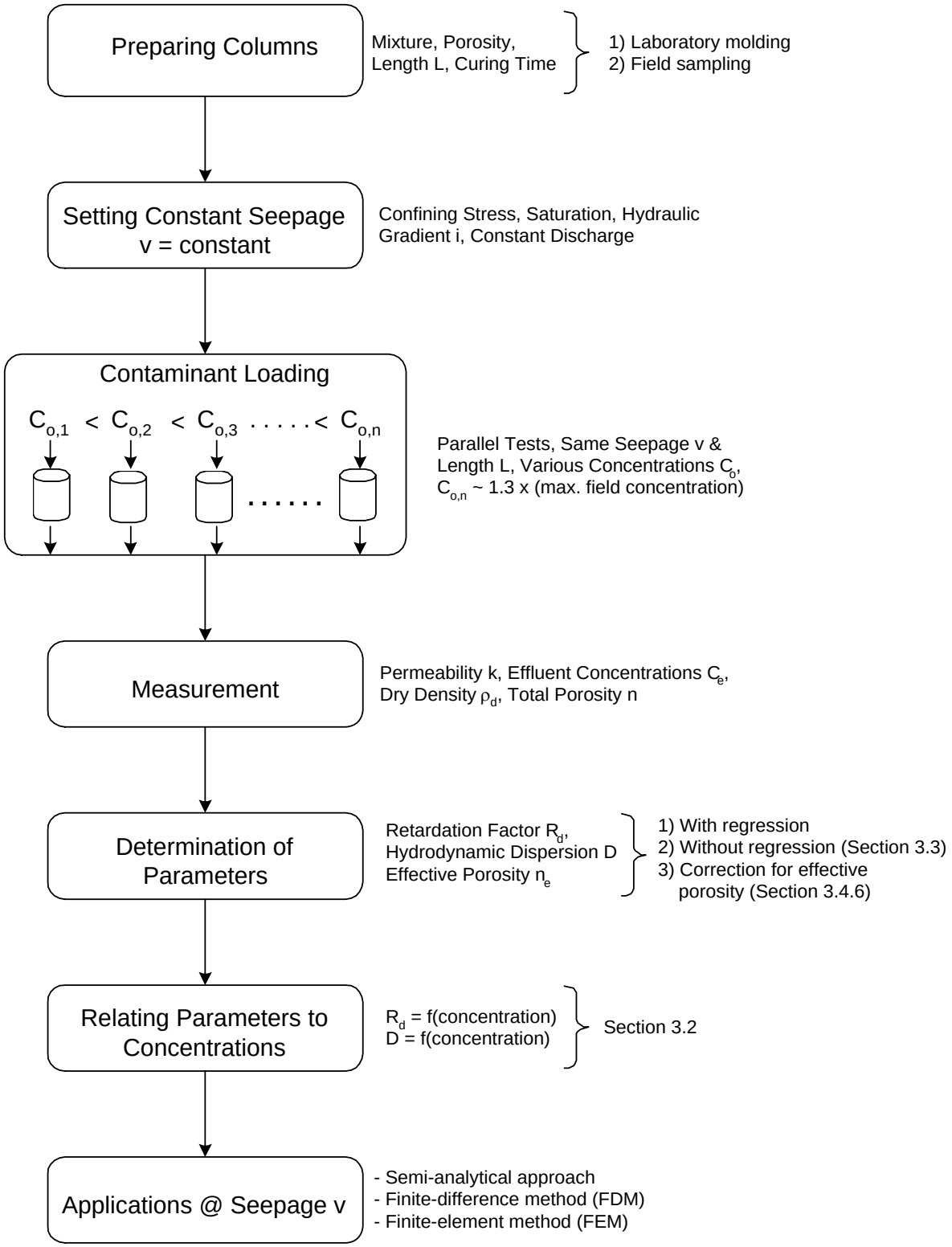

Figure 5.6 Procedure to obtain concentration-dependent parameters.

5.2.2 Examples

From Section 3.4.4, two diffusion tests are performed in this research. The two tests had been made from mix 1 and cured for 28 days before the diffusion of chloride ions from the top of each sample according to Figure 2.10 (left). The initial source concentration of 2,100 mg/L was designed according to the reference concentration of column 12 in Figure 4.20. The concentration drop (as in Figure 2.11) in each source solution was assumed to obey Equation (2.15) and was measured for 6 days. The results of the two tests are shown in Figures 5.7 and 5.8.

Section 3.5.2 explains that the results of column testing at a sufficiently low velocity could be applied to diffusion testing of the same material. Therefore, the column adsorption isotherm in Figure 4.20 and the values of effective diffusion coefficient D^* in Figure 4.21 are input to POLLUTE software (Rowe et al. 1998, Section 3.5.1) to generate theoretical curves for the concentration drops in the source reservoirs. In POLLUTE, retardation factor R_d from Freundlich model is calculated by the secant approach in Equation (2.13). Because the secant approach seen in Figure 2.8 gives a higher retardation factor than the tangent approach in Equation (2.12), the tangent approach was also conducted in the software by replacing K in Equation (2.13) with $K\varepsilon$.

In each test, two effective diffusion coefficients, 2.2×10^{-6} and 8×10^{-6} cm^2/s, were used as a lower bound and an upper bound value, respectively. The first value represents a diffusion rate at high concentration, and the latter value is a rate for low concentration level. An average background concentration of 12 mg/L was specified in the analyses. It is seen in both Figures 5.7 and 5.8 that the specified diffusion coefficients provide a good boundary for the observed concentration drops in the source reservoirs. Furthermore, good agreement between the prediction and the diffusion data can be observed around the upper boundary value due to the fact that the average level of resident concentrations inside the two samples during 6-day diffusion is not high.

The difference between the tangent (solid lines) and secant approaches (dash lines) can also be seen. At the same diffusion rate, the secant approach gives a greater concentration drop because of higher adsorption. The size of the gap between the two approaches depends on the shape of isotherm and the range of concentration considered. However, the effect of different adsorption approaches in this study is not as significant as the variation of diffusion coefficients as a result of the level of resident concentration.

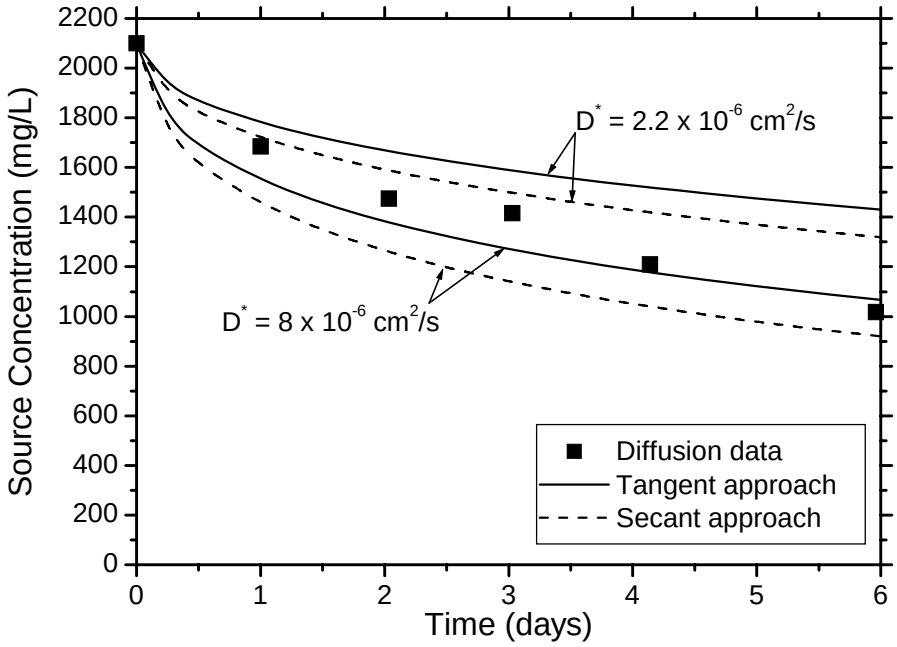

Figure 5.7 Diffusion test no. 1, L = 6.1 cm, H_f = 2.9 cm.

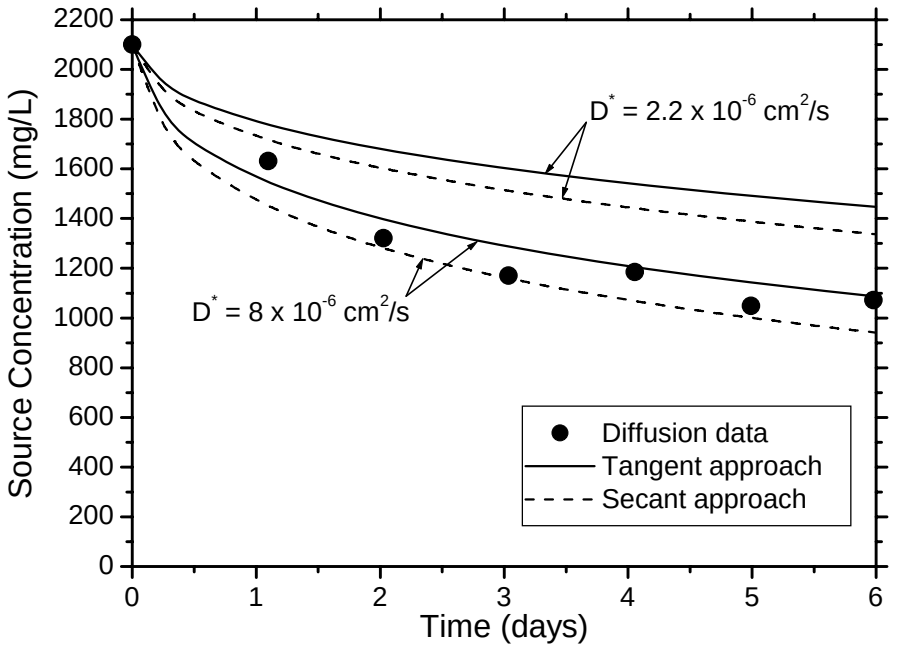

Figure 5.8 Diffusion test no. 2, L = 8.0 cm, H_f = 3.0 cm.

Effect of Effective Porosity

If an effective porosity n_e is assumed to be 0.7, the R_d and D^* values of columns 9, 10, 11 and 12 will increase by 28.57%. By using the same ρ_d (0.265 g/cm^3) and the assumed n_e, a new column adsorption isotherm by regressing Equation (2.12) is $q = 139.45C_R^{0.484}$, with R^2 equal to 0.968. The value 8.04 x 10^{-6} cm^2/s turns to be 1.03 x 10^{-5} cm^2/s at 101.5 mg/L, and the value 2.17 x 10^{-6} cm^2/s changes to 2.79 x 10^{-6} cm^2/s at 626.8 mg/L. The new column adsorption isotherm and D^* values were used to predict the diffusion tests in Figures 5.7 and 5.8 again. It was found that the predicted curves (not shown) were almost coincident with the foregoing analyses due to the fact that R_d and D^* were increased by the same factor n/n_e, under zero seepage velocity in diffusion testing [see Equations (2.1) and (2.14)]. Little discrepancy between the two predictions is attributed to the fitting of the two isotherms. Consequently, the conclusion that concentration level affects the prediction of chloride transport remains unchanged. The D^* values at the low concentration level yield better predictions for both diffusion tests.

5.3 POSSIBLE APPLICATIONS IN CASE OF COMPOSITE WALLS

A composite vertical barrier is constructed by installing jointed geomembrane (GM) panels into a trench backfilled with SB, CB, or other materials. This type of groundwater barrier is analogous to the composite liner system used for waste containment. The GM panels can be joined using some joint systems (e.g., Tachavises and Benson 1997). GM is adequately impervious to the diffusion of inorganic solutes when compared to many organic solutes (Haxo and Lahey 1988; Rowe et al. 1995a).

Figure 5.9 shows the comparison between the composite liner system and the composite vertical barrier. In case of composite walls, if solutes are assumed to uniformly accumulate in front of the GM face as in Figure 5.9(b), then any approaches applied to the composite liner system [Figure 5.9(a)] are also applicable to the composite vertical barrier. According to Foose et al. (2002), there are two pathways for solute transport through composite liners: (1) transport of inorganic and organic solutes through defects in GM and subsequently through the liner, and (2) transport of organic solutes through intact GM and subsequently through the liner. For composite walls, joint systems are more critical than the defects in GM panels because GM sheets for the vertical barriers are not as likely to be damaged as those in the construction of landfills. The hydraulic conductivity of GM joints could be referred to the studies of Cortlever (1988) and Lee and Benson (2000).

POLLUTE software (Rowe et al. 1998) is also able to evaluate the performance of composite systems. The diffusion coefficient and the equivalent hydraulic conductivity of GM must be specified. The equivalent hydraulic conductivity of GM is supposed to take care of the effects of joints and defects in the GM. Apart from POLLUTE, Foose et al. (2002) suggested numerical methods for analyzing solute transport through composite liners and used the methods to compare three composite liners.

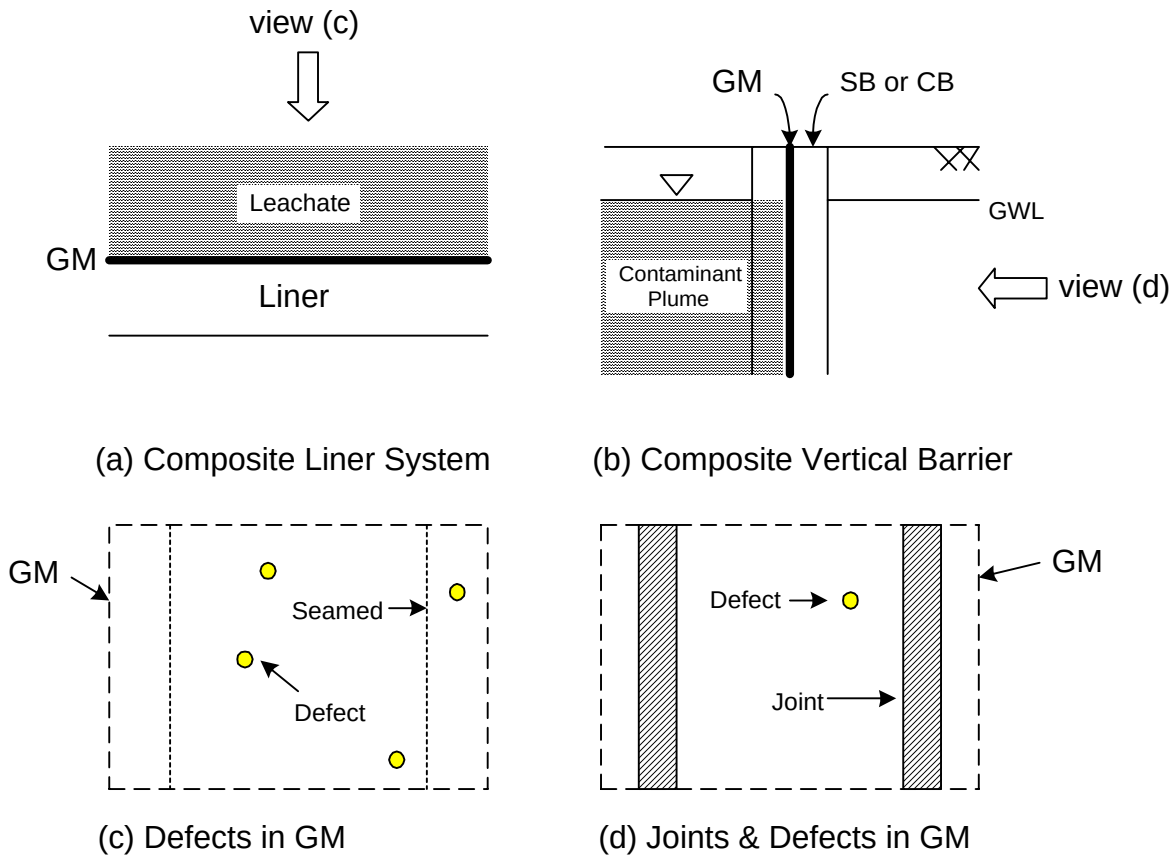

Figure 5.9 Composite liner system versus composite vertical barrier.

5.4 CHAPTER SUMMARY

This chapter intends to complete the last research objective, to propose practical applications of CB walls: design and analysis. The chapter begins with the possible design methods based on two theoretical charts proposed in this research. The design relies on constant parameters and is limited to two specific cases, conservative and economical. The proposed charts can be used to evaluate time, retardation factor, and barrier length. Three examples are given therein.

Then, the following section gives an example of analysis using concentration-dependent parameters. The procedure to obtain concentration-dependent parameters from column testing is depicted by a flow chart. The two diffusion tests performed in this research are predicted by the results from a series of column tests conducted in diffusion-dominated condition. Agreement between the predicted results and diffusion data is explained. Additionally discussed is the effect of effective porosity on the predicted results. The successful prediction may suggest that the approach newly developed in this research (Section 3.2) could be used to determine concentration-dependent transport parameters for the analysis of in-situ problem.

Lastly, possible applications for composite walls with geomembrane panels are suggested by making an analogy between a composite liner system and a composite vertical wall. Solute transport mechanisms in case of composite barriers are shortly explained, and some approaches having been developed by some researchers could be used to analyze the composite vertical wall.

CHAPTER 6
CONCLUSIONS AND RECOMMENDATIONS

6.1 CONCLUSIONS

This research volume deals with the solute transport through cement-bentonite (CB) mixtures under various selected factors. Chloride ions are the solute of interest, and the significant factors believed to influence the migration of chloride ions through CB mixtures are curing period, seepage velocity, concentration, particle size, porosity, and mix design. Chapter 3, Methodology, presents analytical tools and experimental plans; Chapter 4, Results and Discussions, shows a number of experimental results, and Chapter 5, Practical Design and Analysis, proposes design methods and examples of analyses for CB barriers.

In Chapter 3, main conclusions are as follows:

1. A new approach is formulated in order to relate retardation factor R_d and hydrodynamic dispersion coefficient D interpreted from column testing to a timely-averaged or reference concentration C_R which is dependent on column Peclet number P_e. See Section 3.2.
2. A simple algorithm to determine P_e without nonlinear regression has been proposed by two theoretical charts. See Section 3.3. The charts can also be used in the design of single-layer contaminant barriers when a quick solution is needed. See Section 5.1.

There are mainly five kinds of experiments which have been conducted, namely column testing, batch testing, diffusion testing, scanning electron microscopy (SEM), and laser diffraction (LD) technique. Among them, column testing is the most significant experiment because the behaviors of CB mixtures under the attack of chloride have been investigated using this type of experiment. Except the results of diffusion testing, all other experimental results are provided in Chapter 4. Based on this chapter, the following conclusions can be drawn:

1. Conventional batch testing for soils conducted under agitation did not give meaningful information because the hydration of cement hardly worked to harden CB

slurries. Also, the order of material mixing in batch testing is not similar to the real application of CB slurry walls. See Section 4.4.1.

2. At the lowest seepage used in column testing, there was no mechanical dispersion. By regression of (C_R, R_d) data, the resultant column adsorption isotherm was well fitted to Freundlich model with $R^2 = 0.958$. This indicates that adsorption in column testing depends on concentration. The column isotherm did not match with the two batch isotherms. See Section 4.6.1.
3. Calculated D parameters from column testing at the lowest seepage were found to be in the range of effective diffusion coefficients D^*, and their values decreased linearly with the square root of C_R up to the root of 626.8 mg/L, with R^2 valuing 0.999. This also suggests that diffusion is a function of concentration level. Apparent tortuosity factor τ_a was also linked with concentration by using free-solution diffusion coefficient D_o. See Section 4.6.2.
4. NaCl solutions did not significantly affect hydraulic conductivity values in any column tests. It suggests that no significant modification in pore structures occurred during the NaCl permeation. See Section 4.7.
5. Blastfurnace slag decreased hydraulic conductivity, but not as much as bentonite did. See Section 4.7.
6. Prehydration of cement by air moisture before mixing reduced adsorption. See Sections 4.7, 4.8 and 4.10.
7. When seepage v increased, R_d decreased due to shortened reaction time between chloride ions and CB; on the other hand, D increased due to mechanical dispersion. The yielding velocity at which mechanical dispersion started prevailing in CB mixes was about 1×10^{-4} cm/s. See Sections 4.8 and 4.12.
8. When concentration C_R increased, both R_d and D became lower. Lower R_d at high concentration level is convincingly because of concave adsorption isotherm. It is believed that, under high concentration, solute particles interfered one another and thus proceeded slower, resulting in lower D. See Sections 4.6.1, 4.6.2 and 4.9.
9. At a longer curing period, both R_d and D decreased. Decreases in R_d were due to carbonation reaction which is known to reduce pH with time. The lower pH falls, the less adsorption becomes. The carbonation reaction also makes CB pore structure denser; therefore, it contributed to the reductions in both hydraulic conductivity and hydrodynamic dispersion. See Sections 4.7, 4.10 and 4.11.

10. Chloride ions were bound by the formation of Friedel's salt and perhaps some other chloro-complexes. The shape of the salt was hexagonal, seen by SEM. See Section 4.11.
11. The yielding velocities of Barricalla clay and sands are respectively 4×10^{-6} and 3×10^{-4} cm/s which are different from that of CB mixes in this research. The hydrodynamic curves (v, D) of sands, Barricalla clay and CB mixes did not appear coincident. See Section 4.12.
12. The normalized hydrodynamic curves of sands, Barricalla clay and CB mixes also did not match one another. By using prehydrated average particle sizes d_{50} from LD technique, the normalized curve of CB mixes located between the sands and clay curves. Therefore, the normalized curve of sand data, which is found in literatures, shall not be applied to other porous media. See Section 4.13.
13. The level of concentration used in column testing could explain the scatter of data in hydrodynamic curves. See Sections 4.9, 4.12 and 4.13.
14. When porosity decreased, hydraulic conductivity and adsorption decreased. It suggests that chloride binding in CB mixtures was partly controlled by the accessibility of chloride ions to adsorption sites. Dispersion should have decreased. The increased dispersion may be attributed to the boundary effect. See Section 4.14.
15. The effect of blastfurnace slag on R_d and D parameters is unclear in this research. Some influencing factors such as water content, seepage, bentonite and the role of cations may need investigation. See Section 4.15.

Based on Chapter 5, Practical Design and Analysis, the following conclusions are drawn:

1. Some design methods regarding one-layer barriers are proposed. They are based on two theoretical charts developed in Section 3.3. It is possible to determine breakthrough time, retardation factor, and barrier length.
2. Suggestion on the analysis of composite walls is given by making an analogy between the composite walls and composite liner systems in landfills.
3. The soundness of the approach developed in Section 3.2 is substantiated in Section 5.2 where the results of two diffusion tests are predicted by concentration-dependent parameters from column testing conducted at the lowest seepage (Section 4.6). The column adsorption isotherm and selected diffusion rates provided good theoretical

boundary for each diffusion data, and the positions of predicted curves can be explained in terms of concentration.

The application of this research to in-situ CB barriers may follow these recommendations:

1. In order to conduct column testing to find transport parameters, the preparation of CB specimen must be in accordance with the in-situ construction of CB barrier.
2. If possible, field sampling of CB specimen for column testing is preferable, for the specimen from the field is more representative.
3. The measurement of in-situ seepage is necessary because the magnitude of seepage is an input parameter for column testing to find adsorption and hydrodynamic dispersion parameters.
4. The level of concentration used in column testing should be similar to field condition. For barrier designs with constant parameters (Section 5.1), the average in-situ concentration is reasonable; in contrast, for analyses using concentration-dependent parameters, the maximum in-situ concentration is indispensable.
5. The knowledge of real functioning time of a CB wall is important because transport parameters are dependent on curing time. For instance, if a CB barrier is constructed to cut off a moving contaminant plume, transport parameters obtained at early curing may be more appropriate.
6. Column testing must be conducted at constant seepage. It may be necessary to adjust hydraulic gradient to keep seepage constant because seepage velocity is likely to decrease with hydraulic conductivity due to cement hydration.

6.2 RECOMMENDATIONS FOR FUTURE WORK

The author has tried to investigate many aspects of solute transport through CB barriers by using mathematical and experimental approaches. In fact, the methodology in Chapter 3 is not restricted to the study of CB mixtures alone. Many more researches can be extended from the present work by using the basic knowledge in Chapter 2, the approaches in Chapter 3 and the contribution in Chapters 4 and 5. Some subjects which may require further investigation are recommended as follows:

1. Only three CB mix designs have been used in this research. It is possible to experiment more mixtures to make comparisons. Some special additives can be used as well.
2. Many other solutes besides chloride ought to be studied: anions and cations, organic and inorganic. Preliminary experiments showed that the adsorption capacity of CB mixtures is quite effective for anions.
3. Because this research considers CB as a positive adsorbent, the possibility of CB to adsorb cations has not been clarified.
4. It is mentioned in Section 4.13 that the parameter d_{50} may not be suitable for the normalization of hydrodynamic curves. Other characteristic lengths such as average pore diameter might be used to replace d_{avg} in Figure 4.30.
5. Static batch testing according to Tang and Nilsson (1993) seems more realistic to cement-based materials. The test should be conducted on CB mixtures, and the results of the test are encouraged to compare with column adsorption isotherm (see Figure 4.20).
6. The effect of blastfurnace slag in CB mixtures on adsorption and hydrodynamic dispersion needs to be clarified.
7. The approach developed in Section 3.2 is more or less related to scale effect. This means that if two column tests with different lengths are conducted at the same velocity, the results would be a function of length.
8. Due to many disadvantages of batch testing for soils, the approach in this research (Figure 5.6) could be an alternative in the determination of adsorption isotherms for other porous media such as compacted clayey liners.

APPENDIX A
TIMELY AVERAGED CONCENTRATION

From the table below, the values from the second column to the fifth column are calculated using t_{limit} values to obtain M_{pore} equal to 96%, 97%, 98%, and 99% of the total pore capacity V_vC_o. The values in the last column are obtained by extrapolation using parabolic equations with R^2 values more than 0.9994.

$$C_R = \frac{A_{eff}}{V_v} \cdot \frac{1}{t_{limit}} \cdot \int_0^{t_{limit}} \int_0^L C_r(x,t)dxdt \qquad (3.5)$$

P_e	C_R/C_o (96%)	C_R/C_o (97%)	C_R/C_o (98%)	C_R/C_o (99%)	C_R/C_o (100%)
0.1	0.808608	0.828162	0.850951	0.880323	**0.913771**
0.2	0.803294	0.823208	0.846447	0.876448	**0.910634**
0.5	0.788647	0.809455	0.833829	0.865491	**0.901647**
1	0.767753	0.789588	0.815347	0.849120	**0.887843**
2	0.735237	0.758132	0.785452	0.821875	**0.863888**
5	0.675922	0.699122	0.727403	0.766325	**0.811717**
10	0.626387	0.648298	0.675436	0.713725	**0.758725**
15	0.599051	0.619645	0.645348	0.682055	**0.725348**
20	0.581229	0.600720	0.625145	0.660283	**0.701802**
30	0.558864	0.576666	0.599067	0.631539	**0.669978**
40	0.545095	0.561659	0.582546	0.612938	**0.648950**
50	0.535620	0.551240	0.570940	0.599664	**0.633708**
60	0.528645	0.543501	0.562241	0.589596	**0.622023**
70	0.523263	0.537487	0.555431	0.581632	**0.612685**
80	0.518965	0.532662	0.549927	0.575139	**0.605015**
90	0.515449	0.528688	0.545368	0.569722	**0.598577**
100	0.512507	0.525347	0.541516	0.565111	**0.593057**

APPENDIX B1

SPREADSHEET OF HYDRAULIC CONDUCTIVITY

This spreadsheet corresponds with Column Test 3 in Table 4.4.

	A	B	C	D	E	F	G	H	I	J
22								Container	257.47	g
23	Temperature =		25	Celsius				Saturated sample	167.11	g
24	L =		5	cm				Container + dried sample	296.08	g
25	Column Diameter =		6	cm	Area =	28.274	cm^2	Dried sample	38.61	g
26					Volume =	141.3717	cm^3	Water	128.5	g
27	$i = h_{loss}/L$ =		10					w_c	3.32815	
28	**Hydraulic Conductivity:**							ρ_d =	0.27311	g/cm^3
29	cc	sec	Q (cc/s)	Darcy (cm/s)	k (cm/s)			ρ_t =	1.18206	g/cm^3
30	21.26	1180	0.01802	0.0006372	6.37E-05	1st sampling		G_s =	2.99961	
31	22.06	1260	0.01751	0.0006192	6.19E-05	2nd sampling		e =	9.98317	
32	20.14	1158	0.01739	0.0006151	6.15E-05	3rd sampling		n =	0.90895	
33	23.73	1367	0.01736	0.000614	6.14E-05	4th sampling				
34	22.02	1263	0.01743	0.0006166	6.17E-05	5th sampling				
35	22.49	1293	0.01739	0.0006152	6.15E-05	6th sampling				
36	19.88	1151	0.01727	0.0006109	6.11E-05	7th sampling				
37	20.61	1192	0.01729	0.0006115	6.12E-05	8th sampling				
38	23.37	1362	0.01716	0.0006069	6.07E-05	9th sampling				
39	19.02	1112	0.0171	0.0006049	6.05E-05	10th sampling				
40	18.59	1095	0.01698	0.0006004	6E-05	11th sampling				
41	19.15	1134	0.01689	0.0005973	5.97E-05	12th sampling				
42	19.12	1110	0.01723	0.0006092	6.09E-05	13th sampling				
43	19.53	1148	0.01701	0.0006017	6.02E-05	14th sampling				
44	20.04	1178	0.01701	0.0006017	6.02E-05	15th sampling				
45	20.38	1197	0.01703	0.0006022	6.02E-05	16th sampling				
46	21.95	1289	0.01703	0.0006023	6.02E-05	17th sampling				
47	353.34	20489	0.01725	0.0006099	6.1E-05	**Average of samples 1 to 17**				

APPENDIX B2

SPREADSHEET OF COLUMN TESTING

This spreadsheet corresponds with Column Test 3 in Table 4.4.

	A	B	C	D	E	F	G	H	I	J	K	L
1	**Input:**	Influent concentration, C_o =			1063.5	mg/L		C_i =	33	mg/L		
2			Flow rate, Q =		1.725E-02	cm^3/sec =	1490.0	cm^3/day				
3			Length of sample, L =		5	cm						
4			Diameter of sample =		6	cm, Area =	28.274	cm^2				
5			Volume of sample =		141.3717	cm^3						
6				w_c =	3.32815							
7				G_s =	2.99961	e =	9.98317					
8			Porosity, n =		0.9090							
9	1 T =	One pore volume of soil, V_v =			128.50	cm^3 ==	0.09	days =	2.1	hours =	124.2	minutes
10	0.25 T =	32.13	cm^3	h_{loss} =	50	cm						
11				i =	10.0	(gradient)	k =	6.10E-05	cm/sec			
12				v =	6.710E-04	cm/sec (seepage)						
13		Influent pipe volume =			15.3	cm^3, Lag =	1.48E+01	minutes =	887		sec	
14	$Vol_{initial}$	Δ Vol	Vol_{final}	$T_{initial}$	T_{final}	Δ T	$T_{average}$	C_e (mg/L)	C_e-C_i	C_e-C_i/C_o-C_i	IMR	CMR
15	**0**	21.26	21.26	**0**	0.165447	0.165447	0.082724	33.92	0.92	0.0009	0.000148	0.000148
16	21.26	22.06	43.32	0.165447	0.337121	0.171673	0.251284	44.90	11.90	0.0115	0.001982	0.002130
17	43.32	20.14	63.46	0.337121	0.493852	0.156732	0.415486	38.25	5.25	0.0051	0.000799	0.002928
18	63.46	23.73	87.19	0.493852	0.678521	0.184669	0.586187	43.13	10.13	0.0098	0.001816	0.004744
19	87.19	22.02	109.21	0.678521	0.849883	0.171362	0.764202	57.09	24.09	0.0234	0.004006	0.008751
20	109.21	22.49	131.70	0.849883	1.024903	0.175019	0.937393	78.65	45.65	0.0443	0.007754	0.016505
21	131.70	19.88	151.58	1.024903	1.179611	0.154708	1.102257	104.11	71.11	0.0690	0.010675	0.027180
22	151.58	20.61	172.19	1.179611	1.340000	0.160389	1.259805	155.39	122.39	0.1188	0.019049	0.046229
23	172.19	23.37	195.56	1.340000	1.521868	0.181868	1.430934	283.35	250.35	0.2429	0.044182	0.090411
24	195.56	19.02	214.58	1.521868	1.669883	0.148016	1.595875	537.79	504.79	0.4898	0.072505	0.162916
25	214.58	18.59	233.17	1.669883	1.814553	0.144669	1.742218	740.90	707.90	0.6870	0.099381	0.262297
26	233.17	19.15	252.32	1.814553	1.963580	0.149027	1.889066	835.49	802.49	0.7787	0.116053	0.378350
27	252.32	19.12	271.44	1.963580	2.112374	0.148794	2.037977	942.15	909.15	0.8822	0.131273	0.509623
28	271.44	19.53	290.97	2.112374	2.264358	0.151984	2.188366	1020.73	987.73	0.9585	0.145676	0.655298
29	290.97	20.04	311.01	2.264358	2.420311	0.155953	2.342335	1062.43	1029.43	0.9990	0.155792	0.811090
30	311.01	20.38	331.39	2.420311	2.578911	0.158599	2.499611	1083.92	1050.92	1.0198	0.161743	0.972833
31	331.39	21.95	353.34	2.578911	2.749728	0.170817	2.664319	1105.85	1072.85	1.0411	0.177837	1.150670

APPENDIX C

REGRESSION OF COLUMN TESTING

This nonlinear regression corresponds with Column Test 3 in Table 4.4.

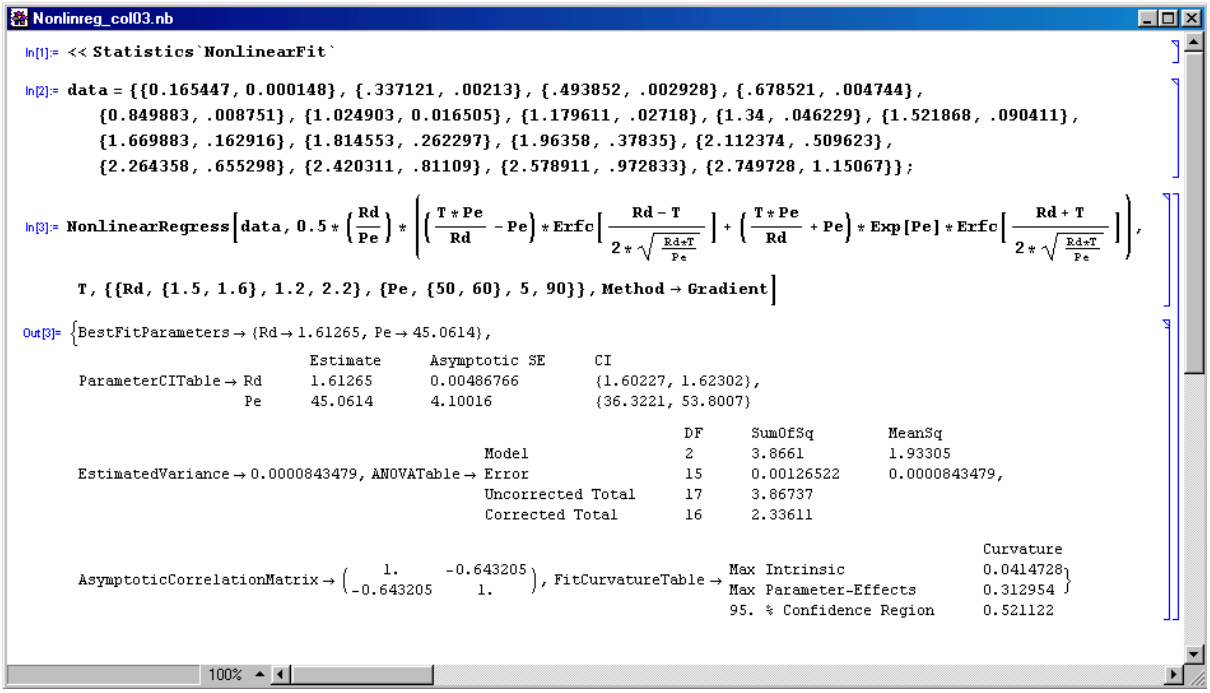

Nonlinreg_col03.nb

```
In[1]:= << Statistics`NonlinearFit`

In[2]:= data = {{0.165447, 0.000148}, {.337121, .00213}, {.493852, .002928}, {.678521, .004744},
          {0.849883, .008751}, {1.024903, 0.016505}, {1.179611, .02718}, {1.34, .046229}, {1.521868, .090411},
          {1.669883, .162916}, {1.814553, .262297}, {1.96358, .37835}, {2.112374, .509623},
          {2.264358, .655298}, {2.420311, .81109}, {2.578911, .972833}, {2.749728, 1.15067}};

In[3]:= NonlinearRegress[data, 0.5 * (Rd/Pe) * ((T * Pe/Rd - Pe) * Erfc[(Rd - T)/(2 * Sqrt[(Rd+T)/Pe])] + (T * Pe/Rd + Pe) * Exp[Pe] * Erfc[(Rd + T)/(2 * Sqrt[(Rd+T)/Pe])]),
          T, {{Rd, {1.5, 1.6}, 1.2, 2.2}, {Pe, {50, 60}, 5, 90}}, Method → Gradient]

Out[3]= {BestFitParameters → {Rd → 1.61265, Pe → 45.0614},
                              Estimate     Asymptotic SE     CI
         ParameterCITable → Rd  1.61265      0.00486766       {1.60227, 1.62302},
                            Pe  45.0614      4.10016          {36.3221, 53.8007}

                                                  DF     SumOfSq        MeanSq
                                        Model     2      3.8661         1.93305
         EstimatedVariance → 0.0000843479, ANOVATable → Error     15     0.00126522     0.0000843479,
                                        Uncorrected Total 17     3.86737
                                        Corrected Total   16     2.33611

                                                                          Curvature
         AsymptoticCorrelationMatrix → (  1.      -0.643205 ), FitCurvatureTable → Max Intrinsic          0.0414728
                                       (-0.643205   1.     )                      Max Parameter-Effects  0.312954
                                                                                  95. % Confidence Region 0.521122}
```

100%

REFERENCES

Achari, G., Chatterji, S., Joshi, R.C., and Bentley, L.R. (1997). "Effect of ion concentration on diffusion through clay." *Soil Science*, 162 (1), 51-55.

ASTM D 5084. "Measurement of hydraulic conductivity of saturated porous materials using a flexible wall permeameter." *American Society for Testing and Materials*, Pennsylvania.

Bear, J. (1972). *Dynamics of Fluids in Porous Media*, Elsevier Scientific Publ. Co, Amsterdam.

Bouazza, A., Manassero, M. and Smith, N. (1999). "Cement bentonite slurry walls for waste containment." *Proc., 8th ANZ Conf. On Geomechanics*, Hobart, Australia, 2, 679-684.

Brandl, H. (1994). "Vertical barriers for municipal and hazardous waste containment." *Developments in Geotechnical Engineering*, Balasubramaniam et al., Eds., Balkema, Rotterdam.

Chatterji, S. (1999). "Evidence of variable diffusivity of ions in saturated cementitious materials." *Cement and Concrete Research*, 29, 595-598.

Cortlever, N.G. (1988). "Geolock." *Geotechnics*, Amsterdam, Holland.

Czurda, K.A. and Haus, R. (2002). "Reactive barriers with fly ash zeolites for in situ groundwater remediation." *Applied Clay Science*, 21(1-2), 13-20.

Danckwerts, P.V. (1953). "Continuous flow systems: distributions of residence times." *Chem. Engrg. Sci*., 2(1), 1-13.

Delagrave, A., Marchand, J., Ollivier, J.P., Julien, S., and Hazrati, K. (1997). "Chloride binding capacity of various hydrated cement paste systems." *Advanced Cement Based Materials*, 6, 28-35.

Dhir, R.K., El-Mohr, M.A.K., and Dyer, T.D. (1996). "Chloride binding in GGBS concrete." *Cement and Concrete Research*, 26(12), 1767-1773.

Fam, M.A., and Santamarina, J.C. (1996). "Study of clay-cement slurries with mechanical and electromagnetic waves." *J. Geotech. Engrg.*, ASCE, 122(5), 365-373.

Fernandez, F. and Quigley, R.M. (1985). "Hydraulic conductivity of natural clays permeated with simple liquid hydrocarbons." *Canadian Geotechnical Journal*, 22, 205-214.

Fetter, C.W. (1999). *Contaminant Hydrogeology*, 2nd Ed., Prentice Hall, Inc., New Jersey.

Foose, G.J., Benson, C.H. and Edil, T.B. (2002). "Comparison of solute transport in three composite liners." *J. Geotech. Geoenviron. Eng.*, ASCE, 128(5), 391-403.

Fratalocchi, E., Manassero, M., Roccato, M., Pasqualini, E. and Spanna, C. (1996). "Predicting hydraulic conductivity of cement-bentonite slurries." *Environmental Geotechnics*, M. Kamon, ed., 503-508.

Fratalocchi, E. and Pasqualini, E. (1998). "Permeability over time of cement-bentonite slurry walls." *Environmental Geotechnics*, P.S. Seco e Pinto, ed., 509-514.

Freeze, R.A. and Cherry, J.A. (1979). *Groundwater*, Prentice Hall, Inc., New Jersey.

Garvin, S.L. and Hayles, C.S. (1999). "The chemical compatibility of cement-bentonite cut-off wall material." *Construction and Building Materials*, 13(6), 329-341.

Halamickova, P. and Detwiler, R.J. (1995). "Water permeability and chloride ion diffusion in Portland cement mortars: relationship to sand content and critical pore diameter." *Cement and Concrete Research*, 25(4), 790-802.

Haxo, H.E. and Lahey, T.P. (1988). "Transport dissolved organics from dilute aqueous solutions through flexible membrane liners." *Hazard. Waste Hazard. Mater.*, 5(4), 275-294.

Hiby, J.W. (1959). *Paper presented at conference on displacement in porous media*, Imperial College, London, March.

Horton, R., Thompson, M.L. and McBride, J.F. (1985). "Estimating transit times of noninteracting pollutants through compacted soil materials." *Proc., 11th Ann. Solid Waste Res. Symp.*, Cincinnati, Ohio, EPA/600/9-85/013, 275-282.

Jefferis, S.A. (1992). "Contaminant-grout interaction." *Proc., Conf. Grouting, Soil Improvement and Geosynthetics*, ASCE, New York.

Jefferis, S.A. (1996). "Contaminant-barrier interaction: friend or foe?" *Mineralogical Society Conference, Chemical Containment of Wastes in the Geosphere*, Keyworth, September.

Jefferis, S.A. (1997). "The origins of the slurry trench cut-off and a review of cement-bentonite cut-off walls in the UK." *Proc., Int. Containment Technology Conf.*, Florida State University, Tallahassee, Florida, USA.

Kamon, M. (1997). "Proper waste disposal and the remediation of contaminated sites." *Proc., 14th Int. Conf. Soil Mech. Found. Eng.*, Hamburg, Germany, 4, 2521-2524.

Kamon, M., Ohta, H., Aoi, M. and Ashida, S. (1998). "Development of new river-protection method by continuous inclined diaphragm wall." *Environmental Geotechnics*, P.S. Seco e Pinto, ed., 35-38.

Khera, R.P. and Tirumala, R.K (1992). "Materials for slurry walls in waste chemicals." *Slurry Walls: Design, Construction, and Quality Control, ASTM STP 1129*, D.B. Paul, R.R. Davidson, and N.J. Cavalli, eds., ASTM, Philadelphia, Pa., 172-180.

Kreft, A. and Zuber, A. (1978). "On the physical meaning of the dispersion equation and its solutions for different initial and boundary conditions." *Chem. Eng. Sci*., 33(11), 1471-1480.

Kreyszig, E. (1993). *Advanced Engineering Mathematics*, 7th ed., John Wiley and Sons, Inc., New York.

Lapidus, L. and Amundson, N.R. (1952). "Mathematics of adsorption in beds. VI: The effect of longitudinal diffusion in ion exchange and chromatographic columns." *J. Phys. Chem*., 56(8), 984-988.

Lee, T. and Benson, C.H. (2000). "Flow past bench-scale vertical ground-water cutoff walls." *J. Geotech. Geoenviron. Eng.*, ASCE, 126(6), 511-520.

Lerman, A. (1979). *Geochemical Processes-Water and Sediment Environments*, John Wiley and Sons, Inc., New York.

Li, Y-H. and Gregory, S. (1974). "Diffusion of ions in sea water and in deep-sea sediments." *Geochimica et Cosmochimica Acta*, 38(5), 703-714.

Liao, W.P. and Daniel, D.E. (1989). "Time of travel of contaminants through soil liners." *Proc., 12th Ann. Madison Waste Conf.*, Univ. of Wisconsin, Madison, 367-376.

Lindstrom, F.T., Haque, R., Freed, V.H. and Boersma, L. (1967). "Theory on the movement of some herbicides in soils; Linear diffusion and convection of chemicals in soils." *Environ. Sci. Technol*., 1, 561-565.

Luo, R., Cai, Y., Wang, C., and Huang, X. (2003). "Study of chloride binding and diffusion in GGBS concrete." *Cement and Concrete Research*, 33, 1-7.

Manassero, M., Fratalocchi, E., Pasqualini, E., Spanna, C., Verga, F. (1995). "Containment with vertical cutoff walls." Key-Note Lecture, *Proc., Int. Conf. The Geoenvironment 2000*, ASCE GSP n. 46, New York.

Manassero, M., Di Molfetta, A., Pacitti, M. and Veggi, S. (1997). "The case history of a landfill for hazardous industrial wastes." Key-Note Lecture, *Proc. 1st ANZ Conference Geoenvironment '97*, A.A. Balkema, Rotterdam.

Manassero, M., Pasqualini, E., and Sani, D. (1998). "Potassium sorption isotherms of a natural clayey-silt for pollutant containment." *Proc., 3rd ICEG*, Lisbon, Balkema, Rotterdam.

Manassero, M., Benson, C.H. and Bouazza, A. (2000). "Solid waste containment systems." *Proc., Int. Conf. GeoEng 2000*, Melbourne, Australia, 1, 520-642.

Mesri, G. and Olson, R.E. (1971). "Mechanisms controlling the permeability of clays." *Clays and Clay Minerals*, 19, 151-158.

Millet, R.A., Perez, J-Y. and Davidson, R.R. (1992). "USA practice slurry wall specifications 10 years later." *Slurry Walls: Design, Construction, and Quality Control*,

ASTM STP 1129, D.B. Paul, R.R. Davidson, and N.J. Cavalli, eds., ASTM, Philadelphia, PA., 42-66.

Mitchell, J.K. (1991). "Conduction phenomena: from theory to geotechnical practice." *Geotechnique*, 41(3), 299-340.

Mitchell, J.K. (1993). *Fundamentals of Soil Behavior*, 2nd Ed., John Wiley & Sons, Inc., 251.

Page, C.L. and Vennesland, O. (1983). "Pore solution composition and chloride binding capacity of silica fume cement pastes." *Materiaux et Constructions*, 16(91), 19-25.

Perkins, T.K. and Johnston, D.C. (1963). "A review of diffusion and dispersion in porous media." *Society of Petroleum Engineering Journal*, 3(1), 70-84.

Petrov, R.J., Rowe, R.K. and Quigley, R.M. (1997). "Selected factors influencing GCL hydraulic conductivity." *J. Geotech. Geoenviron. Eng.*, ASCE, 123(8), 683-695.

Rabideau, A. and Khandelwal, A. (1998). "Boundary conditions for modeling transport in vertical barriers." *J. Environ. Eng.*, ASCE, 124(11), 1135-1139.

Reddi, L.N. and Inyang, H.I. (2000). *Geoenvironmental Engineering*, Marcel Dekker, Inc., New York.

Ressi di Cervia, A.L. (1992). "History of slurry wall construction." *Slurry Walls: Design, Construction, and Quality Control*, *ASTM STP 1129*, D.B. Paul, R.R. Davidson, and N.J. Cavalli, eds., ASTM, Philadelphia, PA., 3-15.

Rowe, R.K. and Booker, J.R. (1985). "1-D pollutant migration in soils of finite depth." *J. Geotech. Eng.*, ASCE, 111(GT4), 479-499.

Rowe, R.K., Caers, C.J. and Barone, F. (1988). "Laboratory determination of diffusion and distribution coefficients of contaminants using undisturbed clayey soil." *Can. Geotech. J.*, 25, 108-118.

Rowe, R.K., Hrapovic, L. and Kosaric, N. (1995a). "Diffusion of chloride and dichloromethane through a HDPE geomembrane." *Geosynth. Int.*, 2(3), 507-536.

Rowe, R.K., Quigley, R.M., and Booker, J.R. (1995b). *Clayey Barrier Systems for Waste Disposal Facilities*, E & FN Spon, London.

Rowe, R.K., Booker, J.R., and Fraser, M.J. (1998). *POLLUTE v6 and POLLUTE-GUI User's Guide*, GAEA Environmental Engineering Ltd., London, Ontario.

Roy, W.R., Krapac, I.G., Chou, S.F.J., and Griffin, R.A. (1991). "Batch-type procedures for estimating soil adsorption of chemicals." *EPA/530/SW-87/006-F*, U.S. Environmental Protection Agency, Washington, D.C.

Scheiddegger, A.E. (1954). "Statistical hydrodynamics in porous media." *J. Appl. Phys.*, 25(8), 994-1001.

Shackelford, C.D. (1989). "Diffusion of contaminants through waste containment barriers." *Trans. Rsrch. Record*, 1219, Transportation Research Board, National Research Council, Washington, DC., 169-182.

Shackelford, C.D. (1990). "Transit-time design for earthen barriers." *Engineering Geology*, Elsevier Publ., Amsterdam, 29, 79-94.

Shackelford, C.D. and Daniel, D.E. (1991). "Diffusion in saturated soil. I: Background." *J. Geotech. Eng.*, ASCE, 117(3), 467-484.

Shackelford, C.D. (1994). "Critical concepts for column testing." *J. of Geotechnical Engineering*, ASCE, 120(10), 1804-1828.

Shackelford, C.D. (1995). "Cumulative mass approach for column testing." *J. of Geotechnical Engineering*, ASCE, 121(10), 696-703.

Shackelford, C.D. and Rowe, R.K. (1998). "Contaminant transport modeling." *Environmental Geotechnics*, P.S. Seco e Pinto, ed., 939-956.

Shackelford, C.D. and Jefferis, S.A. (2000). "Geoenvironmental engineering for in situ remediation." *Proc., Int. Conf. GeoEng 2000*, Melbourne, Australia, 1, 121-185.

Sharma, H.D. and Lewis, S.P. (1994). "Chapter 7: vertical barriers: slurry walls." *Waste Containment Systems, Waste Stabilization, and Landfills*, John Wiley and Sons, Inc., New York.

Spitz, K. and Moreno, J. (1996). *A Practical Guide to Groundwater and Solute Transport Modeling*, John Wiley and Sons, Inc., New York.

Suryavanshi, A.K., Scantlebury, J.D., and Lyon, S.B. (1995a). "Pore size distribution of OPC and SRPC mortars in presence of chlorides."*Cement and Concrete Research*, 25(5), 980-988.

Suryavanshi, A.K., Scantlebury, J.D., and Lyon, S.B. (1995b). "The binding of chloride ions by sulphate resistant Portland cement." *Cement and Concrete Research*, 25(3), 581-592.

Suryavanshi, A.K., Scantlebury, J.D., and Lyon, S.B. (1996). "Mechanism of Friedel's salt formation in cements rich in tri-calcium aluminate." *Cement and Concrete Research*, 26(5), 717-727.

Tachavises, C. and Benson, C.H. (1997). "Hydraulic importance of defects in vertical groundwater cut-off walls." *In situ remediation of the geoenvironment '97, Geotech. Spec. Publ. No. 71*, J. Evans, ed., ASCE, New York, 168-180.

Tang, L. and Nilsson, L. (1993). "Chloride binding capacity and binding isotherms of OPC pastes and mortars." *Cement and Concrete Research*, 23(1), 247-253.

Tedd, P., Paul, V. and Lomax, C. (1993). "Investigation of an eight year old slurry trench cut-off wall." *Proc., Int. Conf. Green '93*, Bolton University, Bolton, Balkema, Rotterdam.

van Genuchten, M.Th. and Alves, W.J. (1982). "Analytical solutions of the one-dimensional convective-dispersive solute transport equation." *Technical Bulletin No. 1661*, U.S. Department of Agriculture.

van Genuchten, M.Th. and Parker, J.C. (1984). "Boundary conditions for displacement experiments through short laboratory soil columns." *Soil Sci. Soc. of Am. J.*, 48(4), 703-708.

Yong, R.N., Mohamed, A.M.O. and Warkentin, B.P. (1992). *Principles of contaminant transport in soils*, Elsevier Science Publishers, 122 & 247 & 253-255.

Yu, D., Jackson, K. and Harmon, T.C. (1999). "Dispersion and diffusion in porous media under supercritical conditions." *Chemical Engineering Science*, 54, 357-367.

NOTE